RUMINAL NUTRIENT AVAILABILITY AND INHERENT STRUCTURAL FEATURES OF SIX BARLEY VARIETIES USING *IN SITU* TECHNIQUE AND MID-IR SPECTROSCOPY

A Thesis Submitted to the College of

Graduate Studies and Research

In Partial Fulfillment of the Requirements

For the Degree of Master of Science

In the Department of Animal and Poultry Science

University of Saskatchewan

Saskatoon

By

NA LIU

PERMISSION TO USE STATEMENT

In presenting this thesis in partial fulfilment of the requirements for a Master of Science degree from the University of Saskatchewan, I agree that the Libraries of this University may make it freely available for inspection. I further agree that permission for copying of this thesis in any manner, in whole or in part, for scholarly purposes may be granted by the professor or professors who supervised my thesis work or, in their absence, by the Head of the Department or the Dean of the College in which my thesis work was done. It is understood that any copying or publication or use of this thesis or parts thereof for financial gain shall not be allowed without my written permission. It is also understood that due recognition shall be given to me and to the University of Saskatchewan in any scholarly use which may be made of any material in my thesis.

Requests for permission to copy or to make other use of material in this thesis in whole or part should be addressed to:

Head of the Department of Animal and Poultry Science

University of Saskatchewan

Saskatoon, Saskatchewan (S7N 5A8)

ABSTRACT

Barley grain is one of the main sources of feed for ruminants in Canada. Although barley varieties may have similar chemical composition, they exhibit different rumen degradation characteristics and nutrient availabilities. These biological differences may be related to structural chemical make-up or structural features among the varieties. The objectives of this study were to use the *in situ* technique and two Mid-IR Spectroscopy techniques, Diffuse Reflectance Fourier Transform IR Spectroscopy (DRIFT) and Synchrotron-based Fourier Transform IR Microspectroscopy (SFTIRM) to determine ruminal nutrient availabilities and inherent structural features in the hull, seed and endosperm of six barley varieties (AC Metcalfe, McLeod, CDC Dolly, CDC Helgason, CDC Trey, and CDC Cowboy) and to study the relationships between structural characteristics, mean and median particle size and nutrient availability. The nylon bag technique was used to incubate coarsely dry-rolled barley samples for 0, 2, 4, 8, 12, 24 and 48 h in the rumen of three mature Holstein dry dairy cows, which were ruminally cannulated. The rumen degradation kinetics of dry matter (DM), crude protein (CP) and starch were determined using first order degradation kinetics equations. Results indicated that there were significant differences in the mean and median particle size, degradation kinetics of each individual nutrient (DM, CP, and starch) among the six barley varieties. CDC Helgason showed the lowest degradation rate and extent of all nutrients (DM, CP, and starch) among the six barley varieties with larger particle size. Compared with other five varieties, CDC Helgason may be more suitable for ruminants feeding because of the

lowest degradation rate and extent. The results also revealed a strong correlation between median particle size and the rate and extent of rumen degradation.

The results also showed that both DRIFT and SFTIR techniques associated with uni- and two multi- variate analyses were capable to efficiently discriminate and classify the inherent molecular structural features among the different varieties of barleys. Uni-variate analyses were conducted using both the DRIFT spectroscopy (hull and whole seed sample) and SFTIR microspectroscopy (endosperm tissue). The results from hull samples showed significant differences in the peak area of aromatic lignin, cellulosic compound, and total carbohydrates (CHO), and the ratio of lignin to cellulosic compound among the six barley varieties. The results from whole seed samples showed significant difference in the peak area and height of Amide I, peak area of total CHO and structural CHO (cellulosic), and the ratio of Amide I to total CHO area, and the ratio of total CHO to structural CHO. Significant differences were also found in the SFTIR results from endosperm tissue. With two multivariate spectral analysis techniques: Agglomerative hierarchical cluster (AHCA) and Principal component analyses (PCA) applied on whole seed sample, the CDC Helgason was distinguished from AC Metcalfe, CDC Dolly, McLeod and CDC Cowboy in fingerprint (1800-800 cm^{-1}) and CHO region (1185-800 cm^{-1}), from AC Metcalfe, McLeod and CDC Cowboy in protein region (1715-1485 cm^{-1}). Information from this study involving probing the seed internal structure of barley may provide a further insight as to why barley varieties exhibit different rumen degradations.

ACKNOWLEDGMENTS

It is a great honour for me to obtain the opportunity to accomplish the master program in Department of Animal and Poultry Science, University of Saskatchewan. I would like to express my special thanks to my supervisor, Peiqiang Yu for his invaluable patience and support. Without his guidance and supervision, I would never have learned and accomplished so much. This experience would be the most important and valued treasure in my life.

I also sincerely thank the advisory committee members David A. Christensen, John J. McKinnon, and Fiona C. Buchanan. Without their help and encouragement, the difficulties during the whole process would never have been overcome.

I would also like to sincerely thank Dr. Jan C. Plaizier, the external examiner, for spending lots of time to review my thesis.

I also sincerely thank Zhiyuan Niu for his kind assistance in experiment and analysis work, Dr. Brian Rossnagel (Crop Development Centre, University of Saskatchewan) for providing barley samples, and Jennifer Bohon (NSLS-BNL, U.S. Department of Energy, NewYork, USA) for helpful data collection at the U2B experimental station. Additionally, many thanks to all cooperating teammates and research peers for providing

help and scientific communication and all people with whom I shared laughs and smiles in this progress.

The author acknowledges financial supports from the NSERC-Individual Discovery Grant and ADF-Saskatchewan for funding this research.

TABLE OF CONTENTS

LIST OF TABLES

LIST OF FIGURES

LIST OF APPENDIX

LIST OF ABBREVIATIONS

ADF	Acid detergent fiber
ADICP	Acid detergent insoluble crude protein
AHCA	Agglomerative hierarchical cluster analysis
C	Carbon
CFat	Crude fat
CHO	Carbohydrate
CNCPS	Cornell Net Carbohydrate and Protein System
CP	Crude protein
D	Potentially degradable fraction
DM	Dry matter
DRIFT	Diffuse reflectance Infrared Fourier transform spectroscopy
DVE	Truly digested protein in the small intestine
ED	Effectively degradability
FSD	Fourier self-deconvolution
FTIR	Fourier Transform infrared Spectroscopy
H	Hydrogen

IR	Infrared
Kd	Degradation rate
Kp	Passage rate
N	Nitrogen
NDF	Neutral detergent fiber
NDICP	Neutral detergent insoluble crude protein
NPN	Non-protein nitrogen
NSC	Non-structural carbohydrates
O	Oxygen
PCA	Principal components analysis
RPM	Rotation per minute
RUDM	Rumen undegradable dry matter
RUP	Rumen undegradable protein
RUST	Rumen undegradable starch
S	Soluble fraction
S/N	Signal to noise
SFTIRM	Synchrotron-based Fourier Transform infrared Microspectroscopy
ST	Starch
U	Undegradable fraction

1. LITERATURE REVIEW

1.1. Barley in ruminant nutrition

1.1.1. Background

1.1.1.1. History, production and seed structure

Barley (*Hordeum vulgare)* was one of the earliest domesticated crops in agricultural history and can be dated to 1500–850 BC. Barley is very adaptive to different environmental conditions (for example, climate, soil salinity, water). About 100 countries grow barley for various usages (Kulp and Ponte 2000; Slafer 2002; von Bothmer 2003). Barley is one of the most important cereal grains in crop production and has been widely used in feed (major use), malting and health food industries. Canada was ranked second in the world in barley production with 11.8 million metric tonnes in 2007 (Food and Agriculture Organization 2007). As a principle source of feed for ruminants, there are more than 50 varieties of barley grown in Canada, ten of which occupy approximately 90% of the total acreage (B. G. Rossnagel, personal communication, 2009). The majority of the national barley acreage is largely attributable to western Canada. In Saskatchewan, production was 4,273,000 tonnes out of a total of 10,580,000 tonnes in western Canada for the 1999-2008 average (Langrell et al. 2008).

The fibrous hull exists in the very outside of the grain. Cellulose and hemicellulose exist in the cell wall to strengthen the plant tissue. The pericarp tightly covers the whole seed. The seed coat (testa) is also protective. Besides the embryo, a large portion of the seed is endosperm tissue, with starch granules for storage. Both starch and the aleurone layer are found in the endosperm tissue of barley. The aleurone layer is composed of cells which physically encompass the starchy parts (Black 2000; Kulp and Ponte 2000). β-glucans and arabinoxylans, the compounds comprising fibre, are abundant in the cell wall of the endosperm and aleurone layer (Holtekjøen et al. 2006).

1.1.1.2. Uses and economic value

As one of the most important annual cereal grains, barley is a primary source for animal feed (cattle, swine and poultry) and for the malting industry in North America. In addition, a small amount of barley is used as a health food because of its continuous and stable sugar release in the gastrointestinal tract (von Bothmer 2003).

Barley is mainly supplied as an energy and protein source for swine, beef and dairy cattle (Kellems and Church 2002). Since barley possesses a good balance of nutrients, it is used widely in Canada. The barley seed coat provides little, if any available energy. However, barley provides more protein (average of 11-12% of DM) compared to cereals such as corn. (Church 1991; Holopainen et al. 2005; OMAF Feed Advisory Program 2009).

1.1.2. Varieties

1.1.2.1. Barley varieties for malting purpose

AC Metcalfe is one of the most popular barley varieties for malting purposes adapted to Western Canada, contributing 35.8% of total barley seeded acreage in 2008 (Langrell et al. 2008). Harrington is another barley variety used for malting purpose, which is usually used as an industry malting quality standard (Harvey and Rossnagel 1984). Additionally, CDC Copeland, CDC Kendall, Newdale, Legacy and Tradition are common barley varieties for malting purposes grown in western Canada (Langrell et al. 2008).

1.1.2.2. Barley varieties for feed purpose

As a main source of feed for ruminants in North America, many barley varieties for feed purpose have been developed for animal consumption. Barley varieties used feed have a higher protein content compared with corn, are used as an ingredient to optimize rumen function and improve animal production. Diverse barley varieties for feed purpose have been developed with various superior properties. For example high yield, disease resistance and excellent total carbohydrate content have been selected for in barley breeding programs. CDC Dolly, McLeod, CDC Helgason, CDC Trey, CDC Cowboy are

all two-rowed, hulled barley varieties (Canadian Food Inspection Agency 2007). CDC Dolly and CDC Helgason are commonly used in Western Canada for feeding purposes (Rossnagel and Harvey 1994; Holtekjøen et al. 2006). CDC Cowboy is a spring barley variety developed for feed and forage purposes (Canadian Food Inspection Agency 2007). Other barley varieties for feed purposes include Valier, with a smaller fraction of rapidly degradable sugars (Yu et al. 2003).

Hull-less barley contributes a small percentage of annual barley production. These varieties usually contain more starch and less cellulose than hulled varieties (Holtekjøen et al. 2006).

1.1.3. Digestion in rumen

1.1.3.1. Nutritional benefits for ruminants

Nutrition is one of the most important factors for success in animal production. Major nutrients include total carbohydrates and protein. Considered to be an important diet ingredient, barley is used extensively for energy in cattle feeding in Canada (Kulp and Ponte 2000; Kellems and Church 2002). Barley can also provide protein for cattle to meet the requirements of maintenance, growth, lactation and reproduction. The soluble fraction of protein is always digested in the rumen by microorganisms prior to entering the small intestine. Rumen undigested protein can be utilized by the host animal since bypass protein absorbed in the small intestine can benefit the host animal directly. It appears that barley grain provides an important contribution to rumen microbial growth as well as to the digestible nutrient requirements for cattle. When placing emphasis on ruminant nutrition, with effective ruminal fermentation, it is usually beneficial to provide more high quality feed nutrients (carbohydrates and proteins) digested in the small intestine. This strategy can reduce the risk of rumen acidosis and other metabolic disorders and increase the nutrient supply to the host animal.

The nutrient composition of barley is given in Table 1.1. Barley has more CP (approximately 11.0% DM) than corn (9.8% DM) and Milo (9.8% DM) (Herrera-Saldana

et al. 1990). Barley contains approximately 16-18% NDF and 5-7% ADF (DM basis). For some varieties, NDF and ADF are found up to 19.5% and 7.8% DM, respectively (Herrera-Saldana et al. 1990). Barley contains 22.6-41.1% non-starch polysaccharides, 51.3-64.2% starch and 8.0%-17.7% cellulose (Nocek and Tamminga 1991; Foley et al. 2006). In addition, barley also contains a small amount of lipids (Kulp and Ponte 2000).

1.1.3.2. Structural characteristic of barley on ruminal nutrient availability

Both the chemical and structural make-up of the barley grain can affect the digestion process in the rumen. For example, the polysaccharides in barley seed are widely diverse in terms of content and composition (Tester et al. 2004; Holtekjøen et al. 2006). Carbohydrates, including starch, cell wall polysaccharides and other digestible carbohydrates, are the most important energy source for ruminants (Nocek and Tamminga 1991). As a result of rumen fermentation, the ruminant can effectively utilize these polysaccharides whereas monogastric animals rely on utilization of starch (Church 1991). Barley varieties differ in starch type and content (Yoshimoto et al. 2000), and therefore exhibit various chemical properties. The properties of starch, including granule size, shape, distribution, association pattern and composition may contribute to its rumen degradation pattern (Tester et al. 2004). The hull is the fibrous outer part of the barley kernel. As a fermentation-resistant factor, the hull content can affect the nutrient availability since lignin, cellulose and hemicelluloses are not easily digestible. In comparison with hull-less cultivars, hulled barley was found to have lower soluble and degradable fractions of DM (Khorasani et al. 2000). Lignin content of barley varieties also varies (Dunteman 1989). Feedstuffs containing more lignin and cellulosic materials appear to have a lower digestibility. This slows down the degradation rate in rumen, and consequently, depresses the nutritive value of the feed.

Table 1.1 Chemical composition of Harrington and Valier barley (Adapted from: Yu et al. 2003).

Item	Barley variety	
	Harrington	Valier
Chemical composition		
DM (g/kg)	903	908
ASH (g/kg DM)	25	22
CFat (g/kg DM)	26	27
CP (g/kg DM)	130	136
CHO (g/kg DM)	818	816
NSC (g/kg DM)	602	502
Starch (g/kg DM)	442	443
Starch (g/kg NSC)	744	883
ADF (g/kg DM)	73	69
NDF (g/kg DM)	256	252
Lignin (g/kg NDF)	45	81
SCP (g/kg CP)	180	176
NPN (g/kg SCP)	415	354
NDICP (g/kg CP)	305	281
ADICP (g/kg CP)	38	20

1.1.3.3. Processed barley

Since feed is the most significant production cost in the animal industry, appropriate processing should be applied to improve the efficiency of feeding and management. Grinding and milling are the most common physical processing methods applied to barley. For ruminants, it is better to roll barley rather than to grind it (Church 1991; Kellems and Church 2002).

Processing methods are important because digestibility and digestion site may be affected due to the particle size. Particle size was found to have a negative correlation with digestibility (Bowman et al. 2001). An earlier study found that a faster passage rate of corn from the rumen may result from decreasing particle size (Nocek and Tamminga 1991). Reduced particle size results in increased surface area accessed by rumen microbes and enzymes, and consequently, increasing digestion rate. Appropriate particle size of feed is especially required for ruminants since it improves nutrient availability and benefits both the rumen microorganisms and the host animal. Whereas excessively small particle size may lead to rapid rumen fermentation and as a result, increase the risk of rumen acidosis or other metabolic disorders (Hale 1973). In addition, exclusively fine particles tend to clump when entering the digestion tract, which may negatively affect palatability (Church 1991). Ruminants may sort out fine particles and leave them in the feed bunk. Harrington (malting-type) and Valier (feed type) were found to exhibit similar degradation characteristics with fine processing through 2 mm screen, though they differed when coarsely processed (Yu et al. 2003). An earlier study also reported that particle size less than 1 mm may eliminate variety differences in degradation rate (Nocek 1988).

1.1.3.4. Degradation behaviours of barley

In general, barley grains exhibit a fast degradation rate of DM compared to forage and have a high effective degradability of nutrients for ruminants (Church 1991; Kulp and Ponte 2000). Barley grain quality is influenced by several factors, such as environmental conditions during the growth of the crop, harvest conditions, cultivars, and processing

methods (Kulp and Ponte 2000). The wide variation of barley genotype leads to a large range of *in situ* characteristics (Khorasani et al. 2000). The rumen digestibility of barley grain varies depending on cultivars, processing methods and other quality conditions (for example, hardness and protein content). In vivo experiments showed that the rumen digestibility of rolled barley ranged from 73.2 to 90.3% of total starch (Nocek and Tamminga 1991). However, studies showed that barley varieties that were coarsely rolled exhibit different rumen degradation characteristics and nutrient availability even though they have similar chemical composition (Yu et al. 2003). These differences disappeared when fine processing was applied to the grain to destroy the kernel structure. This implies the structure of kernels may play a role in the digestibility characteristics of barley. Therefore, traditional chemical analysis is not very effective to explain the different degradation behaviours of different varieties with similar chemical content.

1.1.3.5. Rumen disorders caused by fast degradation

Although ruminants can utilize roughages, such as straw or hay, to ensure high production, concentrate is needed as a nutrient source for high producing animals. The rumen is a semicontinuous fermentation chamber. Rumen microorganisms, including bacteria, fungi, and protozoa, are essential to the host animal (Church 1991; Kellems and Church 2002). They carry out the initial digestion of feed in the rumen. If the diet contains a high percentage of grain, the ruminal degradation rate of nutrients, especially carbohydrates and protein, should be monitored to maintain the animal health (National Research Council 2001; Kellems and Church 2002).

Excessively fast ruminal degradation arising from starch based concentrates usually results in low pH in the rumen, and consequently, leads to potential digestive disorders (Keunen et al. 2002; Ørskov 1986; Plaizier et al. 2008). A high intake of concentrate may lead to extensive fermentation in the rumen, and thus increase the risk of acidosis or other metabolic disorders, such as laminitis, and bloat, even death in severe cases (Bowman et al. 2001; Keunen et al. 2002; Plaizier et al. 2008). Therefore, barley grain with a fast degradation rate may not be a proper source of energy because it may increase acidosis

risk for animals. More research is necessary to evaluate the differences among varieties of barley to understand the availability of the nutrient supply to ruminants.

1.2. Normal feed evaluation methods

1.2.1. In vitro and in vivo techniques and nutrient availability and supply modeling

The in vitro gas production and the *in situ* nylon bag degradability techniques have been reviewed (Valentin et al. 1999). The in vitro techniques involve rumen fluid continuous culture, gas production, enzymatic digestion, dry matter disappearance and volatile fatty acid production (Hale 1973). More methods to determine nutrient digestibility are also summarized (Waldo 1973; Nocek 1988). Both the *in vitro* and *in vivo* techniques are widely employed in ruminant nutrition research.

The *in situ* technique is extensively used to measure rumen digestibility (Ørskov and McDonald 1979; Nocek 1988). The Ørskov model is used to describe the degradation kinetics of feeds. Results may vary due to the variation from bag porosity, particle size, sample size to bag surface ratio, animal effects, dietary effects and microflora effects (Figroid et al. 1972). However, the *in situ* technique is time-consuming and expensive, so it is impossible to carry out for a large amount of samples (Khorasani et al. 2000). In addition, it is not very effective to estimate the differences of digestion features of finely ground samples (Yu et al. 2003). Additionally, a finely ground sample may cause mechanical loss and result in bias (Nocek 1988).

Much effort has been made to develop models to ensure that adequate nutrients are supplied to optimize animal performance. The NRC 2001 dairy model (National Research Council 2001) is effective and widely used for feed evaluation. Besides the NRC models, there are other diet models developed to estimate nutrient availability. The Cornell Net Carbohydrate and Protein System (CNCPS) (Sniffen et al. 1992) is one model, which characterizes the crude protein into PA (non-protein N), PB (true protein, including PB1, PB2 and PB3, depending on various degradation rates) and PC

(unavailable protein) fractions. Similarly, carbohydrates are segregated into CA (rapidly degradable CHO), CB1 (intermediately degradable CHO), CB2 (slowly degradable CHO) and CC (unfermentable CHO) fractions (Sniffen et al. 1992; Yu et al. 2003). The DVE/OEB system (Tamminga et al. 1994; Yu et al. 2003) was developed to evaluate feed nutrients, predict milk production and meet the nutrient requirements of dairy cattle in a detailed and exact manner.

1.2.2. Disadvantages of traditional chemical analysis

Traditional chemical analysis has long been employed to study chemical composition of a feed in animal science. Although chemical analysis methods are in common usage, they fail to take the structural information into account. As reviewed previously, all the traditional "wet" analysis methodologies involve chemical reagents (Wetzel and LeVine 1993). The grinding of the sample usually makes it difficult to explore and evaluate microstructure or chemical distribution of biological samples. The locally distributed compounds are thus diluted and evenly mixed. These undesired influences from traditional chemical analysis make it difficult to restore the original status of the feed, thus resulting in loss of structure. These limitations cannot be overcome unless a new analytical tool is introduced. Therefore, traditional analysis is no longer sufficient for further investigation of grain in feed science, but needs to be complemented with other novel techniques.

1.3. Mid-IR spectroscopy application in feed science

1.3.1. Infrared spectroscopy principles

1.3.1.1. Basic knowledge

The wavelength (λ) of infrared (IR) region is longer than that of visible light. Mid-IR is commonly defined to cover the region of the electromagnetic spectrum from 4000 to 400 cm^{-1} (Messerschmidt and Harthcock 1988).

Atoms vibrate with certain frequencies in a molecule. Vibration of chemical bonds are not completely isolated, but may be affected by other parts of the molecule, especially the neighboring groups. At the same time, with this interaction, the molecule itself does vibrate in different modes (Messerschmidt and Harthcock 1988). Generally, there are two major vibrational modes: stretching and bending. For the stretching vibration, it includes symmetrical stretching vibration (ν_s) and asymmetrical stretching vibration (ν_{as}). For bending vibration, it includes (1) in plane bending vibration (δ), which can be separated to scissoring vibration (δ) and rocking vibration (ρ), and (2) out-of-plane bending vibration (γ), which can be separated to wagging vibration (ϖ) and twisting vibration (τ) (Messerschmidt and Harthcock 1988; Jackson and Mantsch 2000; Stuart 2004). All molecules can be imagined as the superposition of a simple harmonic oscillator formed by atoms. They move around at a certain frequency. The atom mass and the chemical bond between atoms are two factors which can affect this motion (Jackson and Mantsch 2000). Stronger bonds and smaller atom masses usually mean higher vibration frequency (Messerschmidt and Harthcock 1988). When the molecule encounters energy with the same vibration frequency as that of its normal modes of vibration, it can absorb the energy at this frequency. The unabsorbed energy will pass through the sample and can be measured. Different atoms vibrate at different frequencies with different modes, which results in complicated matrix structural information. Different compounds can exhibit their own characteristic IR absorption pattern (Messerschmidt and Harthcock 1988; Jackson and Mantsch 2000; Stuart 2004).

Exposure to IR radiation cause vibration and rotation of molecules between different quantized discrete energy levels E0, E1, E2 (Stuart 2004). Whenever IR radiation transmits through a sample, energy uptake by a molecule occurs and results in transition between different energy levels (Stuart 2004; Barth 2007). Primarily, various IR spectra patterns result from the corresponding vibration, a kind of internal motion of the molecule. Therefore, it is possible to identify the unknown organic compounds and determine the composition of a mixture according to the frequencies, lineshapes, intensities and patterns of the characteristic peaks (Messerschmidt and Harthcock 1988; Jackson and Mantsch 2000; Stuart 2004). There can also be a slight shift of characteristic

peaks resulting from diverse specimens, while the typical IR absorbance patterns do not change. Differences in chemical and structural composition, therefore, can be shown in the IR spectra. By analyzing with uni- and multi- variate analysis methods, informative differences can be probed. Various chemical compounds have various IR spectra. IR spectra are specific and characteristic, which therefore can be used as "fingerprints" for identifying or discriminating sample conformation (Messerschmidt and Harthcock 1988).

IR spectroscopy has been successfully used as an analytical technique in organic chemistry since 1940s. IR spectroscopy is widely applied in analysis of chemical composition, because it can accomplish rapid analysis with simple operation and simultaneously determine multi-nutrient composition in a nondestructive, non-pollutive manner (Barth 2007). This technique only requires a small amount of sample. Additionally, with flexible accessories, IR spectroscopy is capable of analyzing a sample in different status (gases, liquids and solids) or with different composition (organics/inorganics, macro/micro molecules) (Wetzel et al. 1998b; Stuart 2004). Samples are mounted on the path of IR radiation in an IR spectroscope. When a sample is exposed to IR radiation, if the molecules of the sample are "active" to the corresponding IR frequencies, the certain electric dipole moment in the molecule can be altered and characteristic absorption occurs. By measuring the absorption, spectroscopic information can be obtained (Stuart 2004).

1.3.1.2. Spectral band assignments and characteristics

IR spectroscopy is designed to characterize chemical functional groups by measuring the IR absorption in the sample. The IR spectrum is displayed as a function of frequency. All types of chemical functional groups have their own unique absorption frequency associated with energy. When the energy or frequency of IR meets any vibrational frequency of molecules in the sample, absorption occurs. A detector can record the absorption to determine the chemical function groups and examine the chemical composition of the complex matrix (Budevska 2002).

Characteristic absorption peaks can be used to analyze a large variety of compound classes. For example, in the ca. 4000-2500 cm^{-1} region, there are bands caused by O–H, C–H and N–H stretching. Triple-bond stretching usually exhibits absorption in the ca. 2500-2000 cm^{-1} region. In contrast C=C and C=O stretching absorptions are located at the ca. 2000–1500 cm^{-1} region (Jackson and Mantsch 2000; Stuart 2004). The wavenumber range of IR from 1800 to 800 cm^{-1} is the so-called "fingerprint region". The fingerprint region usually accounts for almost all the characteristics of biological molecules. Bands in the fingerprint region are particularly sensitive to molecular structure. However, it should be pointed out that not every band can guarantee the representation of a certain corresponding chemical structure because the vibration of chemical bonds vary in sensitively depending on the sample status and experiment circumstance (Griffiths and De Haseth 1986; Messerschmidt and Harthcock 1988; Yu 2006b).

1.3.2. Spectral analysis

Infrared spectroscopy provides comprehensive information on composition and characteristics of samples. Following exposure to IR radiation, chemical functional groups exhibit characteristic absorption at certain frequencies, which enable the detection of chemical and structural differences. The typical IR absorption peaks of the relevant biopolymers have been well documented (Jackson and Mantsch 2000; Miller 2002). The typical IR spectral bands of biological compounds have been summarized in Table 1.2.

Protein IR absorption bands are related to the corresponding amide group. The corresponding absorbance of amide groups occurs at around 1700-1500 cm^{-1}. Two are commonly used in biological applications. One is amide I (centered at ca. 1650 cm^{-1}), resulting from 80% C=O stretching, 10% C–N stretching and 10% N–H bending (Jackson and Mantsch 1991; Stuart 2004). The amide II absorbance appears at ca. 1550 cm^{-1}, which is from 40% C-N stretching associated with 60% N-H deformation (Wetzel 1993; Stuart 2004). However, the amide II band is usually overlapped with other bands. Hence, it is used less in protein analysis than amide I. Generally, in complex biological specimens, protein conformation is composed of various biopolymer structures. The amide I band can also be used to analyze the secondary structure of the protein because it

usually contains a variety of subcomponents referring to secondary protein structures with 2nd derivative or Fourier self deconvolution (FSD) analysis. For example, this has been used in membrane protein analysis (Stuart 2004) and feed evaluation (Yu 2005c, 2008).

Table 1.2 Brief summary of typical IR spectral bands of biological compounds.

Item	Wavenumber(cm^{-1})	Peak assignment	Reference (s)
Amide I	1650	80% C=O stretching, 10% C–N stretching and 10% N–H bending	Jackson and Mantsch 1991; Stuart 2004
Amide II	1565	40% C-N stretching associated with 60% N-H deformation	Wetzel 1993; Stuart 2004
Lignin	1510	aromatic ring stretching;	Himmelsbach et al. 1998; Wetzel et al. 1998a; Yu 2005b
Cellulosic compound	1246	C-O stretching	Wetzel et al. 1998a; Wetzel and LeVine 2001; Stuart 2004; Yu 2004, 2005b
Carbohydrates	1200-800	C-O and C-C stretching vibrations and C-O-H deformation	Wetzel et al. 1998a; Wetzel and LeVine 2001; Stuart 2004

Carbohydrates have absorption at ca. 3000-2800 cm^{-1} due to C-H stretching. Characteristic IR bands of carbohydrates also appear at ca. 1200-800 cm^{-1}, which are caused by C-O and C-C stretching vibrations and C-O-H deformation (Stuart 2004). However, these bands may be assigned to either structural or nonstructural carbohydrates (Yu 2005b). Starch exhibits absorption bands at ca. 1025 cm^{-1} (Wetzel et al. 1998a; Wetzel and LeVine 2001). For structural CHO, cellulose is characterized at 1170–1150, 1050, 1030 cm^{-1} and hemicellulose is centered at 1732 and 1240 (Wetzel and LeVine 2001; Stuart 2004; Yu 2004, 2005b).

The characteristic lignin absorbance is represented at ca. 1590 and 1510 cm^{-1}, in which the aromatic character can be detected (Himmelsbach et al. 1998; Yu 2005b). The amide I band and lignin band were found overlapped in the pericarp of corn (Yu 2005b). The IR spectra of lipid gives absorption bands at ca. 3000-2800 cm^{-1} due to the C-H stretching. The band at ca. 1745-1725 cm^{-1} is due to the C=O stretching. The C=C-H bending of lipid also results in a peak centered at ca. 967 cm^{-1} (Dumas et al. 2007). Carbon dioxide and H_2O also absorbs IR strongly, thus dry nitrogen is usually used to fill the sample cell (Miller and Dumas 2006).

More information referring to band assignments are detailed and summarized (Wetzel et al. 1998a; Jackson and Mantsch 2000; Wetzel and LeVine 2001; Yu 2004; Yu et al. 2004d, 2004b; Miller and Dumas 2006; Dumas et al. 2007). As previously mentioned, IR spectroscopy can display the characteristic peak patterns of chemical compounds in terms of frequency, lineshape, and intensity. Commonly, data treatments including uni- and multi-variate analyses, are conducted to characterize the sample information after the spectra collection.

1.3.2.1. Univariate spectral analysis

For the interpretation of spectra, converting the spectra to absorbance display mode provides us the opportunity to read the absorbance value and relate it to the relative content of the biopolymers of interest. Peak intensity ratio calculation and mapping analysis of certain chemical functional groups or ratios are also common methods to deal

with IR spectroscopic data (Yu 2005a, 2006a). An earlier study applied this analysis method and found that yellow- and brown-seed canola showed different characteristic peak intensities and chemical functional groups ratios, which indicated microstructure differences between canola varieties (Yu et al. 2005).

1.3.2.2. Multivariate spectral analysis

How to deal with the large and complicated data sets obtained from IR spectra is a primary question that researchers face. In spectral analyzing applications, multivariate methods are more appropriate for complex situations, including agglomerative hierarchical cluster analysis (AHCA), principal component analysis (PCA), artificial neural networks (ANN), linear discriminant analysis (LDA), and fuzzy C-means clustering (FCM) (Dumas et al. 2007).

Hierarchical cluster analysis (AHCA) and principal component analysis (PCA) are commonly applied in statistical data analysis (Jain et al. 1999). Hierarchical cluster analysis is used to sort objectives according to a defined similarity (Kaufman and Rousseeuw 1990). AHCA builds the cluster by combining the objectives according to the distance measurement. The objectives are treated and linked into larger groups by calculating criterion distance step by step. The previously established clusters are progressively merged into larger groups. Eventually, these algorithms form a hierarchical dendrogram to express the possible structure of the data (Romesburg 1984; Kaufman and Rousseeuw 1990; Gan et al. 2007). The dendrogram, appearing as a tree structure, can be generated to visibly present the results.

The PCA is also used to deal with spectral data. This method can transform the original data set into a new data set with smaller dimensions. The new data set is composed of uncorrelated variables, which are principle components (PCs). The first several PCs usually can explain greater than 95% of the total variance. Researchers can use the new data set, which is composed of fewer variables than the original data, to describe as much information as the original observation (Dunteman 1989; Davies and Fearn 2004; Miller et al. 2007).

These two statistical tools are used to reduce the number of variables and extract maximal information content from the informative spectra data. For application in feed science, these two analysis methods have been used to make comparisons between raw and heated flaxseed with amide I FSD spectral information (Yu 2006a), investigate differences in the endosperm molecular structures from wheat, corn and barley (Yu 2005b), and reveal the similarities of normal and transgenic alfalfa (Yu et al. 2009a). Cluster analysis for imaging chemical functional groups has proved powerful in corn structure examination (Yu 2005a).

1.3.3. Fourier transform infrared spectroscopy

Fourier Transform Infrared Spectroscopy (FTIR) detects the signal as a function of the difference of pathlength between the two beams generated by the Michelson interferometer. The mathematical method of Fourier Transform is to convert the symmetric interferogram into functions with frequency components to form the continuous transmittance or absorbance spectra (Stuart 2004). A typical FTIR spectrometer device usually consists of thermal (globar) light source, Michelson interferometer, detector, and computer. The MCT detector is commonly used in FTIR spectroscopy (Stuart 2004). In comparison with conventional dispersive spectroscopy, FTIR spectroscopy exhibits more effective and powerful properties as it has excellent sensitivity, larger optical throughput, and good signal to noise (S/N) ratio. The entire IR region can be detected simultaneously with the FTIR technique. With the faster scan speed, FTIR spectroscopy can produce spectra in less than 2 minutes. It is thereby possible to spend a short time scanning the entire IR region (Stuart 2004). In summary, FTIR methods enable us to apply broadband IR radiation on the sample simultaneously and with multi-scans, high quality spectra can be produced in a short time.

1.3.3.1. Diffuse reflectance Fourier transform infrared spectroscopy

If IR radiation strikes the uneven surface of a solid sample, two kinds of light reflection are generated: specular reflection with the same incidence and reflectance angles, and diffuse reflection, which results in scattered reflectance. When coarse sample is exposed

to IR radiation, the light may be reflected in all directions. Using Diffuse Reflectance Fourier Transform Infrared Spectroscopy (DRIFT), the diffusely reflected energy can be collected and a spectrum produced that is related to the sample chemical composition (Griffiths and De Haseth 1986; Stuart 2004). Diffuse reflectance technique is usually utilized on samples that are powdered, or with irregular surfaces, or on non-transparent samples (Stuart 2004). Therefore, DRIFT spectroscopy is particularly suitable for the examination of feed samples. DRIFT spectroscopy is capable of investigating ground feedstuffs for spectral analysis to reveal structural and chemical differences.

1.3.3.2. Synchrotron-based FTIR microspectroscopy

1.3.3.2.1. Synchrotron

A synchrotron is a particle accelerator using electric fields to speed up electrons and magnetic fields to adjust the direction of the travelling particles in a circular track (Dumas et al. 2007). A synchrotron is composed of six main components, including electron gun, linear accelerator (LINAC), booster ring, storage ring, beamline and experimental station. Electrons, generated from the electron gun, are accelerated in the linear accelerator and booster ring, a circular accelerator. The high-energy electrons are then transmitted into the storage ring (circular vacuum environment), in which they travel at a speed up to 99% of light. A series of magnetic fields transfer the electrons into circular paths. When the track is bent, the high speed electrons emit radiation beam tangentially from the orbit. Synchrotron radiation covers the full region of the spectrum from X-ray, ultraviolet, visible light, to IR. The radiation is transported through the beamline to the experimental stations where the light is available for study (Dumas and Miller 2003; Dumas et al. 2007).

In 1947, synchrotron radiation was accidentally discovered in the USA from high-energy physics application. Today, FTIR microspectroscopy coupled with synchrotron radiation is widely used in biological applications, making it possible to get the visible image and spectral information together, to characterize the microscopic sample area at the cellular or subcellular levels (Marinkovic and Chance 2005; Messerschmidt and Harthcock 1988).

1.3.3.2.2. Advantage of synchrotron light

Conventional thermal (globar) light source has limitations when examination is performed within the cellular dimension (5-30 μm) due to the limitation from the wavelength of IR light and the aperture size of the instrument (Raab and Martin 2001; Marinkovic et al. 2002; Miller and Dumas 2006; Miller et al. 2007). This drawback in terms of diffraction and poor S/N ratio can be overcome by the use of an advanced light source.

Synchrotron light has led to a further development of IR techniques. The synchrotron beam is preferred as the light source in terms of high brightness, continuous bands of spectrum, less signal loss and ultra-spatial resolution, which result from its highly illuminated, well collimated and non-divergent characteristics (Wetzel et al. 1998b; Dumas and Miller 2003). The brightness and effective source size of synchrotron radiation makes it possible to explore the molecular chemistry within cellular dimension of a biological tissue. Synchrotron light source reduces the influence of diffraction and assists researchers to gain high quality spectra with ultra-spatial resolution (3 to 10 μm) on the microscopic area.

1.3.4. Biological application of Mid-IR spectroscopy and recent progress in feed science

Specimens from plant tissue are mixtures of lignin, various CHO, proteins and other biological components. To overcome the difficulties that traditional methods cannot provide with regard to spatial information of the sample, new approaches to detect structural make-up are required. Biological application of Mid-IR spectroscopic techniques can be traced back to the middle period of last century (Dumas et al. 2007). A number of biological investigations were conducted using IR spectroscopy. In the past decade, the use of IR spectroscopy in biology has brought applications to feed science as well.

1.3.4.1. Application of FTIR techniques

There is a broad range of scientific fields that apply FTIR techniques in research for qualitative and quantitative analyses. FTIR spectroscopy is a powerful analytical tool to estimate the chemical composition in conjunction with additional structural information. From paints to pharmaceutical materials and food samples, numerous organic and inorganic materials can be identified and characterized using FTIR spectroscopy (Stuart 2004).

It has been recognized that compositional and structural differences are responsible for the spectroscopic differences. The peak intensity, shape and pattern differences can be detected to reveal structural and chemical characteristics of tissue histopathology. For example, spectroscopic *in situ* analysis has been documented to compare white and gray matter in the rat brain. Peak position and intensity changes were found in diseased brain tissue of mice (Levine and Wetzel 1993; LeVine and Wetzel 1994). Spectroscopic information also revealed the existence of oxidative products in brain tissue of humans with multiple sclerosis (LeVine and Wetzel 1998). Additionally, there have been reports on disease diagnosis and microorganism characterization using FTIR spectroscopy (LeVine et al. 1999; Stuart 2004). This technique was also applied to secondary structure of protein in amyloid plaques and D_2O effects on chemical functional groups in the brain (Wetzel 1998; Wetzel et al. 1998c). Another application was the examination of pathological and normal retina (Homan et al. 2000). The nucleic acids, DNA and RNA, have also been studied using FTIR spectroscopy (Stuart 2004).

1.3.4.2. Application of FTIR microspectroscopy

Integration of the IR microscope and spectrometer as an associated instrument allows us to focus on a particular micro area of biological tissue. FTIR microspectroscopy provides us opportunities for the investigation of localized chemical compounds of plant cells which require no or minimal modification. This technique offers a solution to the problem that chemical agents may destroy the intact structure of sample. Wetzel described that his group first applied FTIR microspectroscopy to investigate wheat

kernels (Wetzel and LeVine 2001). This was an early attempt accomplished with conventional (thermal) FTIR spectrometer. FTIR Microspectroscopy has also been used to investigate other plant tissues, including wheat aleurone cells, primary root cells, rye, corn, oats, and soybean, which have been reviewed previously (Wetzel et al. 1998a). However, conventional FTIR spectroscopy is restricted to exploring microstructure, owing to the properties of conventional light source.

1.3.4.3. Application of synchrotron-based FTIR microspectroscopy (SFTIRM)

In order to expand the ability of FTIR microspectroscopy techniques, synchrotron radiation was developed to overcome the disadvantage of conventional (thermal) light source. Synchrotron radiation has made it possible to reveal the features and distribution of localized chemical compounds. Ideal brightness and the excellent S/N ratio are of particular importance to obtain the spectroscopic information on chemical constituents without the destruction of sample.

Presently, the interdisciplinary application of synchrotron radiation has integrated various sciences. In 1993, a FTIR microspectrometer instrument was equipped with the synchrotron radiation at the National Synchrotron Light Source (NSLS) (Wetzel et al. 1998a). Thereafter many experiments have been conducted to characterize and localize the distribution of chemical compounds within cellular and subcellular dimensions. For example, SFTIRM has served as a powerful tool to investigate single mouse hybridoma B cell, human hair and skin at ultraspatial resolusion (Dumas and Miller 2003; Miller and Dumas 2006; Dumas et al. 2007) and provide data in cancer diagnosis (Dumas et al. 2007) and protein folding research (Marinkovic et al. 2002). The SFTIRM has also been used to probe the biological specimen of plant tissues. A diversity of plants (wheat, barley, soybeans, rye, oats and corn) have been sectioned for FTIR microspectroscopic examination and characterization. Differences in chemical and structural composition from various tissues, including kernel, root, and vascular bundle sheath, have been identified (Wetzel et al. 1998a; Pietrzak and Miller 2005).

The SFTIRM technique is applied in feed science to gradually expand knowledge of crop quality and value of feed. In practice, chemical functional group imaging (or mapping) can graphically reveal the chemical and structural information of specimens by examining the sample in a defined rectangle using SFTIRM techniques. The AHCA and PCA have also been used on SFTIRM spectral data analysis to examine and distinguish different structures. For instance, chemical functional groups, which are associated with nutrients of plant tissue from wheat, barley, corn, canola, and flaxseed have been detected (Yu 2006a; Yu et al. 2004b; 2005; 2007). Ultra-structural studies suggested that SFTIRM can successfully image the structural and chemical features and distribution of barley grain (Yu 2007c; Yu et al. 2004d). The yellow- and brown-seeded *Brassica* rape were also examined using SFTIR technique to reveal the inherent chemical composition (Yu 2004). Barley variety for feed purpose (Valier) and malting purpose (Harrington) were differentiated in the make-up of endosperm tissue (Yu 2004).

Protein secondary structure is difficult to detect due to the complexity and variation of conformation involving α-helices, β-sheets and turns (Nelson and Cox 2005). In previous work, barley varieties have been characterized using SFTIRM to reveal the molecular structure of barley protein (Yu 2007a). The results indicated that large differences in protein structure among barley varieties were detected and with the application of PCA analysis, some varieties could be distinguished with the SFTIR spectral data. The seed protein structure of wheat, feather, winterfat, oats and barley were also examined (Yu 2005c, 2006b, 2007a, 2007b; Yu et al. 2009a). High β-sheets content were detected in feather meal partially accounting for its lower digestibility using multi-component modelling (Yu 2004; Yu et al. 2004c; Yu 2006a). Golden and brown flaxseeds were distinguished by analyzing the amide I FSD spectra and heat treatment was found to have impact on the protein secondary structure of flaxseed tissue (Yu 2006a, 2007b, 2008). A recent study to estimate the quality of alfalfa in terms of protein molecular structure using SFTIR microspectroscopy in conjunction with Gaussian and Lorentzian methods of multi-component peak modeling was conducted (Yu et al. 2009b).

Synchrotron-based FTIR microspectroscopy is capable of exploring the chemical make-up and structural features simultaneously within intact biological tissues at ultra-spatial resolution (3 to 10 μm), therefore, this technique is extremely powerful when dealing with heterogeneous biological specimens. This technique allows us to extend information at a desired cellular or subcellular level and localize the chemical information to the structure of heterogeneous samples.

The above biological applications of FTIR spectroscopy provide evidence as to the potential and power of this technique. Moreover, fluorescence-assisted IR microspectroscopy, near-IR (NIR) spectroscopy, X-ray, Raman and other spectroscopic techniques are also used to examine plant tissues (Wetzel and LeVine 2001; Dumas and Miller 2003; Stuart 2004; Miller and Dumas 2006).

1.4. Conclusions and research hypothesis

Various barley varieties have been developed for feed purpose. They exhibit different rumen degradation characteristics and nutrient availabilities for ruminants although they have similar chemical composition. The differences between barley varieties in biodegradation kinetics and features may be related to their inherent structure and biological component matrix. Therefore, a deeper understanding of the structural and chemical differences among barley varieties is required. Since traditional chemical analysis is limited to reveal the structural and chemical make-up differences of barley, it is needed to develop a complementary method to differentiate barley varieties and evaluate their nutrient values.

The FTIR spectroscopy is sensitive to structural and chemical differences and can therefore be used to identify and discriminate biological materials. Spectroscopic parameters such as wavenumber, intensity and band shape can be used to reflect the chemical constituents and structural information of the sample. Infrared region 1800 to 800 cm^{-1} can be regarded as the fingerprint region for identification, since molecules have their unique absorption patterns in this region. FTIR techniques have a high scan speed, shorter sampling time and good S/N ratio. Associated with PCA and AHCA analysis, it is

possible to effectively deal with a large body of data and interpret maximum information from IR spectra.

Furthermore, with the use of superior synchrotron light source, it is capable to extend our knowledge at cellular or molecular scale of biological materials. Compared to the conventional thermal (globar) source, synchrotron light source is particularly advantageous because of the excellent spatial resolution, brightness, and S/N ratio (without the thermal noise). Therefore, ultra-spatially resolved synchrotron light sourced FTIR microspectroscopy can provide more complementary information referring to the structural and chemical conformation of the barley.

In conclusion, the adoption of IR spectroscopy techniques such as DRIFT and SFTIR techniques for investigating the structural and chemical information of feeds with complex biological tissues may provide advantages such as rapidity, efficiency and specificity over traditional chemical analysis. The hypothesis of this study were to determine if: 1) the *in situ* rumen degradation kinetics of barley varieties are related to particle size and structural and chemical make-up differences among barley varieties; 2) the structural differences among barley varieties can be detected using DRIFT and SFTIRM techniques; 3) these structural characteristics are related to nutrient availability of barley in ruminants.

2. PARTICLE SIZE, CHEMICAL PROFILE AND *IN SITU* RUMEN DEGRADATION KINETICS OF DRY MATTER, CRUDE PROTEIN AND STARCH AMONG SIX BARLEY VARIETIES: EVALUATION AND CORRELATION

2.1. Introduction

Barley is widely used as an ingredient for animal feeding in North America. Canada contributed to world barley production with 11.8 million metric tonnes and ranked second in the world in 2007 (FAO 2007). Saskatchewan produced 4,273,000 out of a total of 10,580,000 tonnes of barley production in western Canada for the 1999-2008 annual average (Langrell et al. 2008). Various barley cultivars have been developed for different purposes. Published results about barley digestibility for ruminants show that there is a great deal of variation in the nutrient value among barley varieties. Barley varieties exhibit different rumen degradation characteristics and nutrient availabilities even though their chemical composition may be similar (Khorasani et al. 2000; Yu et al. 2003).

It has been documented that particle size negatively influences the rumen degradation rate (Nocek and Tamminga 1991). Feeds with smaller particle size have relatively greater surface area which can be accessed by rumen microbes and enzymes. This may result in a faster digestion rate. Excessive ruminal fermentation may lead to an undesired rumen pH drop. Since low rumen pH results from faster degradation of concentrates and can cause metabolic disorders, more attention should be paid to the evaluation of processing methods (Ørskov 1986). Appropriate particle size of feed is required for ruminants since it improves nutrient availability and reduces the risk of digestive disorders. This benefits both the rumen microorganisms and the host animal.

The objectives of this study were: 1) to detect the difference of mean and median particle size of six barley varieties grown in Western Canada; 2) to determine the nutrients (DM, CP and ST) contents and degradation kinetics of six barley varieties using *in situ*

technique; 3) to detect relationship between the mean and median particle size and nutrient degradability and availability.

2.2. Materials and methods

2.2.1. Barley varieties and processing method

Six barley varieties were used in this study, including AC Metcalfe (malting purpose), CDC Dolly (feed purpose), McLeod (feed purpose), CDC Helgason (feed purpose), CDC Trey (feed purpose), CDC Cowboy (feed and forage purpose). All are two-row hulled spring barley varieties. AC Metcalfe has higher yield, larger and plumper seeds than Harrington. CDC Dolly is widely grown in Canada for its high test weight and plumpness. McLeod is developed with good yield and higher test and kernel weight than Harrington. CDC Helgason has similar plumpness, but higher yield and test weight compared to CDC Dolly. CDC Trey is suitable for growing in the eastern Canada Prairies with large and plump seeds. CDC Cowboy has high biomass but somewhat lower grain yield. (B. G. Rossnagel, personal communication 2009; Rossnagel and Harvey 1994; Legge 2003).

The year of the barley grain harvest was 2005. The climate conditions during the year were 17.5°C mean maximum daily temperatures and 455 mm rainfall. Barley samples were obtained from the Crop Development Center (CDC), University of Saskatchewan. All barley varieties were grown without irrigation at the Kernen Crop Research Farm, University of Saskatchewan, Canada, following standard agronomic production practices for barley production. The barley samples were coarsely dry rolled using a 130-teeth roller mill (Sven products, Apollo Machine and products Ltd. Saskatoon, Canada) through 1.59 mm gap with 384 rpm.

2.2.2. Particle size analysis

The particle size data for 2005 year barley samples were reported by Du (2009). Particle size analysis was performed using Pond's Model: $R = 100 \times e^{-k(s-w)}$, where, R = percentage cumulative weight oversize; s = sieve opening size (mm) (six test sieves,

aperture size: 3.36, 2.36, 1.70, 1.19, 0.84, and 0.58 mm); w = the smallest predictable particle size; k = the decay constant of the exponential curve describes the proportionality constant between the percent of particles passed to the next sieve and the percent remained. More details were summarized in Du (2009).

2.2.3. Animal work

2.2.3.1. Animals and diets

Three mature Holstein dry cows were used to measure rumen degradation characteristics. The cows were ruminally cannulated (Bar Diamond Inc., Parma, ID, USA) (internal diameter 10 cm). During the *in situ* experiment period, the cows were housed in pens of approximately 5 m× 5 m. The cows were individually fed twice per day at 0800 and 1600, with 15 kg (7.5 kg at each feeding time) of a total mixed ration consisting of 75% barley silage and 25% pelleted concentrate (as fed). Access to water was *ad libitum*. The care, maintenance and surgical techniques of the animals used in this experiment were carried out according to the guidelines of the Canadian Council on Animal Care (1993).

2.2.3.2. Rumen incubation

The *in situ* technique was used to determine the rumen degradability of the six barley varieties. Seven gram samples were weighed into each coded nylon bags (10 cm×17 cm, ScreenTech Corp, Mississauga ON), then incubated in the rumen for 0, 2, 4, 8, 12, 24 and 48 h according to the “gradual addition/all out” schedule (Yu et al. 2003). The pore size of nylon bag was approximately 40 μm. Sample weight to bag area ratio was approximately 41 mg/cm^2. After incubation, the bags were removed from the rumen and rinsed in cold water without detergent to remove excess ruminal contents. The 0-h incubation samples were washed with the same procedure. Subsequently, all sample bags were dried at 55°C for 48 h. Dry samples were stored at 4 °C until analysis (Yu et al. 2003).

2.2.4. Chemical analysis

Dry matter was determined by drying at 105°C until the sample weight was constant according to the procedure of Association of Official Analytical Chemists (AOAC) Official Method 930.15 (1997). Protein was analyzed by using the LECO FP-528 (LECO Corporation, 3000 Lakeview Ave. St. Joseph, MI, USA) according to the procedure of AOAC Official Method 990.03 (1997). Starch was measured with Megazyme Total Starch Assay Kit (Megazyme international Ireland Ltd., Co. Wicklow, IE) according to the procedure of AOAC Official Method 996.11 (1997).

2.2.5. Rumen degradation kinetics

The first order kinetics degradation model (Ørskov and McDonald 1979) modified by Tamminga et al. (1994) was used to describe the rumen degradation characteristics of these six barley varieties as follows:

DM and CP: $R(t) = U + (100 - S - U) \times e^{-Kd \times (t-T0)}$,

Non-structural carbohydrate -Starch: $R(t) = (100 – S) \times e^{-Kd \times t}$

Where, R(t) is residue of the incubated material after t h of rumen incubation (%), S is rapidly degradable fraction (%), D is slowly degradable fraction (%), U is undegradable fraction, Kd is degradation rate (%/h), Kp is passage rate for concentrate (6%/h), adopted by Tamminga et al. (1994), and T0 is lag time (h).

The effective degradability (ED) values were calculated as:

EDDM (or EDCP) (%) = $S + D \times Kd/(Kp + Kd)$,

EDST (%) =100 - RUST (%) = $100 - U - D \times Kp/(Kp + Kd) = S + D \times Kd/(Kd + Kp)$,

The rumen undegraded feed DM (RUDM), protein (RUP) and starch (RUST) values were calculated as:

RUDM (or RUP) (%) = $U + D \times Kp/(Kp + Kd)$,

RUST (%) = $D \times Kp/(Kp + Kd) + 0.1 \times S$ (Tamminga et al. 1994).

The NLIN procedure of the statistical package SAS software 9.1.3 (SAS Institute, Inc., Cary, NC) (SAS 2003). with iterative least squares regression (Gauss–Newton method)

will be used to describe its degradation accurately. The NLIN program in this study was written by Dr. Yu, Peiqiang (University of Saskatchewan).

2.2.6. Statistical analysis

Statistical analyses were performed using the MIXED procedure of SAS 9.1.3 software (SAS Institute, Inc., Cary, NC). The model used for the analysis was: $Y_{ijk} = \mu + F_i + S_j + e_{ijk}$, where, Y_{ijk} was an observation of the dependent variable ijk; μ was the population mean for the variable; F_i was the effect of barley varieties, a fixed effect; S_j was the replicate effect, a random effect; and e_{ijk} was the random error associated with the observation ijk. Fisher's protected LSD test ($P < 0.05$) was applied to compare treatment means. Proc Corr procedure of SAS package was conducted to examine the correlation between particle size data and degradation characteristics.

2.3. Results and discussion

2.3.1. Comparison of mean and median particle size of coarsely dry-rolled barley grains among six barley varieties

The mean and median particle size parameters of six barley varieties are given in Table 2.1. AC Metcalfe and CDC Trey had the smallest ($P<0.05$) mean (2.82 mm and 2.93 mm, respectively) and median (2.45 mm and 2.55 mm, respectively) particle size among the six varieties. In contrast, CDC Helgason and CDC Dolly had larger ($P<0.05$) particle sizes (means: 3.09 mm and 3.09 mm; medians: 2.75 mm and 2.74 mm, respectively). Although CDC Trey is a barley variety for feed purpose, it was similar in particle size to AC Metcalfe, a barley variety for malting purpose.

Table 2.1 Particle size comparison of six barley varieties

	Barley variety[z]							
Items	AC Metcalfe	CDC Dolly	McLeod	CDC Helgason	CDC Trey	CDC Cowboy	SEM[y]	P value
Particle sizes								
Mean (mm)	2.82 c	3.09 a	3.06 ab	3.09 a	2.93 bc	3.05 ab	0.044	0.0056
Median (mm)	2.45 c	2.74 a	2.66 ab	2.75 a	2.55 bc	2.61 ab	0.048	0.0057

[z] All six varieties of barley were grown at the Kernen Crop Research Farm (University of Saskatchewan, Saskatoon, Canada) and were managed using the same and standard agronomic production practices for all barley production (Crop Development Center).

[y] SEM= standard error of mean. Means with the different letter in the same row are significantly different ($P<0.05$). Mean separation was done by using the Fisher's protected LSD test method.

Cereal processing can modify particle size of a feedstuff, which may influence particle passage rate and degradation rate and consequently, the entire digestion process (Nocek and Tamminga 1991). Larger particle size enhances palatability (Theurer 1986; Church 1991; Kellems and Church 2002). Additionally, the larger particle size may somewhat reduce problems arising from the fast ruminal degradation (Ørskov 1986). As previously reported, differences in particle size was related to the ADF content in grain (Bowman et al. 2001). More research is needed to address the problem of how the chemical and structural composition affect the particle size parameters, and subsequently to understand how chemical conformation influence nutrient digestibility.

2.3.2. Evaluation of chemical profile and *in situ* rumen degradation kinetics of dry matter (DM), crude protein (CP) and starch (ST) among six barley varieties

The degradation kinetics of six barley varieties were determined using the modified Ørskov model (Tamminga et al. 1990; Tamminga et al. 1994). The results are presented in Table 2.2. DM content (%) was similar among the six barley varieties. There were significant differences in DM degradation features among these six barley varieties. The results showed that the barley varieties differed in all degradation characteristics (S, D, U, RUDM and EDDM) except for T0. The S differed ($P<0.01$) from 0.2% (CDC Helgason) to 1.2% (CDC Trey), indicating that CDC Trey, a barley variety for feed purpose, contains higher soluble nutrients. Additionally, the D fraction differed in that CDC Dolly had the lowest ($P<0.05$) D fraction (69.1%) while AC Metcalfe, CDC Trey and CDC Cowboy had the highest D fractions (77.0, 79.0 and 77.6%, respectively). It also showed that these six varieties had similar ($P>0.05$) T0. There were marked differences ($P<0.01$) in Kd and extent (EDDM) ($P<0.01$) among the barley varieties. In comparison with other barley varieties, the Kd of CDC Helgason was lowest (5.62 %/h) ($P<0.01$), followed by CDC Dolly, of which the Kd was 7.84 %/h. The remaining four barley varieties showed relatively faster Kd (10.04 %/h for AC Metcalfe, 9.72 %/h for CDC Trey, 9.63 %/h for McLeod and 8.29 %/h for CDC Cowboy).

Table 2.2 Comparison of six barley varieties: chemical profile and *in situ* rumen degradation kinetics of dry matter (DM).

	Barley variety[z]							
Items	AC Metcalfe	CDC Dolly	McLeod	CDC Helgason	CDC Trey	CDC Cowboy	SEM[y]	P value
In situ rumen degradation kinetics of DM[x]								
Dry matter (DM, %)	91.89	91.78	91.76	91.96	91.94	91.82	-	-
S (%)	0.81 ab	0.39 cd	0.62 bc	0.20 d	1.16 a	0.63 bc	0.146	0.0065
D (%)	76.99 ab	69.05 d	72.10 cd	74.44 bc	79.03 a	77.55 ab	1.512	0.0049
U (%)	22.20 cd	30.56 a	27.28 ab	25.36 bc	19.80 d	21.81 cd	1.576	0.0040
T0 (h)	0.91	1.34	1.00	0.90	0.95	1.04	0.199	0.6555
Kd (%/h)	10.04 a	7.84 b	9.63 ab	5.62 c	9.72 a	8.29 ab	0.671	0.0025
RUDM (g/kg DM)	513.4 d	605.1 b	550.0 c	640.2 a	502.0 d	545.4 c	9.99	<0.0001
EDDM (g/kg DM)	486.7 a	394.9 c	450.0 b	359.8 d	498.0 a	454.6 b	9.99	<0.0001

[z] All six varieties of barley were grown at the Kernen Crop Research Farm (University of Saskatchewan, Saskatoon, Canada) and were managed using the same and standard agronomic production practices for all barley production (Crop Development Center).

[y] SEM= standard error of mean. Means with the different letter in the same row are significantly different (P<0.05). Mean separation was done by using the Fisher's protected LSD test method.

[x] S= rapidly degradable fraction; D= potentially degradable fraction; U= undegradable fraction; Kd = degradation rate; RUDM= rumen undegradable DM; EDDM= effective degradability of DM.

CDC Trey and AC Metcalfe were the highest (P<0.01) in EDDM (498 and 487 g/kg base on DM, respectively). In contrast, CDC Helgason was the lowest in EDDM (360 g/kg base on DM). CDC Helgason had the largest RUDM (640 g/kg DM), whereas the CDC Trey and AC Metcalfe exhibited the smallest RUDM (502 and 513 g/kg base on DM, respectively). These results indicated that the six barley varieties had different ruminal degradation characteristics. Earlier research indicated that the ruminal DM digestibility of barley grain that has been dry rolled varies between 82-621 g/kg (Bowman et al. 2001). A slower degradation rate could result in more bypass nutrients to the host animal and reduce the risk of digestive disorders (Khorasani et al. 2000). Therefore, CDC Helgason, with the slowest degradation rate and smallest EDDM, may supply relatively more nutrients into the small intestine of ruminants. In contrast, other varieties may have more DM digested in the rumen prior to entering the small intestine. In particular, the degradation behaviour of CDC Trey exhibited similar degradation kinetics (S, D, U, Kd, RUDM, EDDM) of DM with AC Metcalfe, implying that it may not be ideal for feed purpose. Additionally, AC Metcalfe and CDC Trey, the two varieties with the smallest mean and median particle size, had the highest Kd and EDDM, suggesting a relationship between degradation kinetics and particle size.

The *in situ* CP degradation results are given in Table 2.3. Protein content varied in the range of 12.4-14.4%, which is consistent with earlier findings (Khorasani et al. 2000; Holtekjøen et al. 2006). AC Metcalfe had the greatest (P<0.05) S protein fraction (3.7%). The other five varieties ranged from 0.7 to 2.4%. CDC Dolly and McLeod had relatively smaller (P<0.05) D fraction (73.4 and 78.1%, respectively). CDC Dolly and McLeod had a relatively greater (P<0.05) U fraction (24.7 and 21.7%, respectively). T0 for AC Metcalfe and CDC Dolly were 0.84 and 1.76 h, respectively. Others were intermediate, ranging from 1.27 to 1.49 h. Slower (P=0.056) Kd of CP was found on CDC Helgason (4.55 %/h). The degradation rate of CDC Trey was 6.95 %/h, which was numerically the highest among the six barley varieties.

Table 2.3 Chemical profile and *in situ* rumen degradation kinetics of crude protein (CP): Comparison of six barley varieties.

	Barley variety[z]							
Items	AC Metcalfe	CDC Dolly	McLeod	CDC Helgason	CDC Trey	CDC Cowboy	SEM[y]	P value
In situ rumen degradation kinetics of CP [x]								
Crude protein (CP, %DM)	14.11	13.08	13.36	13.19	12.35	14.39	-	-
S (%CP)	3.73 a	1.97 b	0.76 c	2.11 b	0.71 c	2.40 b	0.360	0.0002
D (%CP)	78.38 abc	73.35 c	78.05 bc	79.89 ab	83.76 a	81.45 ab	2.194	0.0270
U (%CP)	17.89 b	24.68 a	21.19 ab	18.00 b	15.54 b	16.14 b	2.102	0.0400
T0 (h)	0.84 b	1.76 a	1.27 ab	1.47a b	1.49a b	1.40a b	0.283	0.3705
Kd (%/h)	6.72 a	6.18 ab	6.99 a	4.55 b	6.95 a	5.73 ab	0.551	0.0560
RUP (%CP)	55.31 c	60.96 ab	57.44 bc	63.59 a	54.70 c	57.83 bc	1.250	0.0022
RUP (g/kg DM, DVE[w])	86.6 bc	88.5 abc	85.2 c	93.1 a	75.0 d	92.4 ab	1.88	0.0002
RUP (g/kg DM, NRC[v])	78.0 bc	79.7 abc	76.7 c	83.9 a	67.5 d	83.2 ab	1.69	0.0002
EDCP (%CP)	44.69 a	39.04 bc	42.56 ab	36.41 c	45.30 a	42.17 ab	1.250	0.0022
EDCP (g/kg DM)	63.1 a	51.1 cd	56.9 b	48.0 d	55.9 bc	60.7 ab	1.69	0.0003

[z] All six varieties of barley were grown at the Kernen Crop Research Farm (University of Saskatchewan, Saskatoon, Canada) and were managed using the same and standard agronomic production practices for all barley production (Crop Development Center).

[y] SEM= standard error of mean. Means with the different letter in the same row are significantly different (P<0.05). Mean separation was done by using the Fisher's protected LSD test method.

[x] S= rapidly degradable fraction; D= potentially degradable fraction; U= undegradable fraction; Kd = degradation rate; RUP = rumen undegradable CP; EDCP = effective degradability of CP.

[w] RUP was estimated using the DVE/OEB system (Tamminga et al. 1994).

[v] RUP was estimated using the NRC 2001 model (NRC 2001).

In comparison with the other four varieties, CDC Helgason (63.6%) and CDC Dolly (61.0%) had a higher ($P<0.05$) percentage of rumen undegradable CP (RUP %). Compared with the other barley varieties, CDC Trey showed the lowest ($P<0.01$) RUP (g/kg DM) calculated from the two models (75 g/kg DM from DVE/OEB model and 68 g/kg DM from NRC 2001 model, respectively). The results showed that both the NRC 2001 model and the DVE/OEB model could be used to detect the difference of RUP among the six barley varieties. CDC Helgason and CDC Dolly had lower ($P<0.01$) percentage of EDCP (36.4 and 39.0%, respectively). Others ranged from 42.2 to 45.3%. The EDCP (g/kg DM) of these two varieties were lower than others as well (48 and 51 g/kg DM, respectively), while AC Metcalfe and CDC Cowboy were higher (63 and 61 g/kg DM, respectively). Comparing with other earlier study, the results appeared higher in EDCP than that of steam-rolled barley (Yang et al. 1997). It is conclusive that protein digestibility of different barley varieties differed significantly in the rumen. CDC Helgason may be less extensively fermented in the rumen compared to the other five barley varieties.

The *in situ* starch results (Table 2.4) show that the starch percentage of CDC Dolly (58.6%) compared closely with a previous study of Holtekjøen et al. (2006), but CDC Helgason was lower (56.4%). More variable results of barley varieties were reported earlier (Herrera-Saldana et al. 1990; Khorasani et al. 2000). Previous work indicated that type and amount of polysaccharides impact starch digestibility (Nocek and Tamminga 1991). In this study, the Dutch model (Tamminga et al. 1994) was used to assess the degradation of starch. The results indicate that the starch rate and extent of degradation of six barley varieties were significantly different, though they had similar D fractions ($P>0.05$). CDC Helgason had the lowest ($P<0.05$) Kd (3.67%/h), which indicates that the starch release of CDC Helgason was markedly slower than that of the other five barley varieties in the rumen. In contrast, CDC Trey had the highest Kd of starch (7.11%/h). The degradation rate of the remaining four varied from 4.24 to 7.05%/h, lower than the previous data obtained from steam-rolled barley (Foley et al. 2006) likely because of different processing methods. It has been interpreted that barley starch can be degraded extensively in the rumen (Waldo 1973). However in the small intestine, starch may be

utilized to generate more energy (Bowman et al. 2001) by reducing methane production. There were significant differences observed for the percentage of RUST as well. CDC Helgason revealed the highest ($P<0.01$) percentage of RUST (61.0%). In addition, for RUST (g/kg DM), CDC Helgason and CDC Dolly were relatively higher (344 and 342 g/kg DM, respectively). Differences between varieties were particularly apparent when their EDST were compared. AC Metcalfe and CDC Trey showed higher ($P<0.05$) EDST percentage (55.0 and 54.3%, respectively) compared with other barley varieties, whereas CDC Helgason was the smallest (39.0%). AC Metcalfe showed the highest ($P<0.05$) EDST (322 g/kg DM), comparing with the relatively smaller CDC Helgason (220 g/kg, DM) and McLeod (228 g/kg DM). The others are intermediate. This is also evidence that their ruminal degradation characteristics varied between varieties.

This use of the *in situ* technique to determine the ruminal degradability of barley grain indicated that these six barley varieties exhibited different digestion kinetics characteristics, even though they were grown and processed under the same conditions. This is consistent with the previously published results (Hart et al. 2008; Du et al. 2009). Although the barley digestibility for ruminants has been studied extensively, the ruminal degradation kinetics parameters reported in this study are not very comparable with other reports due to the variation of sample pre-treatment, laboratory conditions and analysis methodologies (Yang et al. 1997; Khorasani et al. 2000; Bowman et al. 2001; Yu et al. 2003; Hindle et al. 2005; Foley et al. 2006; Miller et al. 2007; Du et al. 2009).

Compared with the other five barley varieties, the degradation characteristics of CDC Helgason, in terms of the degradation rate and extent, are extremely attractive. CDC Helgason had the largest rumen undegradable fraction of DM (640 g/kg DM), CP (84 g/kg DM, NRC) and starch (344 g/kg DM) and lowest degradation rate of DM (5.62%/h), CP (4.55%/h) and starch (3.67%/h), respectively. The relatively lower degradation rate and extent may reduce issues with rumen acidosis. These comparative advantages support a perspective that CDC Helgason may be ideal for feed purpose compared with the other five barley varieties.

Table 2.4 Chemical profile and *in situ* rumen degradation kinetics of starch (ST): Comparison of six barley varieties.

	Barley variety[z]							
Items	AC Metcalfe	CDC Dolly	McLeod	CDC Helgason	CDC Trey	CDC Cowboy	SEM[y]	P value
In situ rumen degradation kinetics of ST[x]								
Starch (ST, %DM)	58.44	58.59	48.81	56.39	55.67	54.15	-	-
S (%ST)	2.93	0.51	0.01	2.14	0.18	0.09	1.117	0.2509
D (%ST)	97.07	99.49	99.99	97.86	99.82	99.91	1.117	0.2509
Kd (%/h)	7.05 a	4.24 d	5.28 c	3.67 e	7.11 a	6.16 b	0.176	<0.0001
RUST (%ST)	44.96 e	58.33 b	53.21 c	61.01 a	45.73 e	49.31 d	0.870	<0.0001
RUST (g/kg DM)	262.7 b	341.7 a	259.7 b	344.0 a	254.6 b	267.0 b	4.91	<0.0001
EDST (%ST)	55.04 a	41.67 d	46.79 c	38.99 e	54.27 a	50.69 b	0.870	<0.0001
EDST (g/kg DM)	321.7 a	244.2 d	228.4 e	219.9 e	302.1 b	274.4 c	4.91	<0.0001

[z] All six varieties of barley were grown at the Kernen Crop Research Farm (University of Saskatchewan, Saskatoon, Canada) and were managed using the same and standard agronomic production practices for all barley production (Crop Development Center).

[y] SEM= standard error of mean. Means with the different letter in the same row are significantly different (P<0.05). Mean separation was done by using the Fisher's protected LSD test method.

[x] S= rapidly degradable fraction; D= potentially degradable fraction; U= undegradable fraction; Kd = degradation rate; RUST = rumen undegradable starch; EDST= effective degradability of starch.

An earlier study reported that few differences in chemical composition and starch degradation kinetics were found between AC Metcalfe and the mean of five feed-type barley varieties (Hart et al. 2008). However, with respect to degradation features obtained in this study, undoubtedly, AC Metcalfe, with greater soluble fraction, faster degradation rate and greater effectively degradability, showed its suitability for use in malting. The protein matrix in barley grain was assumed to play a protective role against degradation (Holopainen et al. 2005). Although AC Metcalfe appeared to have numerically higher protein content (14.1%), it is still the most ruminally degradable among the six varieties. Associated with its small particle size, different structural and chemical structure may explain this. The protein matrix of AC Metcalfe may be highly soluble and more easily dissolved in rumen fluid, which can lead to greater ruminal digestibility. In addition, the loose protein-starch conjunction within cellular dimension might imply a faster degradation rate, and result in increased nutrient availability in rumen.

AC Metcalfe, a barley variety for malting purpose, exhibited faster degradation rates of DM (10.04%/h) ($P<0.01$), CP (6.72%/h) ($P=0.056$) and starch (7.05%/h) ($P<0.01$) among the six barley varieties. However, CDC Trey, a barley variety for feed purpose, also had similar degradation features (9.72 for DM, 6.95 for CP, and 7.11%/h for starch, respectively) to AC Metcalfe. Based on these observations, CDC Trey was degraded in the rumen more like a barley variety for malting purpose. Moreover, a large portion (54.3, vs. 55.0% of AC Metcalfe) of starch of CDC Trey was effectively digested in the rumen, while only 45.7% (vs. 45.0% of AC Metcalfe) escaped from ruminal microorganism fermentation. Excessively rapid digestion of starch in the rumen may cause metabolic disorders. It can be argued that CDC Trey may not be suitable for feeding.

2.3.3. Correlation between mean and median particle sizes and degradation rate and extent of dry matter (DM), crude protein (CP) and starch (ST) among barley varieties

The rumen degradation rate and extent are of particular interest to evaluate the quality of grains. The particle size of processed barley grain may be partly responsible for the degradation behaviour (Kellems and Church 2002). In order to further address this

problem, Pearson correlation was determined between particle size parameters and degradation rate and extent (Table 2.5). Negative correlations were observed between the median particle size and effective digestibility of DM ($P<0.05$) and CP ($P<0.05$). Compared with the mean particle size, median particle size revealed relatively strong ($P<0.01$) negative correlations with degradation rate and extent of starch degradation. The median particle size can therefore be considered to be correlated with the rumen fermentation of barley grain. Kd of DM tended to be correlated with median particle size but Kd of CP did not. No significant correlations were detected between mean particle size and starch degradation features (Kd and EDST).

This leads to the conclusion that median particle size, not mean particle size, is associated with the degradation rate and extent of processed barley. These results agree with the earlier conclusion that the large particles are related to slower ruminal degradation (Nocek 1988). Additionally, the results strengthen the concept that the particle size of barley can affect digestibility. Processing destroys the protein starch matrix (Figure 2.1) which surrounds the starch granules and prevents the access of microbial enzymes. Taking the ruminal microbial community into account, smaller particle size implies larger surface area, to which microorganisms and digestive enzymes can efficiently attach. Additionally, smaller particle size may also contribute to the high passage rate. Whereas larger particles appear to need more time to be further broken down in the digestion process with a smaller accessible surface area (Theurer 1986; Nocek and Tamminga 1991; Bowman et al. 2001). There was evidence that particle size has an effect on ruminal passage rate of forage (Welch 1986; Sniffen et al. 1992). Based on related studies (Yoshimoto et al. 2000; You and Izydorczyk 2002; Tester et al. 2004), it is possible that large particle size results from the tight protein structure combining with the starch granules. A speculation was also made that CDC Helgason with larger particle size may be relatively resistant against ruminal degradation and still fermentable in lower gut. As a result, it is probably the most suitable barley variety for feed purpose for ruminants among these six varieties.

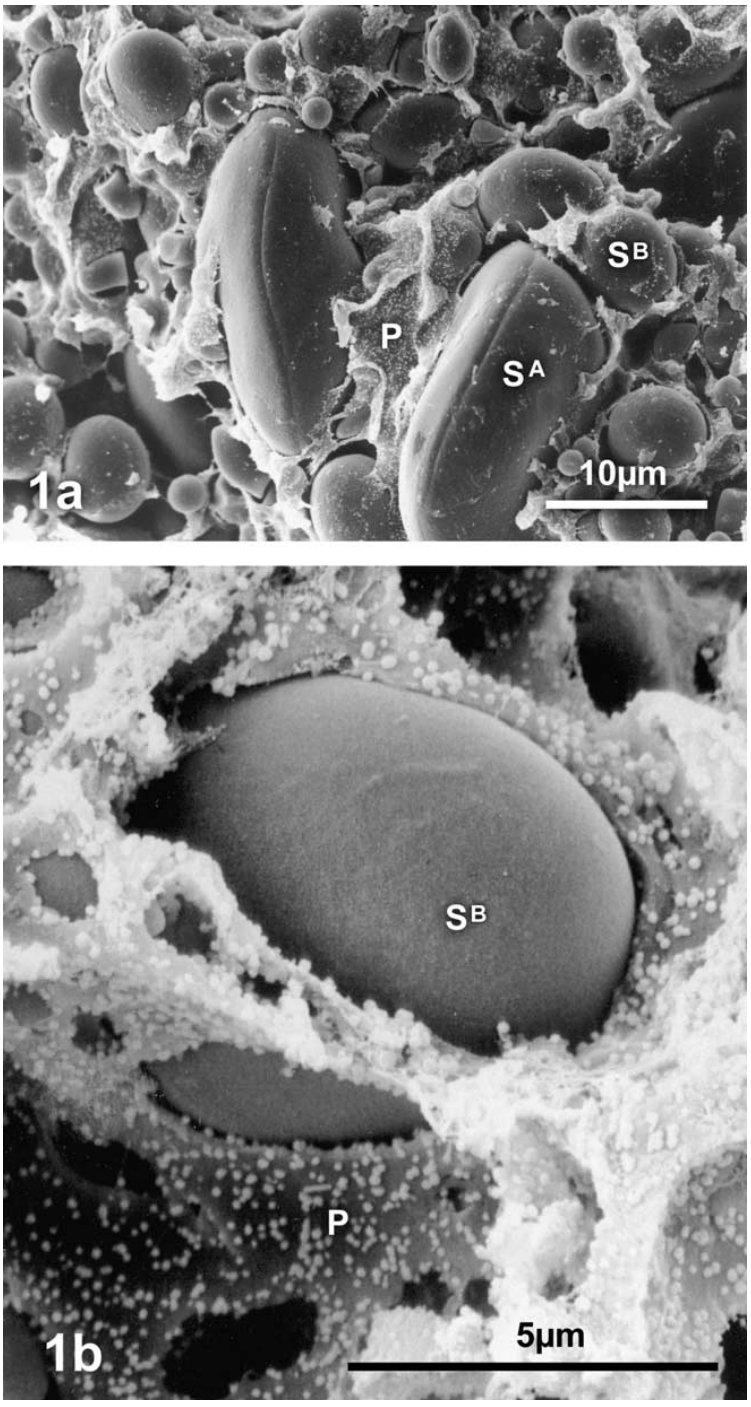

Figure 2.1 Scanning electron micrograph of mature starchy endosperm cells of wheat. (a) Tissue from the central starchy endosperm of cv Bouquet showing small (SB) and large (SA) starch granules embedded in a protein matrix (P). (b) Enlargement to show the protein matrix (P) in starchy endosperm tissue of cv Avalon. (Source: Mills et al. 2005)

Table 2.5 Pearson correlations between *in situ* rumen degradation rate and extent of dry matter (DM), crude protein (CP) and starch (ST) from six barley varieties and mean and median of particle sizes.

	Mean particle size[z]		Median particle size[z]	
Items	Correlation coefficient	P value	Correlation coefficient	P value
In situ rumen degradation kinetics of DM[y]				
Kd (%/h)	-0.774	0.071	-0.784	0.065
EDDM (%)	-0.760	0.079	-0.894	0.016
In situ rumen degradation kinetics of CP[y]				
Kd (%/h)	-0.799	0.057	-0.593	0.215
EDCP (%)	-0.784	0.065	-0.885	0.019
In situ rumen degradation kinetics of ST[y]				
Kd (%/h)	-0.686	0.133	-0.955	0.003
EDST (%)	-0.658	0.156	-0.954	0.003

[z] Mean and median particle sizes were determined by Pond's model.

[y] Kd = degradation rate; EDDM, EDCP, EDST= effective degradability of DM, CP and starch, respectively.

Regression analysis between median particle size and *in situ* degradation features of DM, CP, and starch was conducted using Proc Mixed procedure of SAS package to give a possible answer regarding the magnitude of particle size affecting the various digestion behaviours. The results are presented in Table 2.6. The results showed that the four regression models are significant ($P<0.05$). It was indicative that 79.9% effective digestibility of DM, 78.3% of CP and 91.0% of ST could be explained by median particle size, respectively.

Table 2.6 Regression analysis to predict rumen degradability using median particle size (x) with regression model as follows: Model: Y (degradability) = Median.

Predicted variables (Y)	Model: Y= a + b*x	R^2 value	RSD [z]	P value
EDDM	Y = 153.00 – 41.47 * x	0.799	2.68	0.016
EDCP	Y = 110.28 – 26.11 * x	0.783	1.77	0.019
Kd (ST)	Y = 51.04 – 15.96 * x	0.912	0.64	0.003
EDST	Y = 195.48 - 54.68 * x	0.910	2.21	0.003

[z]RSD= Residue standard deviation.

2.4. Conclusions

The results indicated that under the same growth and processing conditions (dry-rolled though 1.59 mm gap), the six barley varieties appeared to significantly differ in their digestion characteristics and mean and median particle sizes, and thus, had different nutrient supply to ruminants.

CDC Helgason is distinguished from other varieties due to its lowest degradation rate and extent of DM, CP and ST (5.62%/h, 360 g/kg for DM, 4.55%/h, 48 g/kg DM for CP, and 3.67%/h, 220 g/kg DM for starch, respectively) among the six barley varieties. Results indicate that CDC Helgason may be the desirable barley variety for feed purpose compared with the other five barley varieties.

Significant correlation was found between median particle size (not mean particle size) and the rate and extent of rumen degradation (P value was 0.016 for EDDM, 0.019 for EDCP, 0.003 for Kd of starch and 0.003 for EDST). Results indicate that the median

particle size, to a greater extent than mean particle size, can affect the degradation rate and extent of barley grain. The differences in particle size of the processed barley grains may explain the various degradation characteristics exhibited in the rumen among the six barley varieties. Associated with the nutrient availability, particle size could be an important factor to affect barley feed quality, fermentation, and nutrient availability for ruminants. Therefore, preventing inappropriate processing is of importance for the ruminant feeding industry.

With similar chemical composition, the barley varieties exhibited different degradation behaviours. More information about the biological constitution of grain must be taken into account to explain this. It is not sufficient to solve this problem with only *in situ* degradation characteristics and mean and median particle sizes. Further study is required to investigate the inherent structural and chemical make-up characteristics between the barley varieties which may provide more information as to why barley varieties exhibit different biodegradation behaviours in the rumen and lower gut.

3. USING DIFFUSE REFLECTANCE FOURIER TRANSFORM INFARED SPECTROSCOPY (DRIFT) AND SYNCHROTRON-BASED FTIR MICROSPECTROSCOPY (SFTIRM) TO CHARACTERIZE SEED INHERENT STRUCTURE AMONG SIX BARLEY VARIETIES

3.1. Introduction

The results of chapter 2 show that barley varieties exhibit different ruminal degradation rates. Knowledge of their chemical and structural differences may lead to an understanding of the reasons for these differences. Further study of the relationship of biological characteristics of barley grain in relation to spectral characteristics may provide useful understanding of how to best utilize the various varieties.

Grinding is usually required in chemical analysis. In addition, harsh chemical reagents can unavoidably destroy or even obliterate the histological structure of the sample (Wetzel and LeVine 2000, 2001). Structural and chemical information detection is beyond the capacity of traditional chemical analysis, owing to the destructive pre-treatment. These disadvantages necessitate a new and rapid tool to overcome these limitations.

As a potential analytical tool, FTIR technique is widely applied in various scientific fields. Different vibration and complex absorption modes result in different characteristic spectral features. Based on the monitored spectral signal, chemical and structural features can be revealed (Stuart 2004). FTIR technique has been applied to monitor the metabolic changes caused by D_2O in rat cerebellum tissue (Wetzel et al. 1998c). The detailed spectroscopic characterization of biological specimen has been summarized and reviewed (Jackson and Mantsch 2000; Wetzel 2000).

Conventional FTIR techniques show comparable performance to synchrotron when working with large aperture size (>20-30 μm) (Diem et al. 2004). However, it is inferior to synchrotron at ultra-spatial resolution when detecting biological or biomedical specimens (5-30 μm) (Miller et al. 2000). To overcome the weakness of conventional

(thermal) light source, synchrotron light is used because it is extremely advantageous for small aperture setting (Miller and Dumas 2006).

The induction of synchrotron radiation allows simultaneous sample viewing and IR data collection at ultra-spatial resolution. Using synchrotron source to substitute for conventional thermal (globar) source, results in the potential to improve S/N ratio (Miller 2002; Miller and Dumas 2006). The combining of microscopy with FTIR spectroscopy enables observations both visually and spectroscopically. Ultra-spatial resolved synchrotron IR microspectroscopy is used to monitor the intrinsic distribution of chemical compounds in biological and biomedical specimens. Accordingly, taking advantage of the brilliance, broadband and concentration (Miller and Dumas 2006), the application of synchrotron light associated with FTIR technique makes it possible to probe further on the inherent structure of biological materials at a cellular or sub-cellular dimension without thermal noise (Dumas and Miller 2003).

Working with the SFTIR spectroscopy, high quality mapping of sample sections can be generated. For instance, chemical functional groups associated with nutrients of plant tissue from wheat, barley, corn, canola, flaxseed have been detected using FTIR microspectroscopy in conjunction of advanced synchrotron light source (Yu 2005b; 2006a; Yu et al. 2004b; 2005; 2007; 2009a). The photomicrograph and chemical compounds (protein, lipid, lignin, structural and non-structural carbohydrates) mapping of Valier (feed type) and Harrington (malting-type) barley have been obtained using SFTIR technique (Yu 2004; Yu et al. 2004a; 2004d; 2008). The protein molecular structure of alfalfa affected by Lc-gene transformation were firstly reported using SFTIR (Yu et al. 2009b).

A diversity of biological materials have been examined using conventional (globar) or advanced (synchrotron) FTIR techniques in conjunction with powerful statistical analysis methodologies. Agglomerative hierarchical cluster analysis (AHCA) and principal components analysis (PCA) can be used to treat the tremendous amount of information relating to matrix conformation, chemical and structural make-up and compound

distribution. The AHCA can classify the objects into different clusters (groups) based on their similarity (Romesburg 1984; Kaufman and Rousseeuw 1990; Gan et al.2007). PCA can visibly present the analysis in scatter plots of principle components (PCs), of which maximal information of original data can be carried out in organized manner (Dunteman 1989; Jolliffe 2002; Yu 2006b). Previously for feed science application, AHCA and PCA analysis have been applied on discrimination of Harrington and Valier barley with their amide I FSD spectra (Yu et al. 2007). These two analysis methods have also been used to detect the differences between various tissues from wheat (Yu et al. 2007). Previous work indicated that these two multivariate spectral analysis methodologies could successfully distinguish flaxseed structure change caused by autoclaving (Doiron 2009).

These mid-IR techniques enable us to establish a correlation of spectral information to structural and chemical features of plant tissue, furthermore, to feedstuff quality. The objectives of this study were: 1) using DRIFT spectroscopy to identify the differences in functional group characteristics associated with nutrient utilization in barley hull sample and whole seed sample among the six barley varieties; 2) using synchrotron-based FTIR microspectroscopy to determine structural make-up features and identify the structural differences in chemical functional groups in endosperm tissue among the six barley varieties; 3) using multivariate spectral analyses (AHCA and PCA) to detect spectral differences among the six barley varieties; 4) to analyze correlation between *in situ* nutrients degradation (rate and extent) and chemical functional groups features determined by DRIFT and SFTIRM spectroscopy.

3.2. Materials and methods

3.2.1. Barley varieties and growth condition

The six barley varieties were the same mentioned previously in Chapter 2 (AC Metcalfe, CDC Dolly, McLeod, CDC Helgason, CDC Trey, and CDC Cowboy).

3.2.2. Sample preparation for DRIFT spectroscopy

The hull samples of six barley varieties were produced using Laboratory Dehuller (Model LH 5095, Codema Inc. Minneapdis, Minnesota) at 100 psi for 30 sec, and then screened through a 1.2 mm pore size sieve to remove fines and dusts. Hull and whole seed samples from the six barley varieties were ground through 0.25 mm screen twice with Retsch Grinder ZM100 (Brinkmann Instruments Ltd, ON, Canada) and then mixed into KBr powder with a ratio of 4: 1.

3.2.3. DRIFT Spectroscopy

Mid-IR spectra from DRIFT spectroscopy technique were collected using Bio-Rad FTS-40 (Bio-Rad, Cambridge, MA) with a globar IR source in the Saskatchewan Structural Sciences Centre (SSSC), University of Saskatchewan.

3.2.4. DRIFT data collection and processing

Win-IR software, the coupled computer system with Bio-Rad FTS-40 was used to record IR spectra. Spectra within the mid-IR region (ca. 4000-400 cm^{-1}) were collected with 256 coadded scans. Spectral resolution was set as 4 cm^{-1}. Background spectra were collected with the same measurement setting prior to formal spectra collection. Nicolet OMNIC software 7.3 (Spectra Tech, Madison, WI) was used to analyze spectral data. For normalization of the spectral information, baseline correction was applied on all spectra data. Outlier spectra, which might be due to the instrumental and environmental contributions, were eliminated prior to evaluation.

3.2.5. Sample preparation for SFTIR microspectroscopy

Five seeds of each barley variety (six varieties) were randomly selected to cut transversely across the endosperm tissue. The thin cross sections of tissues (ca. 6 μm) were unstained and immediately mounted on barium fluoride (BaF_2) discs (2 mm thick, 13 mm diameter, Spectral Systems, Hopewell Junction, NY, USA) for synchrotron FTIR microspectroscopic work in transmission mode.

3.2.6. SFTIR microspectroscopy

The experiment was performed using a Thermo Nicolet Magna 860 Step-Scan FTIR (Thermo Fisher Scientific Inc., Waltham, MA) spectrometer equipped with a Spectra Tech Continuum IR Microscope (Spectra-Tech, Inc., Shelton, CT) and liquid nitrogen-cooled mercury cadmium telluride (MCT) detector. The IR microspectroscopy instrument was coupled with synchrotron radiation from U2B beamline, Brookhaven National Laboratory National Synchrotron Light Source, U.S. Department of Energy (NSLS-BNL, Upton, NY).

3.2.7. SFTIRM data collection and processing

The spectra were collected from five seeds of each barley variety. Spot samples (30-60) were randomly selected in endosperm area between 100-600 μm from outside of the seed section on each window. The spectra were collected through an aperture of 10 × 10 μm in a transmission mode within mid-IR spectral range of ca. 4000-800 cm^{-1}. The spatial resolution was set as 4 cm^{-1} and 128 scans were coadded on each spot to produce an IR spectrum. Background spectra were collected using the same measurement setting. Atlμs software (Thermo Nicolet, Madison, WI, USA) was used to produce the visual image of the sample. Nicolet OMNIC software 7.3 (Spectra Tech, Madison, WI, USA) was used to collect and analyze spectral data. After baseline correction, the absorption peak parameters (baseline, region, relative height and area) were recorded for further univariate analysis. More details on SFTIRM data collection were documented in Marinkovic et al. (2002) and Yu et al. (2004a).

3.2.8. Multivariate spectral analysis

Agglomerative hierarchical cluster analysis (AHCA) and principal component analysis (PCA) were applied using Statistica 8 (StatSoft Inc, Tulsa, OK, USA) to accomplish the multivariate spectral analyses. The Ward's algorithm method (Miller et al. 2000) and Euclidean Distance were applied to conduct the AHCA analysis and graphically present

the similarity among barley varieties. The 1st principal component (PC1) vs. the 2nd principal component (PC2) scatter plots were generated to present the results.

3.2.9. Statistical analysis

Statistical analyses were performed using the MIXED procedure of SAS 9.1.3 (SAS Institute, Inc., Cary, NC). Fisher's protected LSD test was used to compare means with $P < 0.05$ considered significant.

The DRIFT spectroscopic data were analyzed with a CRD model: $Y_{ij} = \mu + T_i + e_{ij}$, where Y_{ij} was an observation of the dependent variable ij; μ was the population mean for the variable; T_i was the effect of the barley varieties, as a fixed effect, and e_{ij} was the random error associated with the observation ij.

The SFTIR spectroscopic data were analyzed using a completed nested design. The model used for the analysis was: $Y_{ij} = \mu + T_i + S(T)_j + e_{ij}$, where, Y_{ij} was an observation of the dependent variable ij; μ was the population mean for the variable; T_i was the effect of the barley varieties, as a fixed effect, $S(T)_j$ is the seeds nested within treatments, as a random effect, and e_{ij} was the random error associated with the observation ij. The detailed methodology was reported in Yu (2004).

Correlation between *in situ* degradation rate and extent of DM, CP, and starch and mid-IR spectral characteristics among the barley varieties were analyzed using the Corr procedure of SAS software (SAS Institute, Inc. 2003).

3.3. Results and discussion

The DRIFT and SFTIRM techniques were used to characterize inherent seed structure among these six barley varieties. The spectra observed in the region of 4000-800 cm^{-1} were analyzed to show the absorption characteristics attributed to the chemical functional groups of barley grains.

3.3.1. Using DRIFT spectroscopy to characterize and compare structure and chemical make-up of hull samples from six barley varieties

Differences in structural and chemical make-up of barley hull from six barley varieties were identified using DRIFT spectroscopy. Figure 3.1 exhibits a typical spectrum of hull samples from barley seeds. The complex spectrum is composed of a series of unique absorption peaks and the spectral data can be associated with the chemical compounds in barley hulls. Since certain compounds only absorb at the frequencies that match the molecular vibrations, it is possible to identify and characterize the structural and chemical make-up by spectra analysis. The detailed absorption band assignments (baseline and boundaries definitions) are shown in Figure 3.1, including defined boundaries of peak areas. The region 1800-800 cm^{-1} (Figure 3.1 b) can be considered as fingerprint region because almost all molecules present characteristic peaks in this region. Lignin exhibits obvious IR absorption band (Figure 3.1 c) which is centered at ca. 1510 cm^{-1} (Wetzel et al. 1998a; Dumas et al. 2004). As shown in Figure 3.1 (d), there is a strong and complex peak in the range of 1192-932 cm^{-1}, attributed to carbohydrates (Wetzel et al. 1998a; Jackson and Mantsch 2000; Wetzel and LeVine 2000; Dumas et al. 2004). The band at 1245 cm^{-1} represents the cellulosic compound (Figure 3.1 e). The assignments of frequently-used bands in life science application have been detailed and reviewed (Wetzel et al. 1998a; Yu 2005b).

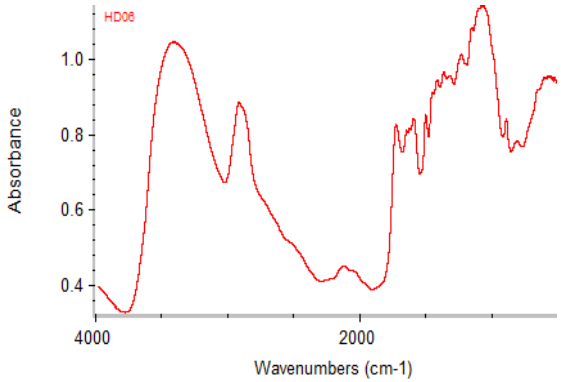

(a) Typical DRIFT spectrum in the region: ca 4000-800 cm^{-1}

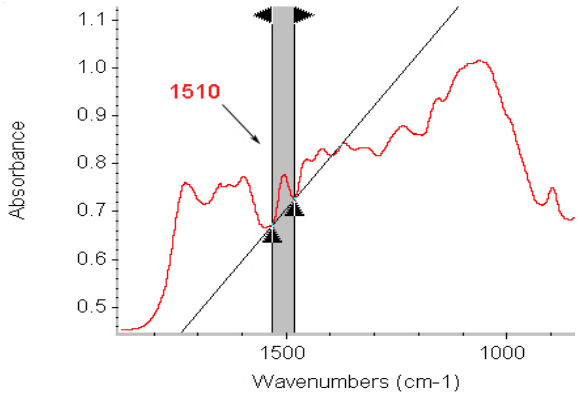

(c) Aromatic lignin peak area (Region: ca. 1536-1484 cm^{-1})

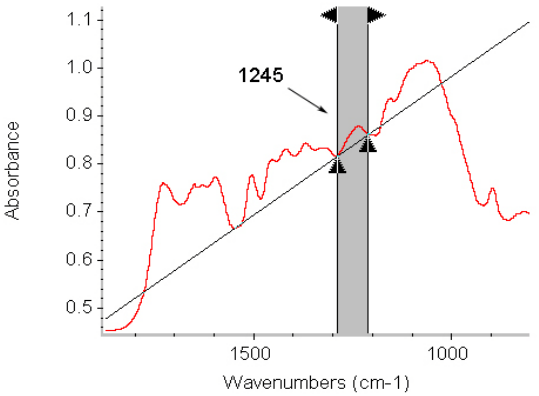

(e) Cellulosic compound peak area (Region: ca.1293-1212 cm^{-1})

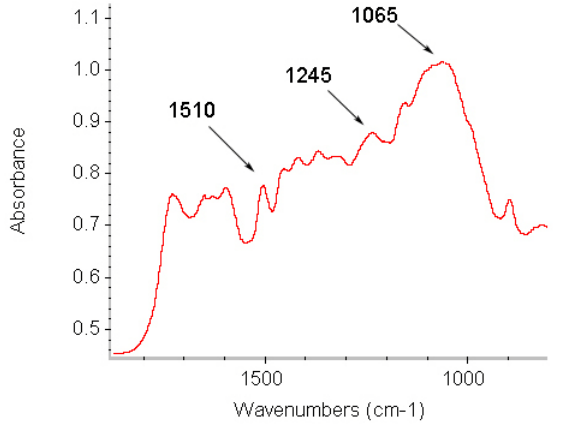

(b) Molecular FTIR Spectrum in the region: 1800-800 cm^{-1}

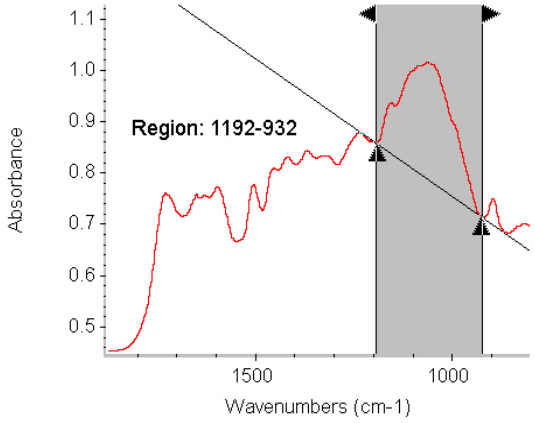

(d) Total carbohydrate peak area (Region: ca.1192-932 cm^{-1})

Figure 3.1 Typical FTIR spectrum of barley hull: (a) whole mid-IR region: ca. 4000-800 cm^{-1}; (b) Fingerprint region: ca. 1800-800 cm^{-1}; (c) Aromatic lignin peak area: ca. 1510 cm^{-1}; (d) Total carbohydrate peak area region: ca. 1192-932 cm^{-1}; (e) Cellulosic compound peak area: ca 1245 cm^{-1}.

The characteristic IR absorption parameters obtained for hull samples are given in Table 3.1. Since less non-structural CHO and protein are contained in hull samples, lignin and cellulosic compounds were more concentrated. As expected, the results showed significant differences in the peak area of aromatic lignin, cellulosic compound, total CHO, and the ratio of lignin to cellulosic compound. The results indicate the obvious presence of lignin in the samples due to the aromatic characteristic peak at 1510 cm^{-1}. A high percentage of lignin may negatively affect the digestibility of the seed for ruminants. CDC Helgason had the largest ($P<0.05$) absorption peak area (2.51), implying a relatively higher concentration of lignin compared to the other barley varieties. This may be responsible for the slower degradation rate exhibited in *in situ* experiment. CDC Dolly had the smallest ($P<0.05$) lignin peak area (1.91) among the six barley varieties. The remaining four varieties were moderate from 1.99 to 2.26. The cellulosic absorption band at 1245 cm^{-1}, was also different between varieties (Table 3.1). The cellulosic compound peak area of CDC Helgason and CDC Cowboy was 1.75 and 1.66, respectively. The other varieties showed lower band intensity (from 1.18 to 1.53) of cellulosic material. In this study, the CHO absorption peak was defined at the region from 1192 to 932 cm^{-1}. CDC Helgason had a distinct higher ($P<0.05$) value (32.30) compared with other five varieties, which varied from 19.68 to 25.86.

Table 3.1 The structural characteristics of aromatic lignin, cellulosic compound and total carbohydrate and their ratios in the barley hull, revealed using DRIFT spectroscopy: Comparison of six barley varieties (n = 10 samples per each type of barley hull).

Items	Peak center (cm^{-1})	Region (cm^{-1})	Baseline (cm^{-1})	Molecular characteristics of barley hull in terms of the mid-IR absorbed peak area and their ratios (Infrared absorbed intensity unit)						SEM[z]	P value
				AC Metcalfe	CDC Dolly	McLeod	CDC Helgason	CDC Trey	CDC Cowboy		
				----------Based on the peak area----------							
Aromatic lignin peak area	~1510	1536-1484	1536-1484	2.26 ab	1.91 c	1.99 bc	2.51 a	2.06 bc	2.26 ab	0.097	0.0006
Cellulosic compound peak area	~1245	1293-1212	1293-1212	1.36 c	1.18 d	1.53 b	1.75 a	1.34 c	1.66 a	0.037	<0.001
Total carbohydrate (CHO) area	-	1192-932	1192-932	22.33 b	19.80 b	25.86 ab	32.30 a	19.68 b	22.26 ab	2.548	0.0087
				----------Based on the peak area ratio----------							
Ratio of Lignin to total CHO	-	-	-	0.12	0.12	0.11	0.08	0.18	0.43	0.126	0.5062
Ratio of Cellulosic to total CHO	-	-	-	0.07	0.07	0.08	0.06	0.12	0.25	0.075	0.4900
Ratio of Lignin to Cellulosic	-	-	-	1.67 a	1.62 ab	1.30 d	1.43 bcd	1.54 abc	1.37 cd	0.072	0.0036

[z] SEM = pooled standard error of means; Means with the different letter in the same row are significantly different ($P<0.05$). Mean separation was done by using the Fisher's protected LSD test method.

Cellulosic materials and lignin resist microbial breakdown (Nocek and Tamminga 1991). An earlier study showed that in contrast to hulless varieties, hulled barley had less soluble and degradable fractions, implying that the hull may be of importance in barley quality evaluation (Khorasani et al. 2000). As previously reported, most fibrous materials exist in the hull, which may also contribute to its poor digestibility (Bowman et al. 2001). Due to the presence of lignin, feedstuffs may more resistant to digestion in the rumen and lower digestive tract than that with less lignin (Tamminga et al. 1994). Cellulosic compounds also contribute to the variation in digestibility in the rumen. It is therefore expected that cellulosic compounds from the hull may also contribute to the decreased digestion rate of this material. This may also partly explain the lower ruminal digestibility of CDC Helgason compared to the other five barley varieties. Resistant compounds, such as lignin and cellulosic materials that are resistant to digest, can negatively affect the feed digestibility in the rumen. CDC Dolly had a similar particle size (Mean: 3.09 mm; Median: 2.74 mm) than CDC Helgason (Mean: 3.09 mm; Median: 2.75 mm), but a faster degradation rate, which may be attributed to its lower lignin (1.91) and cellulosic compound (1.18) contents. This may also partly explain the slowest degradation rate and smallest EDST of CDC Helgason. The relevant nutrients compounds ratios (lignin to total CHO, cellulosic compounds to total CHO and lignin to cellulosic compounds) were also determined. The results are presented in Table 3.1. Ratio of lignin to CHO and cellulosic to CHO were not different ($P>0.05$) among the six barley varieties. However, the ratio of lignin: cellulosic differed ($P<0.01$) among the six barley varieties, varying from 1.30 to 1.67.

Differences in the spectral data are dependent on the chemical make-up of the biological tissue. The differences observed in this study indicate that the hull of different barley varieties vary in structural and chemical make-up. These differences may contribute to the diverse rumen degradation behaviours. Based on this study, it is reasonable to assume that CDC Helgason may have a slower rumen degradation rate than other five barley varieties in rumen due to relatively higher lignin and cellulosic contents in the hull. This may also contribute to the significantly low effectively degradability of DM, CP and ST of CDC Helgason determined in the animal trial. By far, there is no information available

on the spectral information of barley hull. In order to provide more relevant information, the whole seed was used to differentiate the chemical make-up of these six barley varieties.

3.3.2. Using DRIFT spectroscopy to characterize and compare structure-chemical make-up of whole seed samples from the six barley varieties

A typical spectrum from whole barley seed is shown in Figure 3.2. The amide I peak, centered at ca.1650 cm^{-1} (predominantly C=O stretching vibration), represents protein. The peak of cellulosic compounds appears at ca. 1246 cm^{-1}. The bands in the region of 1188-955 cm^{-1} accounts for the presence of total CHO.

The peak absorption parameters from whole seed samples of barley are shown in Table 3.2. The protein components were examined by detecting characteristic bands caused by C=O stretching (amide I), C–N stretching and N–H bending (amide II) and O–C–N bending vibration. Relatively higher protein content in the biological tissue may be implied by the stronger IR absorption of amide I (ca. 1600-1700 cm^{-1}) and amide II (ca. 1500-1560 cm^{-1}) bands (Wetzel and LeVine 2001; Stuart 2004). In the amide I region (1721-1574 cm^{-1}), there were significant differences in band intensities. The amide I peak area data indicated that the whole seed sample of CDC Cowboy may contain the highest ($P<0.01$) concentration of protein (27.61). The amide I peak height data from the DRIFT spectra illustrated that the AC Metcalfe and CDC Cowboy had a relatively higher value (0.36 and 0.35, respectively), while CDC Helgason and CDC Trey were lowest (0.30).

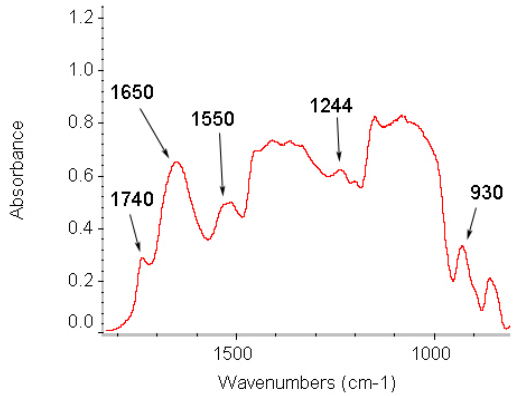

(a) FTIR spectrum in the region: ca 1800-800 cm^{-1}

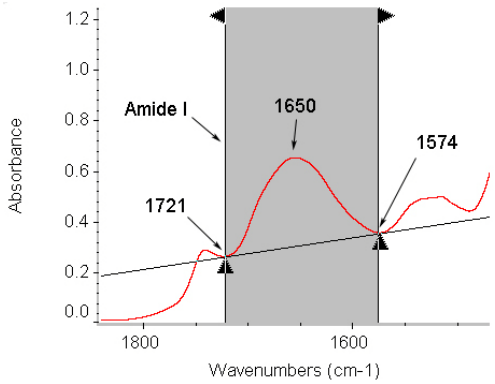

(c) Amide I peak area
(Region: ca. 1721-1574 cm^{-1})

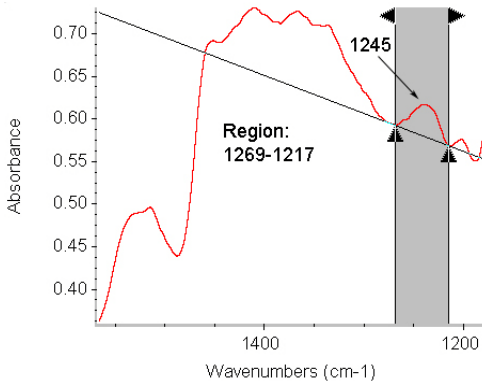

(e) Cellulosic compound peak area
(Region: ca.1269-1217 cm^{-1})

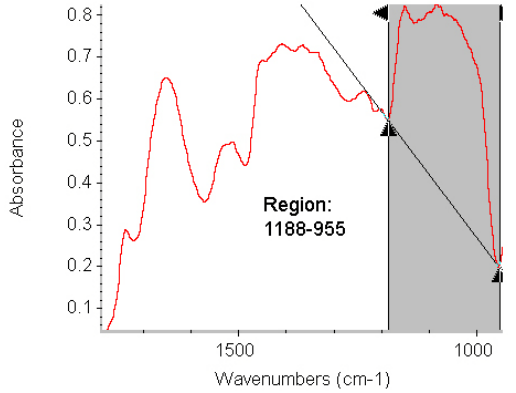

(b) Total carbohydrate peak area
(Region: ca.1188-955 cm^{-1})

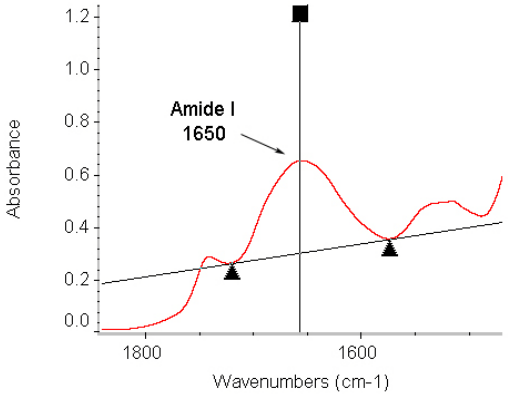

(d) Amide I peak height
(Region: ca. 1721-1574 cm^{-1})

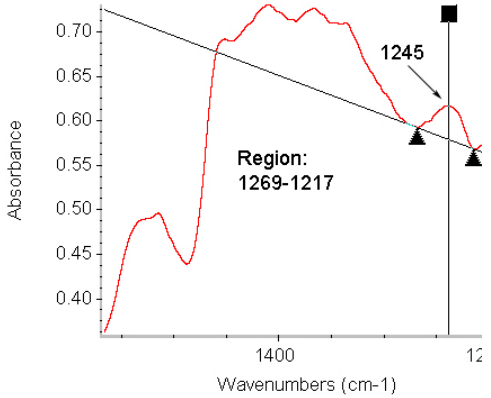

(f) Cellulosic compound peak height
(Region: ca.1269-1217 cm^{-1})

Figure 3.2 Typical FTIR spectrum of whole barley seed: (a) Fingerprint region: ca. 1800-800 cm^{-1}; (b) Total carbohydrate peak area region: ca. 1188-955 cm^{-1} (c,d) Amide I peak area and height: ca. 1650 cm^{-1}; (e,f) Cellulosic compound peak area and height: ca 1245 cm^{-1}.

Table 3.2 The structural characteristics of protein amide I and II, carbohydrates, structural carbohydrate (cellulosic compound) and their ratios in the whole barley seed, revealed using DRIFT spectroscopy: Comparison of six barley varieties (n = 10 samples per each type of whole barley seed).

Items	Peak center (cm^{-1})	Region (cm^{-1})	Baseline (cm^{-1})	Molecular characteristics of whole barley seed in terms of the mid-IR absorbed peak area and their ratios (Infrared absorbed intensity unit)						SEM[z]	P value
				AC Metcalfe	CDC Dolly	McLeod	CDC Helgason	CDC Trey	CDC Cowboy		
				----------Based on the amide I peak area and height----------							
Amide I peak area	~1650	1721-1574	1721-1574	24.91 b	23.77 c	23.44 c	23.95 c	24.04 c	27.61 a	0.222	<0.0001
Amide I peak height	~1650	1721-1574	1721-1574	0.36 a	0.35 b	0.33 c	0.30 d	0.30 d	0.35 ab	0.003	<0.0001
				----------Based on the carbohydrate peak area----------							
Total Carbohydrate (CHO)	-	1188-955	1188-955	63.69 b	62.90 b	58.49 c	54.83 d	59.21 c	70.69 a	1.120	<0.0001
Structural CHO (cellulosic)	~1246	1269-1217	1269-1217	0.97 ab	0.95 bc	0.92 cd	0.84 e	0.88 de	1.00 a	0.015	<0.0001
				----------Based on the amide I and CHO peak area----------							
Ratio of Amide I to CHO area	1721-1574 / 1188-955		-	0.39 bc	0.38 c	0.40 b	0.44 a	0.41 b	0.39 bc	0.007	<0.0001
Ratio of total CHO to Structural CHO	1188-955/1269-1217		-	65.52 bc	66.16 bc	63.75 c	65.21 bc	67.28 ab	70.50 a	1.142	0.0031

[z] SEM = pooled standard error of means; Means with the different letter in the same column are significantly different (P<0.05). Mean separation was done by using the Fisher's protected LSD test method.

In addition, Table 3.2 shows that there was a significant difference in the CHO spectra absorbance of the barley varieties, with the CDC Cowboy having the highest ($P<0.05$) absorbance value of carbohydrate (70.69), while CDC Helgason had the lowest (54.83). The other four varieties were intermediate, ranging from 58.49 to 63.69. Similarly, for the structural CHO (cellulosic), CDC Cowboy and AC Metcalfe revealed a relatively higher peak height (1.00 and 0.97, respectively). CDC Helgason and CDC Trey exhibited lower ($P< 0.05$) values (0.84 and 0.88, respectively). The results indicate that CDC Helgason was found to have a relatively higher CHO content in the hull. However, in the whole seed sample, CDC Helgason had the lowest total CHO peak intensity, indicating there was a higher concentration of CHO existed in barley hull. This leads to the conclusion that CDC Helgason has the lowest CHO in whole seed, with a large portion of CHO in hull, may contribute to its lowest degradation rate and extent compared to other five barley varieties.

Amide I to CHO area ratio is given in Table 3.2. CDC Helgason showed the highest ($P< 0.01$) ratio. Amide I absorption peak contributes to evaluating protein, thus, it is possible to assume that there is more protein surrounding CHO in CDC Helgason to protect against the degradation in rumen. This may also partially explain the lowest EDCP (Table 2.3) and EDST (Table 2.4) of CDC Helgason. The ratio of total CHO to structural CHO (cellulosic) was also calculated and significant differences were revealed among the six barley varieties (Table 3.2). CDC Cowboy had the highest ($P< 0.05$) ratio compared with other five barley varieties, indicating that CDC Cowboy may contain a relatively higher percentage of cellulosic compounds in the seed structure. Barley varieties differ in type and composition of starch and non-starch polysaccharides (Holtekjøen et al. 2006). This property influences the barley quality in either malting or feeding industry. Type and amount of structural carbohydrate may affect site and extent of starch digestion (Nocek and Tamminga 1991). A high starch content may be associated with greater digestibility (Bowman et al. 2001). However, CDC Cowboy exhibited moderate digestibility of starch in *in situ* experiments. It is probably because of the starch distribution in the endosperm tissue. But comparative data are too limited to confirm this conclusion.

The adoption of DRIFT spectroscopy for examining the complex biopolymers of plant tissue provides advantages over traditional chemical analysis techniques. The DRIFT spectroscopy method has proven to be a powerful tool in terms of characterizing and discriminating structural and chemical differences of barley varieties. This technique may be used as an effective approach to rapidly differentiate and analyze of such samples.

3.3.3. Using Synchrotron-based FTIR microspectroscopy (SFTIRM) to characterize and compare structural and chemical make-up of seed endosperm tissue among six barley varieties

For SFTIRM, the barley seed specimens were optically observed with the coupled microscope (Figure A4) and spot sampling was done randomly on endosperm tissue (between 100-600 µm from outside of the seed section) of each barley variety to produce the spectral data. Figure 3.3 (a) illustrates the typical SFTIR spectrum of the endosperm tissue in the region of ca. 4000-800 cm^{-1}. The IR spectra of characteristic bands associated with specific nutrients (protein, cellulosic compound in Figure 3.3 and carbohydrates in Figure 3.4) are shown as well.

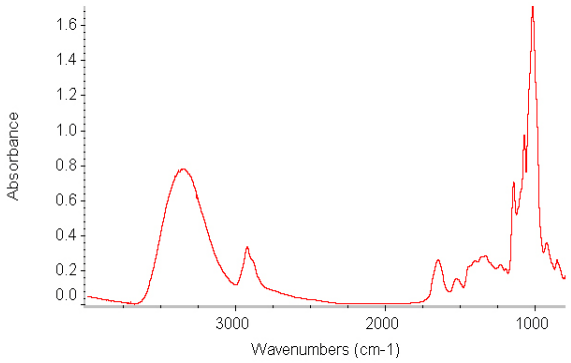

(a) Typical synchrotron-based FTIR spectrum in the region: ca 4000-800 cm^{-1} in the endosperm tissue

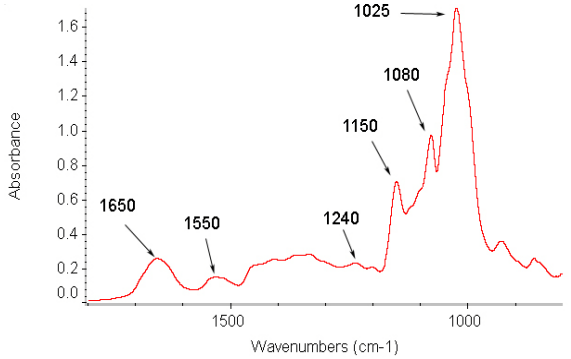

(b) FTIR spectrum in the fingerprint region: ca 1800-800 cm^{-1}

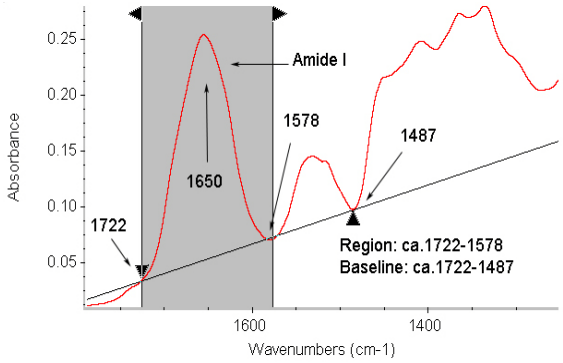

(c) Amide I peak area (Region: ca. 1722-1587 cm^{-1})

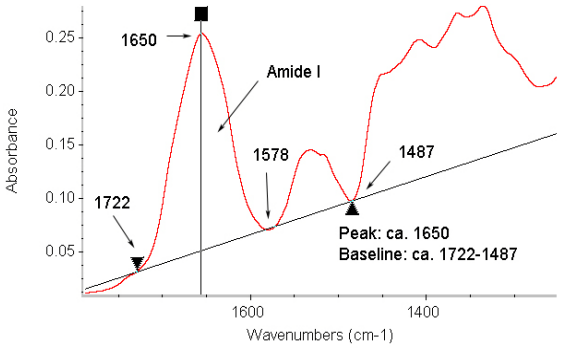

(d) Amide I peak height (Region: ca. 1722-1578 cm^{-1})

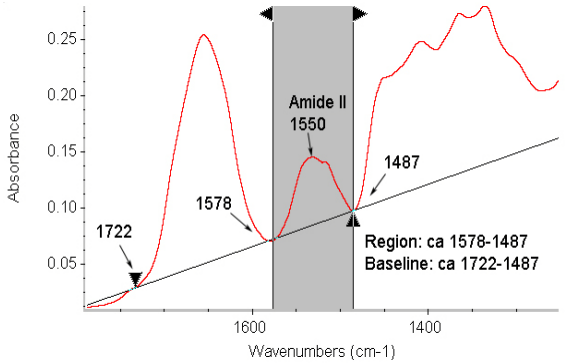

(e) Amide II peak area (Region: ca.1587-1487 cm^{-1})

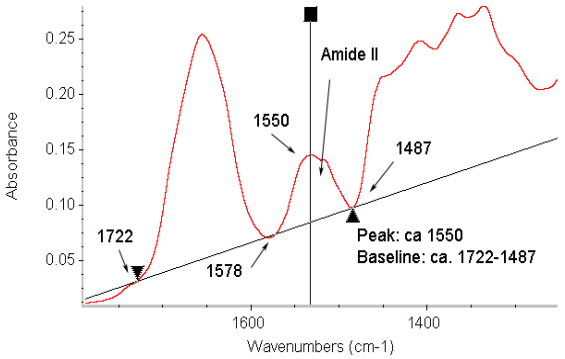

(f) Amide II peak height (Region: ca. 1587-1487 cm^{-1})

Figure 3.3 Typical synchrotron-based FTIR spectrum of endosperm tissue within a cellular dimension: (a) Whole mid-IR region: ca. 4000-800 cm^{-1}; (b) Fingerprint region: ca. 1800-800 cm^{-1}; (c,d) Amide I peak area and height: ca. 1650 cm^{-1}; (e,f) Amide II peak area and height: ca. 1550 cm^{-1}; (g, h) Cellulosic material peak area and height: ca 1240 cm^{-1};

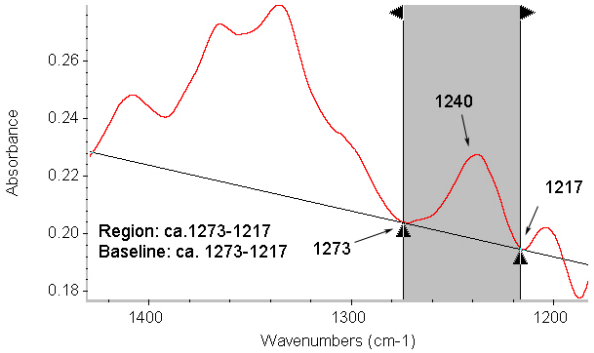

(g) Cellulosic compound peak area (Region: ca.1273-1217 cm^{-1})

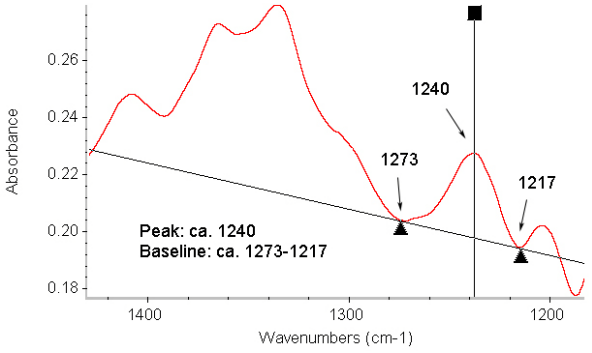

(h) Cellulosic compound peak height (Region: ca.1273-1217 cm^{-1})

Figure 3.3 (continued) Typical synchrotron-based FTIR spectrum of endosperm tissue within a cellular dimension: (a) Whole mid-IR region: ca. 4000-800 cm^{-1}; (b) Fingerprint region: ca. 1800-800 cm^{-1}; (c,d) Amide I peak area and height: ca. 1650 cm^{-1}; (e,f) Amide II peak area and height: ca. 1550 cm^{-1}; (g, h) Cellulosic material peak area and height: ca 1240 cm^{-1};

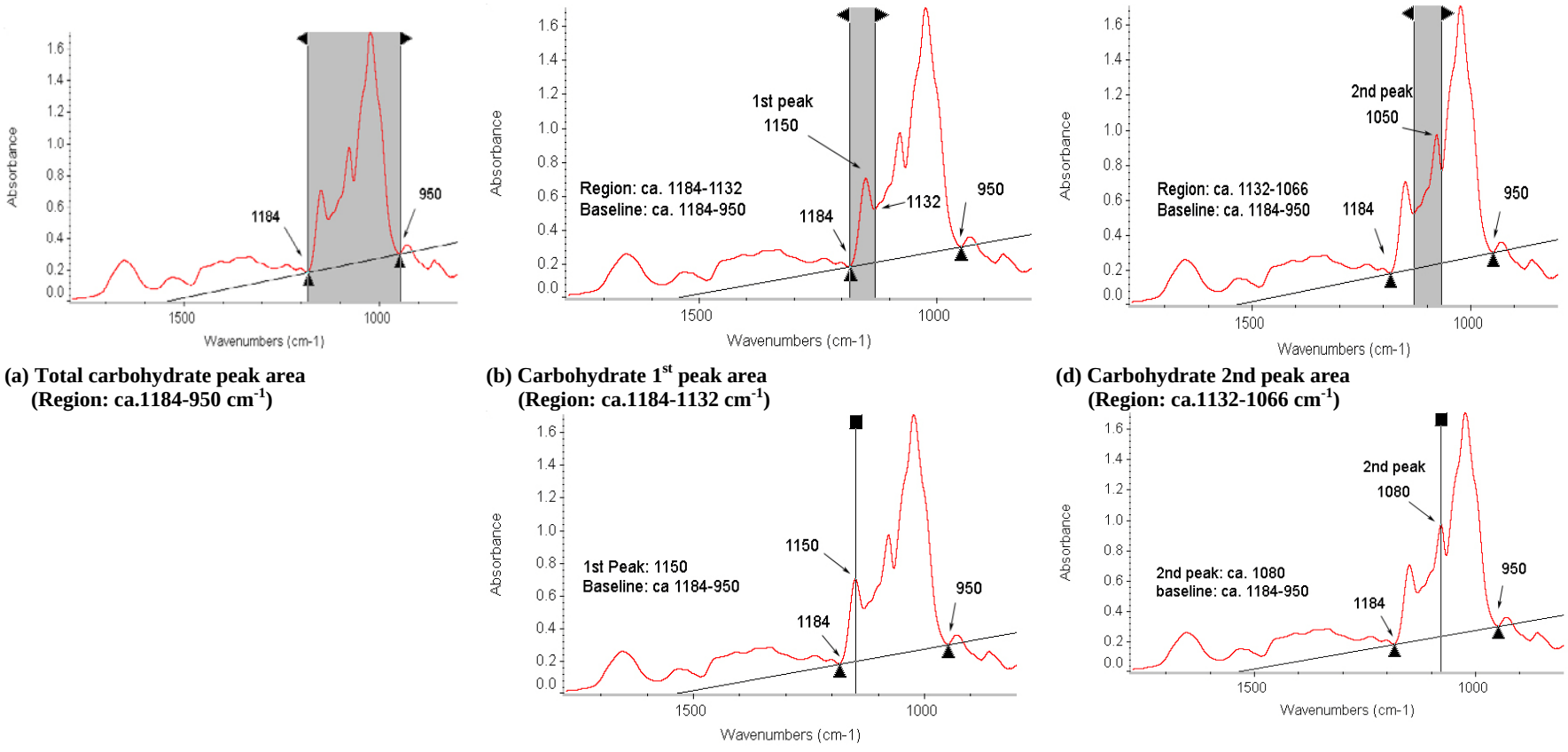

(a) Total carbohydrate peak area (Region: ca.1184-950 cm^{-1})

(b) Carbohydrate 1st peak area (Region: ca.1184-1132 cm^{-1})

(d) Carbohydrate 2nd peak area (Region: ca.1132-1066 cm^{-1})

(c) Carbohydrate 1st peak height (Region: ca.1184-1132 cm^{-1})

(e) Carbohydrate 2nd peak height (Region: ca.1132-1066 cm^{-1}

Figure 3.4 Typical synchrotron-based FTIR spectrum of endosperm tissue within a cellular dimension: (a) Total carbohydrate peak area region: ca. 1184-950 cm^{-1}; (b,c) Carbohydrate 1st component peak area and height: ca. 1150 cm^{-1}; (d,e) Carbohydrate 2nd component peak area and height: ca. 1080 cm^{-1}; (f,g) carbohydrate 3rd component peak area and height: ca. 1025 cm^{-1}.

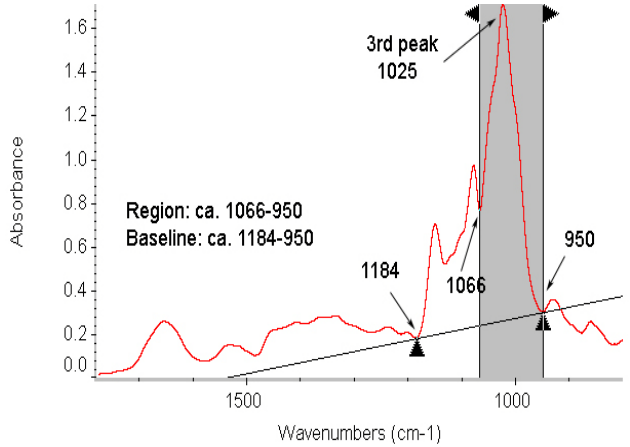

(f) Carbohydrate 3rd peak area (Region: ca. 1066-950 cm^{-1})

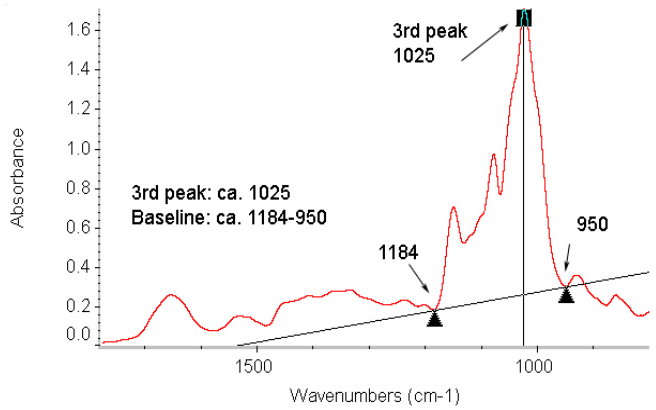

(g) Carbohydrate 3rd peak height (Region: ca. 1066-950 cm^{-1})

Figure 3.4 (continued) Typical synchrotron-based FTIR spectrum of endosperm tissue within a cellular dimension: (a) Total carbohydrate peak area region: ca. 1184-950 cm^{-1}; (b,c) Carbohydrate 1st component peak area and height: ca. 1150 cm^{-1}; (d,e) Carbohydrate 2nd component peak area and height: ca. 1080 cm^{-1}; (f,g) carbohydrate 3rd component peak area and height: ca. 1025 cm^{-1}.

The characteristic absorbance bands of the amide groups can be used to probe and characterize the structural and chemical make-up of the plant tissue. The amide I (ca. 1650 cm^{-1}) and amide II (ca. 1550 cm^{-1}) peak areas and height definition used for univariate analysis are shown in the Figure 3.3 (c, d, e, f). The peak centered at approximately 1240 cm^{-1} (Figure 3.3 g, h) was considered to represent the structural carbohydrates (cellulosic compounds) (Wetzel et al. 1998a; Stuart 2004; Yu 2005b). The total carbohydrate peak area is located at region from ca.1184 to 951 cm^{-1} because of C-O and C-C stretching vibrations and C-O-H deformation (Wetzel et al. 1998a; Stuart 2004; Yu 2005b). The CHO band intensities were determined by calculating the peak heights and areas of specific bands: carbohydrate 1^{st} peak area occurs at region of ca.1184-1132 cm^{-1}, carbohydrate 2^{nd} peak area occurs at region of ca.1132-1066 cm^{-1} and carbohydrate 3^{rd} peak area occurs at region of ca. 1066-950 cm^{-1}. These three peaks are regarded to represent total carbohydrate compounds (Figure 3.4).

To detect the chemical features associated with nutrients, synchrotron-based IR microspectroscopy was used to examine barley endosperm tissue. Spectroscopic data from spot samples within cellular dimensions are detailed in Table 3.3 to 3.5. It should be realized that the peak intensity parameters (area or height for instance) cannot be considered as representation of accurate biological compound contents.

Table 3.3 The structural characteristics of protein amides I and II in the endosperm tissue of barley varieties, revealed using Synchrotron-based FTIR Microspectroscopy: Comparison of six barley varieties.

Items	Peak center (cm^{-1})	Region (cm^{-1})	Baseline (cm^{-1})	Molecular characteristics of whole barley seed in terms of the mid-IR absorbed peak area and their ratios (Infrared absorbed intensity unit)						SEM[z]	P value
				AC Metcalfe	CDC Dolly	McLeod	CDC Helgason	CDC Trey	CDC Cowboy		
Amide molecular spectral features				----------Based on the amides I and II peak area and height----------							
Amide I peak area	~1650	1722-1578	1722-1487	7.99 bc	8.23 abc	10.02 a	7.33 c	9.01 ab	9.23 ab	0.582	0.004
Amide I peak height	~1650	1722-1578	1722-1487	0.11 cd	0.12 bcd	0.16 a	0.11 d	0.14 ab	0.13 bc	0.091	<0.0001
Amide II peak area	~1550	1578-1487	1722-1487	1.94 b	1.97 ab	2.57 a	1.86 b	2.20 ab	2.34 a	0.182	0.024
Amide I plus II area	-	1722-1578	1722-1487	9.93 bc	10.20 abc	12.59 a	9.19 c	11.22 ab	11.56 a	0.754	0.005

[z] SEM = pooled standard error of means; Means with the different letter in the same row are significantly different ($P<0.05$). Mean separation was done by using the Fisher's protected LSD test method.

Table 3.4 The structural characteristics of carbohydrates, and structural carbohydrate (cellulosic compounds) in the endosperm tissue of barley varieties, revealed using Synchrotron-based FTIR Microspectroscopy: Comparison of six barley varieties.

Items	Peak center (cm^{-1})	Region (cm^{-1})	Baseline (cm^{-1})	Molecular characteristics of whole barley seed in terms of the mid-IR absorbed peak area and their ratios (Infrared absorbed intensity unit)						SEM[z]	P value
				AC Metcalfe	CDC Dolly	McLeod	CDC Helgason	CDC Trey	CDC Cowboy		
Carbohydrate (CHO) molecular spectral features				----------Based on the carbohydrate peak area and height----------							
Cellulosic compound area	~1240	1273-1217	1273-1217	0.54 a	0.53 ab	0.48 b	0.54 a	0.47 b	0.49 b	0.020	0.003
Total carbohydrate peak area	-	1184-951	1184-951	71.10 a	75.20 a	62.68 b	76.71 a	72.30 a	72.31 a	2.889	0.022
CHO: 1st component peak area	~1150	1184-1132	1184-951	8.25 b	8.67 ab	7.03 c	9.02 a	8.14 b	8.19 b	0.374	0.006
CHO: 1st component peak height	~1150	1184-1132	1184-951	0.29 a	0.30 a	0.24 b	0.27 ab	0.28 a	0.28 a	0.012	0.048
CHO: 2nd component peak area	~1080	1132-1066	1184-951	10.41 ab	11.24 a	9.54 b	11.14 a	10.74 ab	10.64 ab	0.460	0.175
CHO: 2nd component peak height	~1080	1132-1066	1184-951	0.42 ab	0.45 a	0.38 b	0.44 a	0.42 ab	0.42 ab	0.017	0.144
CHO: 3rd component peak area	~1025	1066-951	1184-951	44.92 b	47.38 ab	39.59 c	48.66 a	46.08 ab	46.30 ab	1.791	0.014
CHO: 3rd component peak height	~1025	1066-951	1184-951	0.66 ab	0.69 ab	0.59 b	0.72 a	0.72 a	0.72 a	0.029	0.014

[z] SEM = pooled standard error of means; Means with the different letter in the same row are significantly different ($P<0.05$). Mean separation was done by using the Fisher's protected LSD test method.

Table 3.5 The structural characteristics of the ratios of protein amide I and II, and structural (cellulosic compounds) and non-structural (NSC, starch) carbohydrates (CHO) in the endosperm tissue of barley varieties, revealed using Synchrotron-based FTIR Microspectroscopy: Comparison of six barley varieties.

Items	Peaks area regions (baseline) (cm^{-1})	Molecular characteristics of whole barley seed in terms of the mid-IR absorbed peak area and their ratios (Infrared absorbed intensity unit)						SEM[z]	P value
		AC Metcalfe	CDC Dolly	McLeod	CDC Helgason	CDC Trey	CDC Cowboy		
		--------Based on the Amide I and CHO peak area and height ratios --------							
Ratio of total CHO peak area / Amides I plus II peak area	1184-951 (baseline: 1184-951) / 1722-1487 (baseline 1722-1487)	8.90 b	9.15 abc	7.11 c	9.89 ab	10.81 a	9.49 ab	0.618	0.002
Ratio of NSC (starch) peak area (CHO 3rd peak) / Amides I peak area	1066-951 (baseline:1184-951) / 1722-1487 (baseline 1722-1487)	6.91 b	6.86 abc	5.35 c	7.68 ab	8.25 a	7.58 ab	0.505	0.003
Ratio of NSC (starch) peak height (CHO 3rd peak) / Amide I height	~1025 (baseline: 1184-951) / ~1650 (baseline: 1722-1487)	6.91 bc	7.24 bc	5.16 c	7.90 b	8.41 ab	9.97 a	0.789	<0.001
Ratio of amides I & II peak area / cellulosic compounds peak area	1722-1487 (baseline: 1722-1487) / 1273-1217 (baseline: 1273-1217)	19.41 b	20.98 ab	26.44 a	17.99 b	23.64 a	24.29 a	1.568	<0.0001
Ratio of amide I peak area /cellulosic compounds peak area	1722-1587 (baseline: 1722-1487) / 1273-1217 (baseline: 1273-1217)	15.44 b	16.92 ab	21.03 a	14.27 b	18.96 a	19.36 a	1.190	<0.0001
Ratio of Amide I peak height /Cellulosic compounds peak height	~1650 (baseline: 1722-1487) / 1273-1217 (baseline: 1273-1217)	5.90 c	6.36 bc	9.77 a	5.67 c	7.87 b	7.67 b	0.501	<0.0001
Ratio of total CHO peak area / Cellulosic compound peak area	1184-951 (baseline: 1184-951) / 1273-1217 (baseline: 1273-1217)	137.14 bc	144.80 abc	130.89 c	144.99 abc	157.57 a	148.60 ab	5.963	0.022
Ratio of NSC (starch) peak area (CHO 3rd peak) /Cellulosic compound peak area	1066-951 (baseline: 1184-951) / /1273-1217 (baseline: 1273-1217)	87.08 bc	91.26 abc	82.65 c	92.71 abc	101.24 a	95.32 ab	3.936	0.011
Ratio of NSC (starch) peak height (CHO 3rd peak)/Cellulosic compound peak height	~1025 (baseline: 1184-951) / 1273-1217 (baseline: 1273-1217)	34.56 d	36.47 cd	35.82 cd	38.45 bc	42.47 a	40.93 ab	1.271	<0.0001

[z] SEM = pooled standard error of means; Means with the different letter in the same row are significantly different (P<0.05). Mean separation was done by using the Fisher's protected LSD test method.

The amide bands representing protein at 1650 and 1550 cm^{-1} exhibited significant differences among the six barley varieties. Table 3.3 indicated that McLeod had the largest ($P<0.05$) amide I peak area (10.02), indicating a greater concentration of protein in the endosperm tissue. In contrast, CDC Helgason showed the lowest value (7.33). The other four values were in between. For amide I peak height value, the data varied significantly from 0.11 to 0.16. The peak areas and height centered at 1550 cm^{-1} (amide II) bands of McLeod exhibited the highest value (2.57, 0.05 respectively), again implying a greater concentration of protein in the endosperm tissue. By analyzing the peak of the total amides I and II area (Table 3.3), McLeod was still the greatest (12.59), while the CDC Helgason was the smallest (9.19). This may partially explain the lowest EDCP of CDC Helgason among the six barley varieties. If these six barley varieties are ranked based on their amide groups intensities, it is obvious that all the amide groups parameters show a similar trend that CDC Helgason exhibited the smallest value whereas McLeod showed the greatest peak intensity. The remaining four, in which AC Metcalfe and CDC Dolly had relatively smaller values, and CDC Trey and CDC Cowboy were relatively higher. These results also agree with the previous work that McLeod was developed as a high protein content barley (Camm 2008; Mikel and Kolb 2008). The protein may play a protector role if combined with carbohydrate, which may be related with the digestibility of barley.

Shown in Table 3.4 are the absorbance peak area and height data of non-structural and structural carbohydrates (cellulosic compounds) in the endosperm tissue of barley varieties. CDC Trey had the relatively smaller value (0.47) of the peak area at ca. 1240 cm^{-1} (cellulosic compounds band). In particular, there were differences found in the region around 1184-951 cm^{-1}, revealing the various CHO contents of the endosperm tissue of barley varieties. McLeod had the lowest ($P<0.05$) value of total carbohydrate

peak area (62.68). The three characteristic absorption peaks fell in CHO region (1184-951 cm^{-1}) were analyzed respectively and it was observed similar trends. McLeod had the smallest ($P<0.01$) area of the 1st CHO peak (7.03), contrasting to the CDC Dolly and CDC Helgason (8.67 and 9.02, respectively). Compared to the other varieties, McLeod and CDC Helgason exhibited relatively lower ($P<0.05$) peak height of the 1st CHO peak (0.24 and 0.27, respectively). There was no significant ($P>0.05$) difference of 2nd CHO peak intensity shown here. At ca. 1066-951 cm^{-1}, there was an obvious absorption band which can be assigned to starch. The peak maxima appeared at ca. 1025 cm^{-1} (Wetzel et al. 1998a). Consistent with other CHO peak parameters, McLeod had the smallest ($P<0.05$) 3rd CHO peak area and relatively smaller peak height (0.59), suggesting the lowest enrichment of starch in endosperm tissue among the six barley varieties. Starch is abundant in endosperm tissue with different granule size, type and content (Takeda et al. 1999; You and Izydorczyk 2002). These variable molecular characteristics of barley endosperm tissue may have a strong influence on ruminal fermentation.

In order to extend the analysis of the structural and chemical make-up of the barley endosperm, relative intensity ratios of specific bands associated with nutrients were calculated. All items analyzed are presented in Table 3.5. The ratio analysis was calculated using absorbance intensity (area or height) of one characteristic peak observed in the spectrum to divide that of another one. McLeod had the relatively smaller ratio of total CHO peak area to amides I and II peak area (7.11). The ratio of 1205 cm^{-1} band assigned to starch: amide I band at 1650 cm^{-1} were significantly different among the six barley varieties. McLeod showed a relatively smaller value for both of the area and height ration comparison (5.35 and 5.16, respectively). According to the chemical composition analysis, McLeod has relatively more protein and less CHO content, which may be a reason of the smallest the CHO: amide ratio. Valier, another feed-type barley, was found

to have lower starch: protein ratio in earlier study, implying that protein may protect starch from degradation in rumen (Yu 2006a).

There was also a notable difference in the ratio of the amide band to cellulosic compounds in the 1273-1217 cm^{-1} region. CDC Helgason, AC Metcalfe and CDC Dolly had relatively smaller ratio of amides I: cellulosic peak area (14.27, 15.44 and 16.92, respectively). The same trend was also found in peak area ratio comparison of amide I: cellulosic compounds. Whereas McLeod had the greatest ($P<0.05$) height ratio of amide I: cellulosic compounds (9.77). This is further evidence to support the opinion that cellulosic compounds significantly contribute to the lower digestibility.

Another large difference ($P<0.05$) was seen at peak area ratio of total CHO: cellulosic compounds. The higher starch content and lower undigestible fibrous materials may result in the better nutrients value, which has been noted in earlier study (Bowman et al. 2001). In comparison with CDC Trey (157.57) and CDC Cowboy (148.60), McLeod was merely 130.89. The ratio of non-structural CHO (starch) peak area (CHO 3rd peak): cellulosic compounds peak area exhibited a similar trend among these six barley varieties. CDC Trey and CDC Cowboy had a relatively higher ($P<0.05$) peak height ratio of non-structural CHO (starch) peak area (CHO 3rd peak): cellulosic compounds (42.47 and 40.93, respectively). Others were ranging from 34.56 to 38.45.

The protein matrix provides adhesion for starch granules in endosperm tissue (Holopainen et al. 2005). Cellulosic compounds in cell wall also take effort to support and maintain microstructure of seed. This association may influence the hardness of cereal, the particle size distribution, and as a result, nutritional value. With protein encompassing the starch granules, cultivars containing more protein may be associated

with a harder structure. The protein content, structure, distribution and conjunction may partially explain the grain characteristics. Whereas, documents are lacking in individual spots sampling on barley grain using IR spectroscopic analysis. Little information is comparable. More study is needed to examine whether the spots sampling with Mid-IR spectroscopy can be used to predict nutrients availability of grain.

We can draw the conclusion that in conjunction with synchrotron light source, chemical-structural information can be obtained *in situ* via FTIR technique with intact tissue sections. Compared to traditional chemical analysis methodologies, for which grinding is always required, SFTIRM is obviously superior on probing the internal biological matrix with minimal artificial influence. Again, the results confirm earlier statements that with the advanced SFTIRM techniques, chemical-structural information of feedstuffs can be revealed. DRIFT data can be used to produce spectroscopic information of ground specimens, while the SFTIRM data can provide the ultrastructural-chemical make-up information of original biological tissue. Further research using SFTIRM techniques is needed since the results are limited.

3.3.4. Correlations between mean and median particle sizes, *in situ* degradation features of DM, CP, and starch and Mid-IR spectral characteristics among barley varieties

To extend this research, the correlation procedure was used in an attempt to relate spectral information with ruminal degradation characteristics. Pearson correlation coefficients were computed using Proc Corr procedure of SAS package to investigate the relationship between spectral data (from DRIFT and SFTRM) and degradation data (degradation rate and extent of DM, CP and ST in Table 3.6 to 3.10; S and D of DM, CP and ST in Table 3.11) for nutrient availability evaluation. The results displayed that the

DRIFT spectroscopic data from hull samples were weakly correlated with the degradation characteristics (Table 3.6). Ratio of cellulosic to CHO was correlated with EDDM (P=0.082) and EDST (P=0.111). Aromatic lignin peak area was correlated with Kd of CP (P=0.082). However, no significant correlation was detected between the spectral data from whole seed sample and degradation rate and extent of DM, CP, and ST (Table 3.7). The correlation tendency also appeared between SFTIR information and degradation features, though not all of them were significant (Table 3.8 to 3.11). CHO: 1st component peak area was correlated with Kd of CP (P=0.101) (Table 3.9). Cellulosic compound area was correlated with S (%) of CP (P=0.068) and S (%) of ST (P=0.041) (Table 3.11). More spectroscopic analysis on seed tissues is necessary to clarify this assumption that whether the chemical-structural make-up of endosperm tissue is linked to degradation performance of grain.

Weak correlations indicate that six barley varieties might not be sufficient enough to interpret the relationship between spectroscopic information and nutrients value of barley grain. In this case, it may due to the similarities and limitations of the barley varieties (only six barley varieties were examined). Differences among the varieties may not be large enough to reveal the actual relationship between the spectroscopic data and ruminal degradation data. Chemical and physical composition of plant tissue may affect the digestion process, but relevant reports referring to mid-IR spectroscopy have not been well documented yet. We aim at a further understanding of the relationship between IR spectroscopic information and nutrition value of feedstuffs. More studies involving a diverse range of samples with biological differences may thereby be necessary.

Table 3.6. Pearson correlation results between structural characteristics from hull sample and *in situ* rumen degradation rate and extent of six barley varieties. (The structural characteristics include aromatic lignin, cellulosic compound and total carbohydrate and their ratios in the barley hull, revealed using DRIFT spectroscopy).

Items	In situ rumen degradation kinetics of DM [z]				In situ rumen degradation kinetics of CP [z]				In situ rumen degradation kinetics of ST [z]			
	Kd (%/h)		EDDM (%)		Kd (%/h)		EDCP (%)		Kd (%/h)		EDST (%)	
	Correlation coefficient	P-value	Correlation coefficient	P-value	Correlation coefficient	P-value	Correlation coefficient	P-value	Correlation coefficient	P-value	Correlation coefficient	P-value
Aromatic lignin peak area	-0.557	0.251	-0.305	0.556	-0.757	0.082	-0.358	0.486	-0.251	0.632	0.139	0.793
Cellulosic compound peak area	-0.501	0.311	-0.309	0.551	-0.644	0.167	-0.360	0.483	-0.365	0.477	0.232	0.659
Total carbohydrate (CHO) area	-0.670	0.145	-0.633	0.177	-0.701	0.121	-0.647	0.165	-0.576	0.232	0.576	0.231
Ratio of Lignin to CHO	0.503	0.309	0.440	0.382	0.655	0.158	0.477	0.339	0.371	0.469	-0.336	0.515
Ratio of Cellulosic to CHO	0.616	0.193	0.756	0.082	0.550	0.258	0.731	0.099	0.574	0.234	-0.714	0.111
Ratio of Lignin to Cellulosic	0.176	0.739	0.141	0.790	0.185	0.725	0.163	0.758	0.285	0.584	-0.199	0.706

[z] Kd = degradation rate; EDDM, EDCP, EDST= effective degradability of DM, CP and starch, respectively.

Table 3.7. Pearson correlation results between structural characteristics from whole seed sample and *in situ* rumen degradation rate and extent of six barley varieties. [The structural characteristics include protein amide I and II, carbohydrates, structural carbohydrate (cellulosic compound) and their ratios in the whole barley seed, revealed using DRIFT spectroscopy.]

Items	In situ rumen degradation kinetics of DM [z]				In situ rumen degradation kinetics of CP [z]				In situ rumen degradation kinetics of ST [z]			
	Kd (%/h)		EDDM (%)		Kd (%/h)		EDCP (%)		Kd (%/h)		EDST (%)	
	Correlation coefficient	P-value	Correlation coefficient	P-value	Correlation coefficient	P-value	Correlation coefficient	P-value	Correlation coefficient	P-value	Correlation coefficient	P-value
Amide I peak area	0.021	0.969	0.251	0.631	-0.207	0.694	0.189	0.719	0.192	0.715	0.348	0.500
Amide I peak height	0.356	0.489	0.205	0.697	0.266	0.610	0.215	0.682	0.364	0.478	0.318	0.539
Amide I & II area	0.110	0.835	0.205	0.697	-0.118	0.825	0.165	0.754	0.285	0.584	0.388	0.418
Total Carbohydrate (CHO)	0.296	0.569	0.372	0.468	0.145	0.785	0.339	0.511	0.352	0.494	0.440	0.382
Structural CHO (cellulosic)	0.448	0.373	0.392	0.442	0.325	0.529	0.384	0.453	0.453	0.367	0.412	0.416
Ratio of Amide I to CHO area	-0.580	0.228	-0.410	0.419	-0.583	0.224	-0.432	0.393	-0.461	0.358	-0.379	0.459
Ratio of Amide I & II to CHO	-0.559	0.248	-0.518	0.292	-0.622	0.187	-0.524	0.286	-0.367	0.474	-0.302	0.561
Ratio of Structural to CHO	-0.224	0.670	-0.516	0.295	-0.127	0.811	-0.464	0.354	-0.275	0.598	-0.416	0.412

[z] Kd = degradation rate; EDDM, EDCP, EDST= effective degradability of DM, CP and starch, respectively.

Table 3.8. Pearson correlation results between structural characteristics from seed endosperm tissue and *in situ* rumen degradation rate and extent of six barley varieties. (The structural characteristics include protein amides I and II in the endosperm tissue of barley varieties, revealed using Synchrotron-based FTIR Microspectroscopy.)

Items	In situ rumen degradation kinetics of DM [z]				In situ rumen degradation kinetics of CP [z]				In situ rumen degradation kinetics of ST [z]			
	Kd (%/h)		EDDM (%)		Kd (%/h)		EDCP (%)		Kd (%/h)		EDST (%)	
	Correlation coefficient	P-value	Correlation coefficient	P-value	Correlation coefficient	P-value	Correlation coefficient	P-value	Correlation coefficient	P-value	Correlation coefficient	P-value
Amide I peak area	0.610	0.198	0.529	0.281	0.644	0.168	0.538	0.271	0.381	0.456	0.394	0.440
Amide I peak height	0.569	0.239	0.463	0.355	0.625	0.185	0.480	0.335	0.330	0.523	0.317	0.540
Amide II peak area	0.498	0.315	0.434	0.390	0.513	0.298	0.437	0.386	0.290	0.578	0.312	0.547
Amide II peak height	0.513	0.298	0.443	0.379	0.512	0.299	0.448	0.373	0.324	0.531	0.329	0.524
Amide I & II area	0.587	0.220	0.510	0.302	0.617	0.192	0.517	0.293	0.362	0.480	0.377	0.461

[z] Kd = degradation rate; EDDM, EDCP, EDST= effective degradability of DM, CP and starch, respectively.

Table 3.9. Pearson correlation results between structural characteristics from seed endosperm tissue and *in situ* rumen degradation rate and extent of six barley varieties. [The structural characteristics include carbohydrates and structural carbohydrate (cellulosic compounds) in the endosperm tissue of barley varieties, revealed using Synchrotron-based FTIR Microspectroscopy.]

Items	In situ rumen degradation kinetics of DM [z]				In situ rumen degradation kinetics of CP [z]				In situ rumen degradation kinetics of ST [z]			
	Kd (%/h)		EDDM (%)		Kd (%/h)		EDCP (%)		Kd (%/h)		EDST (%)	
	Correlation coefficient	P-value	Correlation coefficient	P-value	Correlation coefficient	P-value	Correlation coefficient	P-value	Correlation coefficient	P-value	Correlation coefficient	P-value
Cellulosic compound area	-0.511	0.300	-0.553	0.255	-0.560	0.247	-0.550	0.258	-0.321	0.535	-0.418	0.410
Cellulosic compound height	-0.349	0.497	-.0522	0.288	-0.257	0.623	-0.494	0.320	-0.347	0.500	-0.480	0.336
CHO: 1st component peak area	-0.711	0.113	-0.556	0.252	-0.728	0.101	-0.582	0.225	-0.515	0.296	-0.435	0.389
CHO: 1st component peak height	-0.021	0.968	0.058	0.914	-0.059	0.912	0.045	0.933	0.097	0.855	0.140	0.792
CHO: 2nd component peak area	-0.646	0.166	-0.505	0.307	-0.609	0.199	-0.528	0.282	-0.527	0.283	-0.426	0.399
CHO: 2nd component peak height	-0.630	0.180	-0.503	0.309	-0.610	0.199	-0.523	0.287	-0.484	0.331	-0.407	0.423
CHO: 3rd component peak area	-0.660	0.154	-0.449	0.372	-0.687	0.132	-0.486	0.329	-0.471	0.346	-0.336	0.515
CHO: 3rd component peak height	-0.509	0.302	-0.201	0.702	-0.579	0.229	-0.255	0.626	-0.313	0.546	-0.098	0.853
Total carbohydrate peak area	-0.668	0.147	-0.484	0.330	-0.680	0.137	-0.515	0.295	-0.487	0.327	-0.374	0.465

[z] Kd = degradation rate; EDDM, EDCP, EDST= effective degradability of DM, CP and starch, respectively.

Table 3.10. Pearson correlation results between structural characteristics ratios from seed endosperm tissue and *in situ* rumen degradation rate and extent of six barley varieties. [The structural characteristics include protein amide I and II, and structural (cellulosic compounds) and non-structural (NSC, starch) carbohydrates (CHO) in the endosperm tissue of barley varieties, revealed using Synchrotron-based FTIR Microspectroscopy.]

Items	In situ rumen degradation kinetics of DM [z]				In situ rumen degradation kinetics of CP [z]				In situ rumen degradation kinetics of ST [z]			
	Kd (%/h)		EDDM (%)		Kd (%/h)		EDCP (%)		Kd (%/h)		EDST (%)	
	Correlation coefficient	P-value	Correlation coefficient	P-value	Correlation coefficient	P-value	Correlation coefficient	P-value	Correlation coefficient	P-value	Correlation coefficient	P-value
Ratio of total CHO peak area / Amides I & II peak area	-0.279	0.593	0.030	0.955	-0.322	0.533	-0.012	0.982	-0.098	0.853	0.102	0.848
Ratio of NSC (starch) peak area (CHO 3rd peak) / Amides I peak area	-0.295	0.571	0.045	0.933	-0.380	0.457	-0.007	0.990	-0.081	0.879	0.138	0.795
Ratio of NSC (starch) peak height (CHO 3rd peak) / Amide I height	-0.294	0.572	0.042	0.937	-0.434	0.390	-0.026	0.961	-0.109	0.837	0.143	0.788
Ratio of amides I & II peak area / cellulosic compounds peak area	0.552	0.256	0.489	0.325	0.596	0.212	0.495	0.319	0.317	0.540	0.351	0.495
Ratio of amide I peak area / cellulosic compounds peak area	0.555	0.253	0.489	0.325	0.607	0.202	0.496	0.317	0.315	0.544	0.348	0.499
Ratio of Amide I peak height / Cellulosic compounds peak height	0.509	0.303	0.413	0.415	0.574	0.234	0.428	0.398	0.263	0.614	0.264	0.613
Ratio of total CHO peak area / Cellulosic compound peak area	-0.171	0.746	0.117	0.826	-0.175	0.741	0.076	0.887	-0.089	0.867	0.136	0.797
Ratio of NSC (starch) peak area (CHO 3rd peak) / Cellulosic compound peak area	-0.169	0.750	0.139	0.793	-0.190	0.718	0.094	0.860	-0.069	0.896	0.165	0.754
Ratio of NSC (starch) peak height (CHO 3rd peak) / Cellulosic compound peak height	-0.125	0.813	0.185	0.726	-0.155	0.770	0.134	0.801	-0.085	0.873	0.177	0.737

[z] Kd = degradation rate; EDDM, EDCP, EDST= effective degradability of DM, CP and starch, respectively.

Table 3.11. Pearson correlation results between structural characteristics from seed endosperm tissue and *in situ* rumen degradation characteristics of six barley varieties. [The structural characteristics include structural carbohydrate (cellulosic compounds) and amide I: cellulosic compound ratio in the endosperm tissue of barley varieties, revealed using Synchrotron-based FTIR Microspectroscopy.]

	Degradation characteristics of DM[z]				Degradation characteristics of CP[z]				Degradation characteristics of ST[z]			
	S (%)		D (%)		S (%/)		D (%)		S (%/)		D (%)	
Items	Correlation coefficient	P-value	Correlation coefficient	P-value	Correlation coefficient	P-value	Correlation coefficient	P-value	Correlation coefficient	P-value	Correlation coefficient	P-value
Cellulosic compound area	-0.614	0.195	-0.281	0.590	0.779	0.068	-0.507	0.304	0.830	0.041	-0.677	0.140
Cellulosic compound height	-0.527	0.283	-0.628	0.182	0.500	0.313	-0.823	0.044	0.404	0.427	-0.684	0.134
Ratio of amide I peak area /cellulosic compounds peak area	0.442	0.380	0.035	0.948	-0.648	0.164	0.213	0.685	-0.860	0.028	0.531	0.278

[z] S = soluble fraction; D= potentially degradable fraction of DM, CP and starch, respectively.

3.3.5. Using Mid-IR spectroscopy with multivariate molecular spectral analysis to discriminate and classify molecular structure difference of barley seed: Comparison among barley varieties

DRIFT technique was used to detect structural characteristics and identify the structural differences in chemical functional groups of the ground barley seed. Two multivariate analysis methodologies, AHCA and PCA were applied to the SFTIR spectroscopic data sets to organize the produced spectral data for comparison purposes. Since the fingerprint region can be used to identify the type of chemical compounds, primary interests were emphasized on the fingerprint region (1800-800 cm^{-1}) to conduct the multivariate spectral analyses. As the most distinctive variety, CDC Helgason was compared to other five varieties using AHCA and PCA analysis in attempt to access the attributes of varieties. The separation results are visually presented in Figure 3.5. We realized that the analysis results of the six barley varieties overlapped together. Therefore, in this study, the six barley varieties were contrasted to each other respectively to achieve the separation.

The AHCA analysis of the spectra of CDC Helgason compared with other five barley varieties was carried out and shown in Figure 3.5 (left column). Note that except CDC Trey, in other four paired comparisons, spectral data from different varieties can be obviously separated into two individual clusters within a linkage distance 100, implying that CDC Helgason has a different spectroscopic features in contrast with the other four varieties. However, the mixed dendrogram of CDC Helgason and CDC Trey showed similarities of spectral data in fingerprint region between these two varieties.

I: Cluster Analysis (CLA): Fingerprint region **1800-800 cm^{-1}** (barely seed)

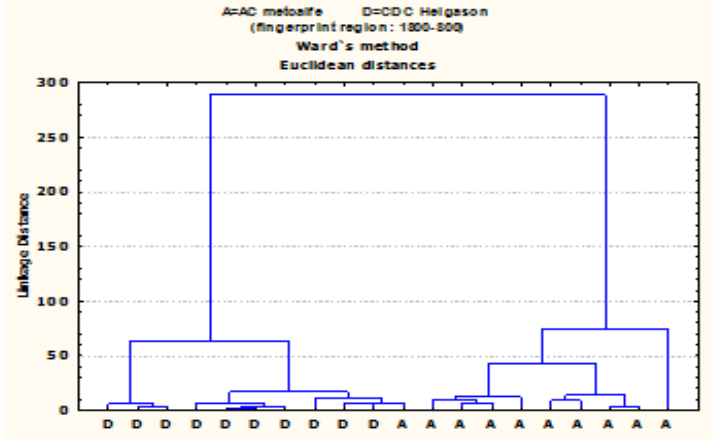

(1) Comparison of CDC Helgason (D) and AC Metcalfe (A)

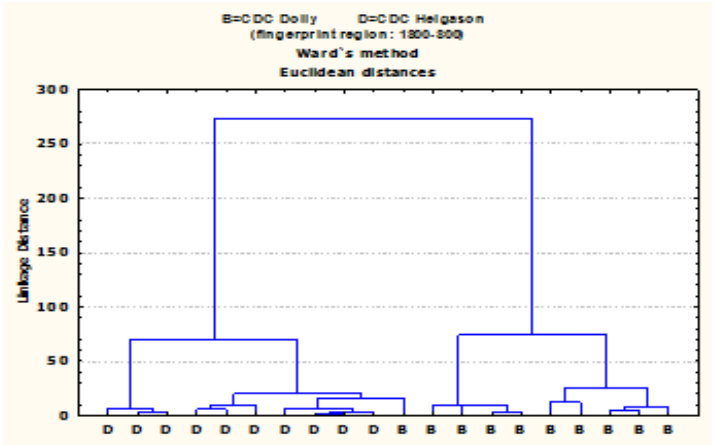

(2) Comparison of CDC Helgason (D) and CDC Dolly (B)

II: Principal component analysis (PCA): Fingerprint region **1800-800 cm^{-1}** (barely seed)

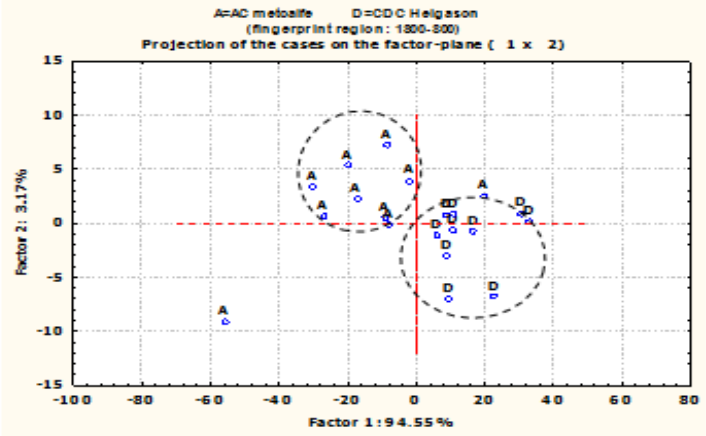

(1) Comparison of CDC Helgason (D) and AC Metcalfe (A): PC1 and PC2 explain 94.55 and 3.17% of the variances, respectively.

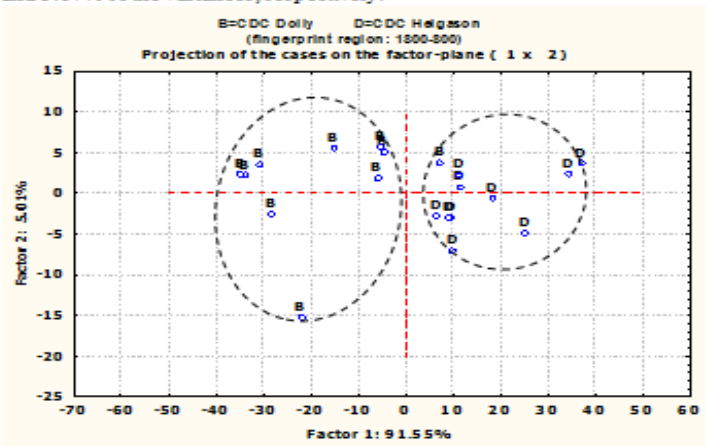

(2) Comparison of CDC Helgason (D) and CDC Dolly (B): PC1 and PC2 explain 91.55 and 5.01% of the variances, respectively.

Figure 3.5 Multivariate spectral analyses of barley structures in the whole seed: comparison of CDC Helgson (D) with other five barley varieties (AC Metcalfe (A), CDC Dolly (B), McLeod (C), CDC Trey (E) and CDC Cowboy (F) I: cluster analysis (1) Select spectral region: fingerprint region: ca. 1800 to 800 cm^{-1}; (2) Distance method: Euclidean; (3) Cluster method: Ward's algorithm; II: principal component analysis: Scatter plots of the 1st principal components (PC1) vs. the 2nd principal components (PC2).

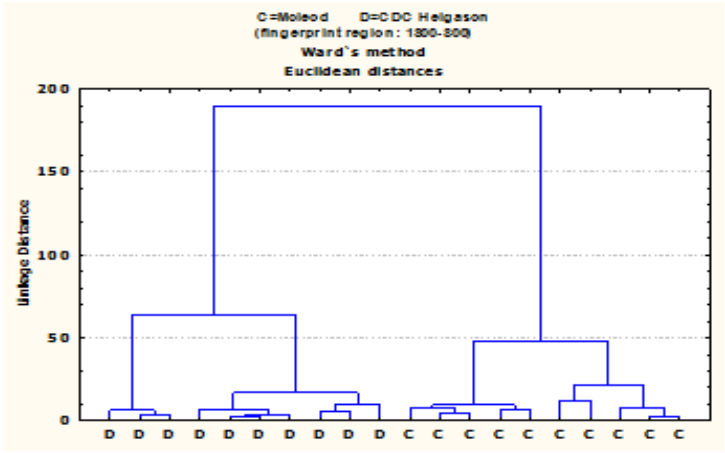

(3) Comparison of CDC Helgason (D) and McLeod (C)

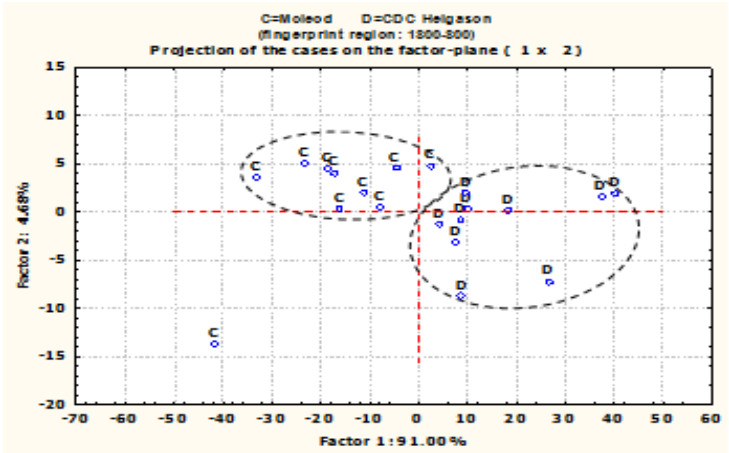

(3) Comparison of CDC Helgason (D) and McLeod (C): PC1 and PC2 explain 91.00 and 4.68% of the variances, respectively.

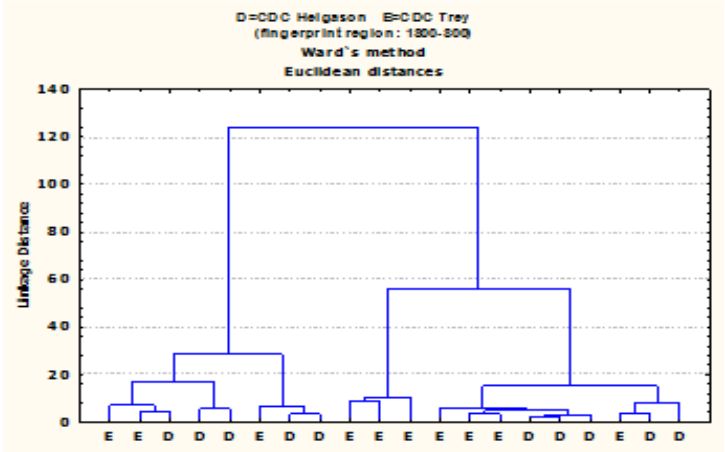

(4) Comparison of CDC Helgason (D) and CDC Trey (E)

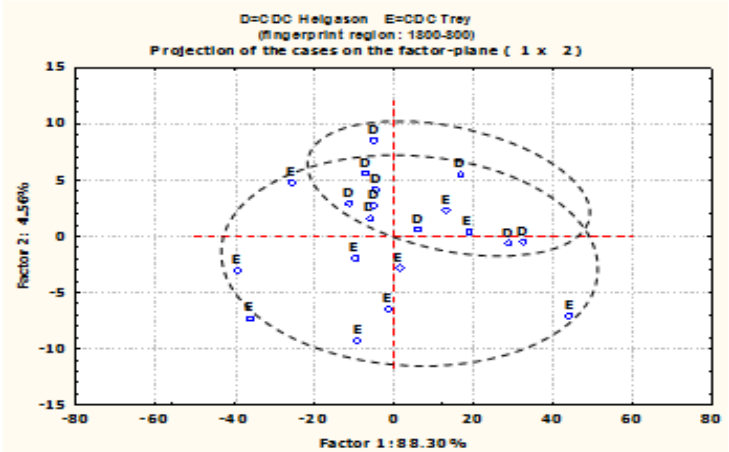

(4) Comparison of CDC Helgason (D) and CDC Trey (E): PC1 and PC2 explain 88.30 and 4.56% of the variances, respectively.

Figure 3.5 (continued) Multivariate spectral analyses of barley structures in the whole seed: comparison of CDC Helgson (D) with other five barley varieties (AC Metcalfe (A), CDC Dolly (B), McLeod (C), CDC Trey (E) and CDC Cowboy (F) I: cluster analysis (1) Select spectral region: fingerprint region: ca. 1800 to 800 cm^{-1}; (2) Distance method: Euclidean; (3) Cluster method: Ward's algorithm; II: principal component analysis: Scatter plots of the 1st principal components (PC1) vs. the 2nd principal components (PC2).

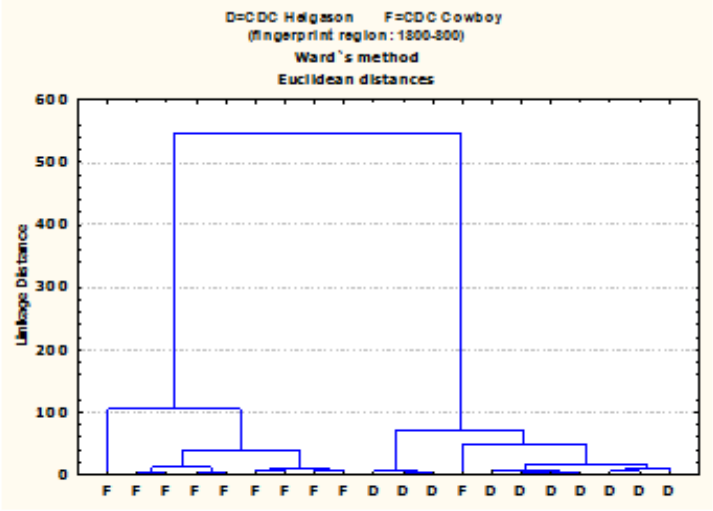

(5) Comparison of CDC Helgason (D) and CDC Cowboy (F)

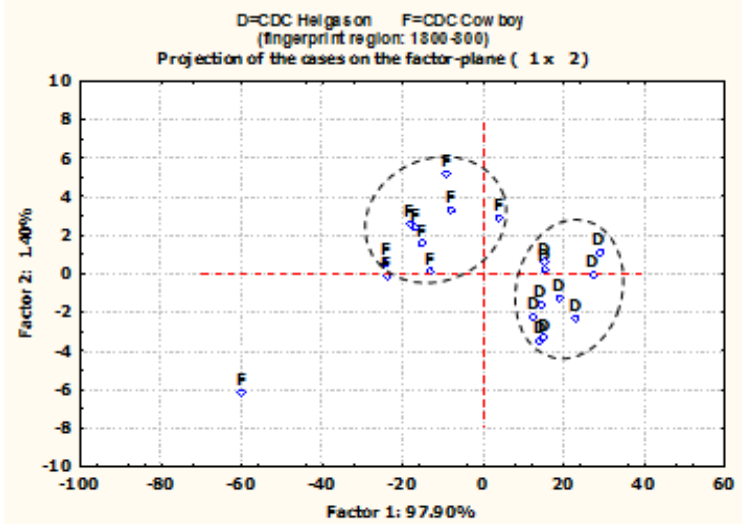

(5) Comparison of CDC Helgason (D) and CDC Cowboy (F): PC1 and PC2 explain 97.90 and 1.40% of the variances, respectively.

Figure 3.5 (continued) Multivariate spectral analyses of barley structures in the whole seed: comparison of CDC Helgson (D) with other five barley varieties (AC Metcalfe (A), CDC Dolly (B), McLeod (C), CDC Trey (E) and CDC Cowboy (F) I: cluster analysis (1) Select spectral region: fingerprint region: ca. 1800 to 800 cm^{-1}; (2) Distance method: Euclidean; (3) Cluster method: Ward's algorithm; II: principal component analysis: Scatter plots of the 1st principal components (PC1) vs. the 2nd principal components (PC2).

PCA analysis results of CDC Helgason compared with other five barley varieties are shown as the 1st principal component (PC1) vs. the 2nd principal component (PC2) plot figure in Figure 3.5 (right column). The first two principal components explained predominant variation (88.30-97.90% for PC1 and 1.40-5.01% for PC2, respectively) of the spectral data. PCA analysis illustrates the same results as that from AHCA analysis, which clearly shows that CDC Helgason was distinguishable with AC Metcalfe, CDC Dolly, McLeod and CDC Cowboy in the PC1 vs. PC2 scatter plot. The barley varieties were grouped in different ellipses to detect the differences of chemical functional groups. It is possible to distinguish CDC Helgason from other barley varieties with the exception of CDC Trey. CDC Trey and CDC Helgason overlapped with each other, implying they have similar spectroscopic information, which may arise from their similarities of chemical and structural composition. Further study is necessary to detect the biological differences between CDC Helgason and CDC Trey.

The paired comparison also exhibited that CDC Cowboy could be clearly distinguished from AC Metcalfe, McLeod and CDC Trey in fingerprint region (see Appendix supplementary material Figure A1).

AHCA and PCA analysis provide statistical evidences that differences exist in chemical and structural conformation among the six barley varieties. This again supports our conclusion that CDC Helgason is particularly unique. Due to the insufficiency of related data from barley, more research is needed to make the classification and comparison among varieties to determine the biological effects on microstructure and other features associated with feed quality. As previously mentioned, in order to gain deeper insights of the chemical differences among these six barley varieties, attention was subsequently focused on the carbohydrates and protein. Comparisons, in collaboration of the multivariate methods, were also made in amide I and II region (1715-1485 cm^{-1}) and CHO region (1185-800 cm^{-1}).

The dendrograms and PCs scatter plots of barley varieties comparisons in protein (amide I and II) region are presented in Figure 3.6. Both the AHCA and PCA analysis illustrate

similar results which are linked to the differences of spectroscopic information associated with chemical and physical properties of barley. As shown in Figure 3.6 (left column), the appearing two cluster indicate that the examined varieties have distinct spectroscopic features in amide I and II region. Except CDC Trey and CDC Dolly, CDC Helgason and other three barley varieties were well separated, forming two clusters.

This separation of varieties is more obviously exhibited in PCA analysis in Figure 3.6 (right column), shown as the scatter plots of the first two PCs. We note that different distribution in PCA plot represent different spectroscopic features linked to inhomogeneous conformation. This segregates varieties into different groups. Although CDC Helgason and CDC Trey form two individual ellipses in y-axis direction, the PC2 only explained 0.68% variation, which is not sufficient to demonstrate their dissimilarity in protein matrix conformation. Correspondingly, the results emphasize that CDC Helgason has thus been successfully differentiated from AC Metcalfe, CDC Dolly, McLeod and CDC Cowboy in amide I and II region, illustrating their dissimilarities in protein amide I and II region of 1715-1485 cm^{-1}. Additionally, CDC Cowboy and CDC Trey can be grouped into different family in protein region, indicating their differences in protein conformation (see Appendix supplementary material Figure A2).

Whereas the relevant information is lacking, it is still difficult to conclude that CDC Helgason and CDC Trey have the same protein structural and chemical make-up. In addition, AHCA and PCA showed inconsistent results of comparison between CDC Dolly and CDC Helgason. An earlier study found that both the β-sheet and α-helices contribute to amide absorption respectively (Jackson and Mantsch 1991). More characterizing methods, such as FSD involving protein secondary structure analysis, may provide new angles on similarities and dissimilarities of chemical and structural information of protein matrix of barley grain. This information may be helpful for rapid evaluation of barley nutrient availability for ruminants.

I: Cluster Analysis (CLA): Fingerprint region **1715-1485 cm^{-1}** (barely seed)

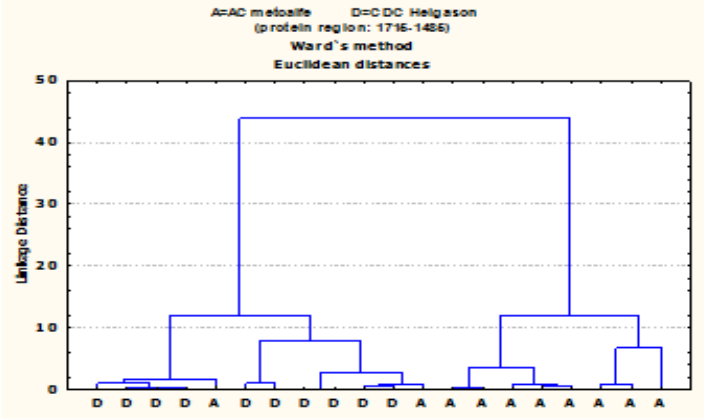

(1) Comparison of CDC Helgason (D) and AC Metcalfe (A)

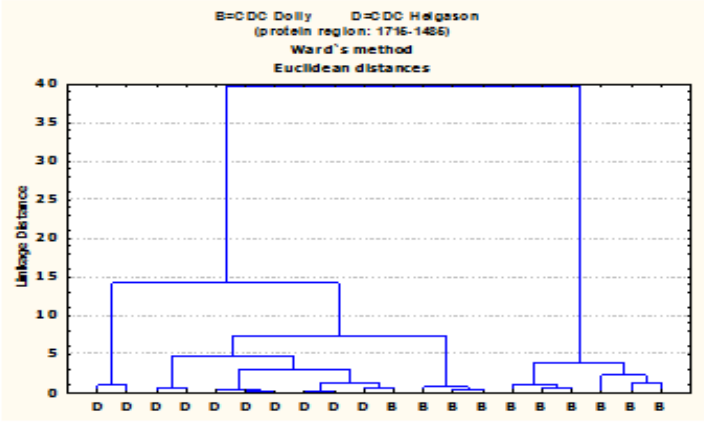

(2) Comparison of CDC Helgason (A) and CDC Dolly (B)

II: Principal component analysis (PCA): Fingerprint region **1715-1485 cm^{-1}** (barely seed)

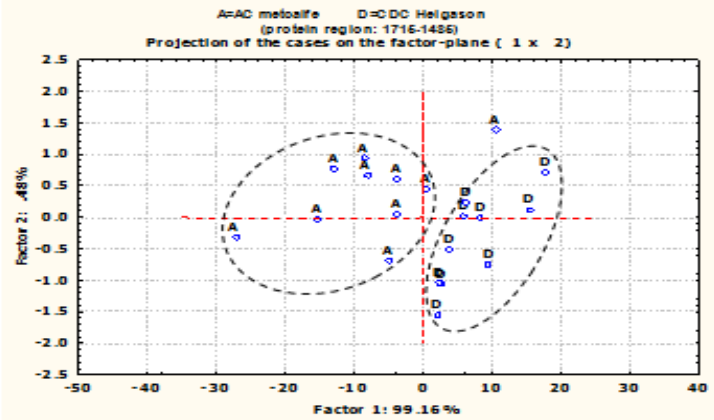

(1) Comparison of CDC Helgason (D) and AC Metcalfe (A): PC1 and PC2 explain 99.16 and 0.48% of the variances, respectively.

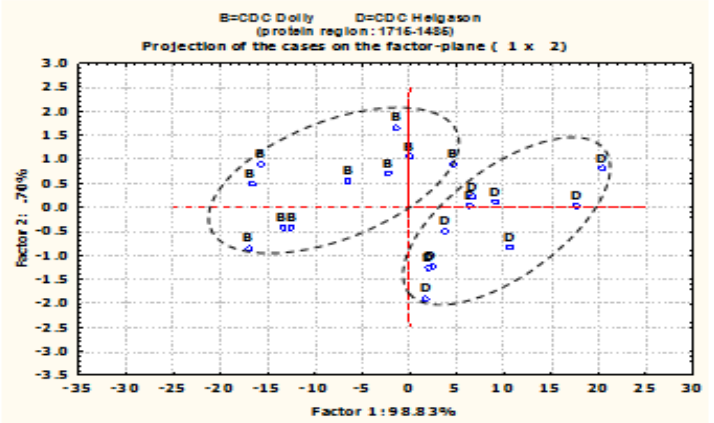

(2) Comparison of CDC Helgason (D) and CDC Dolly (B): PC1 and PC2 explain 98.83 and 0.70% of the variances, respectively.

Figure 3.6 Multivariate spectral analyses of barley structures in the whole seed: comparison of CDC Helgason (D) with other five barley varieties (AC Metcalfe (A), CDC Dolly (B), McLeod (C), CDC Trey (E) and CDC Cowboy (F) I: cluster analysis (1) Select spectral region: amides I and II region: ca. 1715 to 1485 cm^{-1}; (2) Distance method: Euclidean; (3) Cluster method: Ward's algorithm; II: principal component analysis: Scatter plots of the 1st principal components (PC1) vs. the 2nd principal components (PC2).

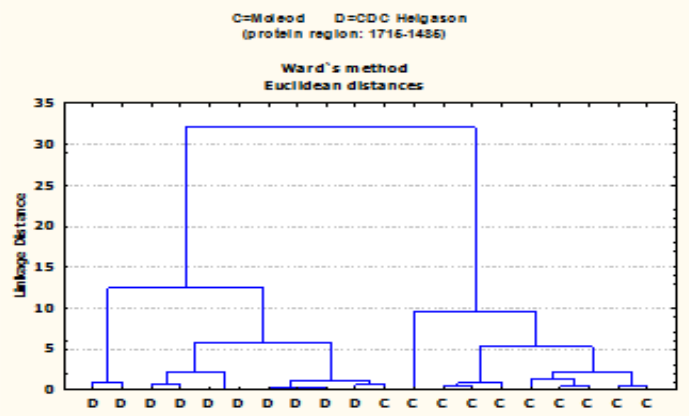

(3) Comparison of CDC Helgason (D) and McLeod (C)

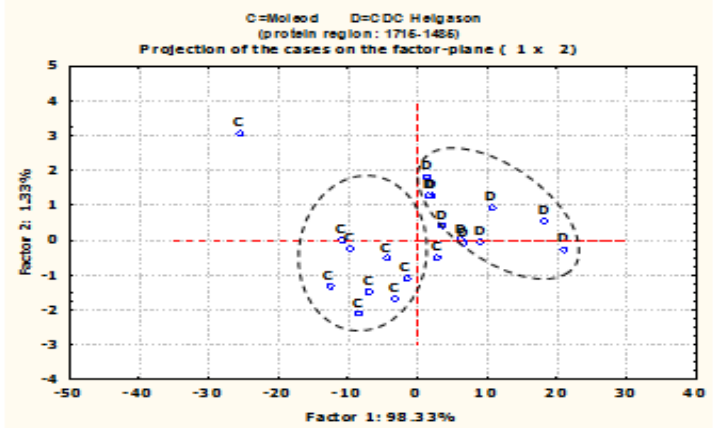

(3) Comparison of CDC Helgason (D) and McLeod (C): PC1 and PC2 explain 98.33 and 1.33% of the variances, respectively.

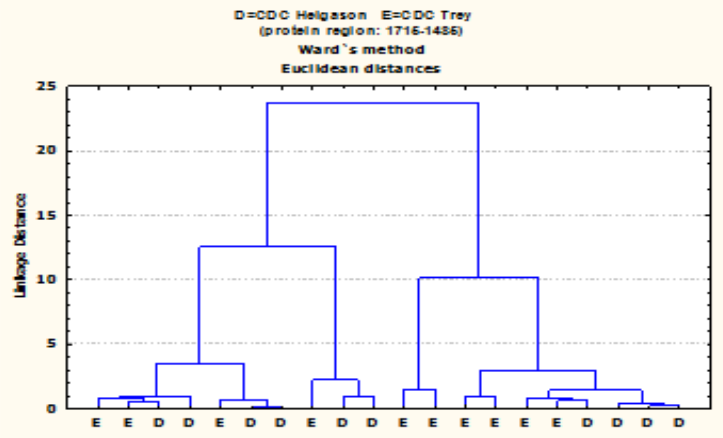

(4) Comparison of CDC Helgason (D) and CDC Trey (E)

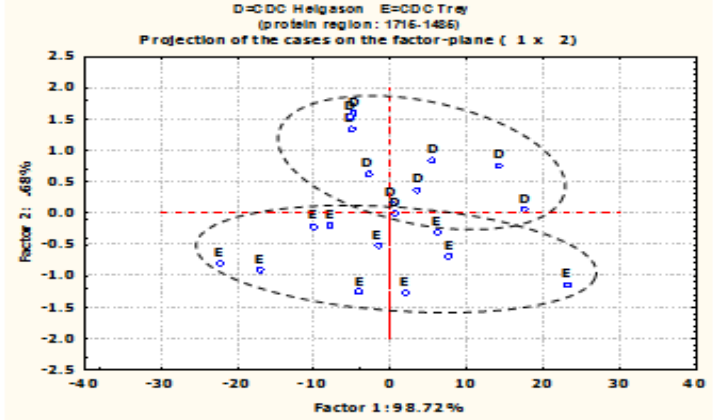

(4) Comparison of CDC Helgason (D) and CDC Trey (E): PC1 and PC2 explain 98.72 and 0.68% of the variances, respectively.

Figure 3.6 (continued) Multivariate spectral analyses of barley structures in the whole seed: comparison of CDC Helgason (D) with other five barley varieties (AC Metcalfe (A), CDC Dolly (B), McLeod (C), CDC Trey (E) and CDC Cowboy (F) I: cluster analysis (1) Select spectral spectral region: amides I and II region: ca. 1715 to 1485 cm^{-1}; (2) Distance method: Euclidean; (3) Cluster method: Ward's algorithm; II: principal component analysis: Scatter plots of the 1st principal components (PC1) vs. the 2nd principal components (PC2).

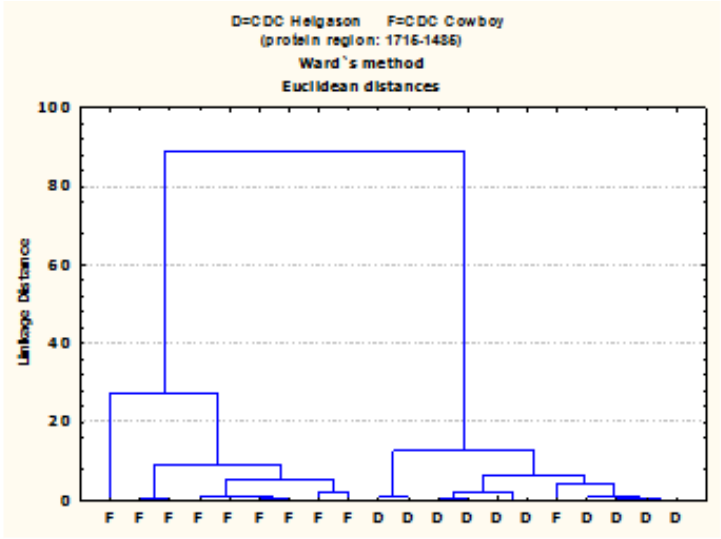

(5) Comparison of CDC Helgason (D) and CDC Cowboy (F)

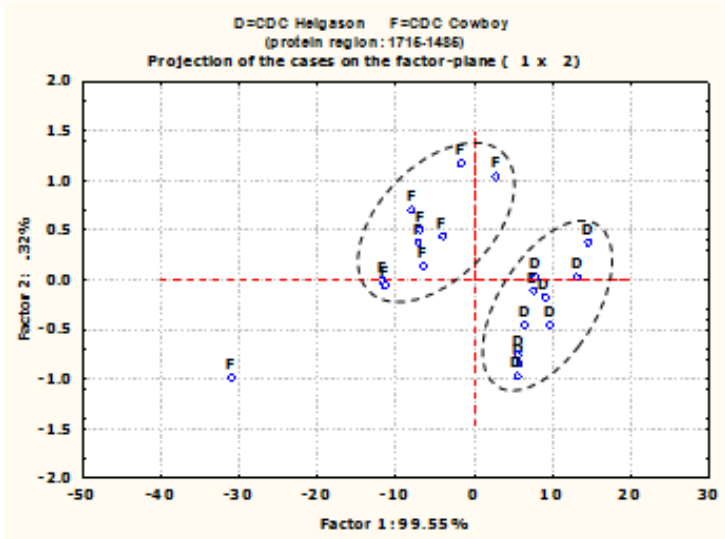

(5) Comparison of CDC Helgason (D) and CDC Cowboy (F): PC1 and PC2 explain 99.55 and 0.32% of the variances, respectively.

Figure 3.6 (continued) Multivariate spectral analyses of barley structures in the whole seed: comparison of CDC Helgason (D) with other five barley varieties (AC Metcalfe (A), CDC Dolly (B), McLeod (C), CDC Trey (E) and CDC Cowboy (F) I: cluster analysis (1) Select spectral spectral region: amides I and II region: ca. 1715 to 1485 cm^{-1}; (2) Distance method: Euclidean; (3) Cluster method: Ward's algorithm; II: principal component analysis: Scatter plots of the 1st principal components (PC1) vs. the 2nd principal components (PC2).

Comparisons were also made in spectral region assigned to CHO from 1185 to 800 cm^{-1} to further analyze the heterogeneity among the six varieties of the barley grain. As illustrated in Figure 3.7, the characteristic bands were examined as well using AHCA and PCA, two multivariate analysis methods. The dendrograms and the PCs scatter plots derived from the original spectral data graphically reveal the differences of structural and chemical make-up. Except CDC Trey, the uniqueness of CDC Helgason in structural and chemical differences was descriptive compared with other four barley varieties. CDC Trey and CDC Helgason could not be completely discriminated even though their degradation rate and extent of starch are significantly different. Presumably, CHO is more diverse than protein in barley, which is in agreement with the earlier study that barley varieties vary markedly in carbohydrates composition (Yu 2007a). Nevertheless, the information of CHO spectral difference using AHCA and PCA is completely lacking. No more references could be found to do further discussion.

By comparing the analysis results, variations were detected among different barley varieties, which evidenced that the protein amides I and II and/or CHO structural and chemical make-up properties of barley may account for the cultivar differences in digestibility for ruminants. The results indicated that the application of AHCA and PCA, two multivariate techniques, with the IR spectroscopy, makes it possible to efficiently discriminate and classify the inherent molecular structural features among the different barley varieties. These methods are especially helpful when unknown tissue is examined. Although the AC Metcalfe and CDC Dolly did not show significant differences using AHCA and PCA analysis of the original spectral data set in this study, another previous work (Yu 2007a) exhibited that these two barley varieties could be distinguished by applying PCA analysis with Fourier self-deconvolution (FSD) spectral data in amide I region (1710-1576 cm^{-1}), indicating more spectral analysis methodologies can be used to expand our understanding of the molecular information of the feed structure.

I: Cluster Analysis (CLA): Fingerprint region **1185-800 cm^{-1}** (barley seed)

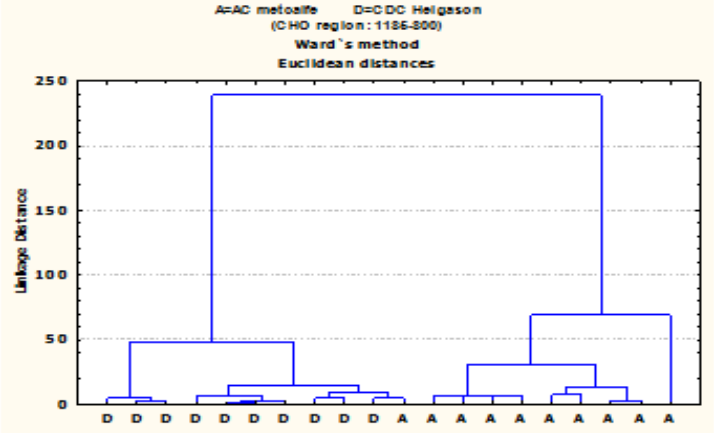

(1) Comparison of CDC Helgason (D) and AC Metcalfe (A)

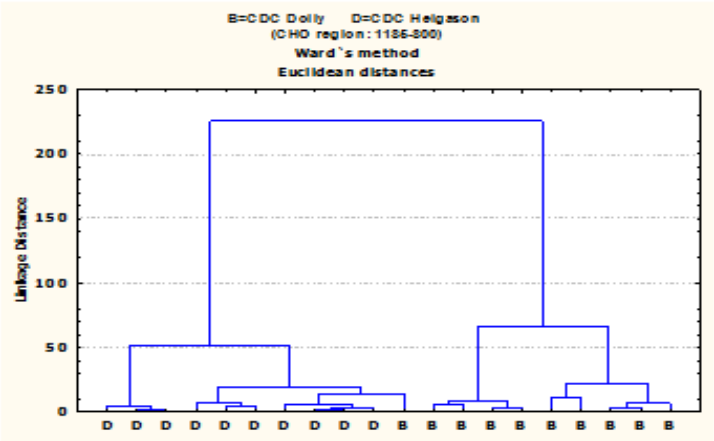

(2) Comparison of CDC Helgason (A) and CDC Dolly (B)

II: Principal component analysis (PCA): Fingerprint region **1185-800 cm^{-1}** (barley seed)

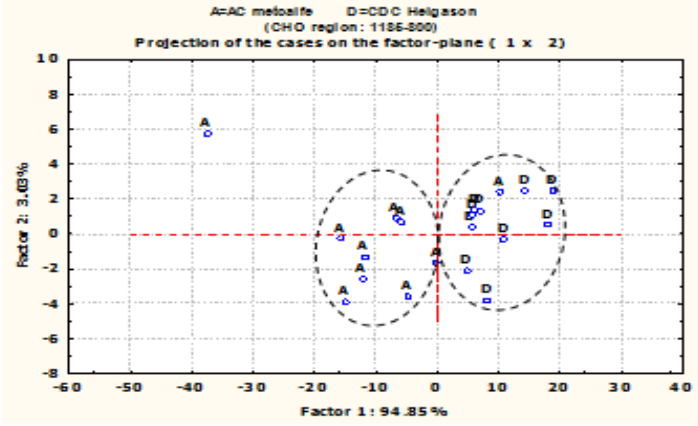

(1) Comparison of CDC Helgason (D) and AC Metcalfe (A): PC1 and PC2 explain 94.85 and 3.03% of the variances, respectively.

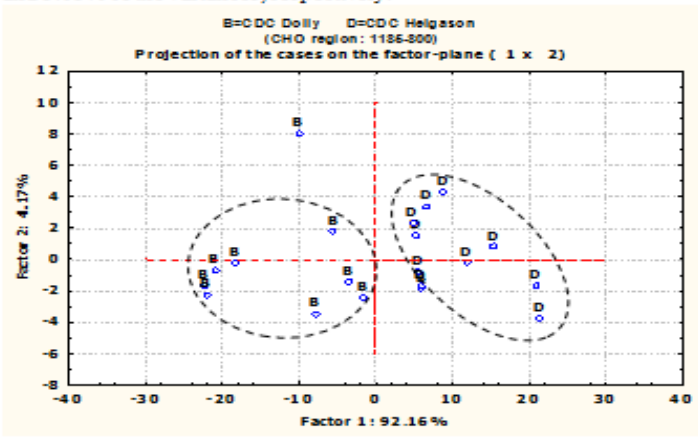

(2) Comparison of CDC Helgason (D) and CDC Dolly (B): PC1 and PC2 explain 92.16 and 4.17% of the variances, respectively.

Figure 3.7 Multivariate spectral analyses of barley structures in the whole seed: comparison of CDC Helgason (D) with other five barley varieties (AC Metcalfe (A), CDC Dolly (B), McLeod (C), CDC Trey (E) and CDC Cowboy (F) I: cluster analysis (1) Select spectral region: carbohydrate region: ca. 1185 to 800 cm^{-1}; (2) Distance method: Euclidean; (3) Cluster method: Ward's algorithm; II: principal component analysis: Scatter plots of the 1st principal components (PC1) vs. the 2nd principal components (PC2).

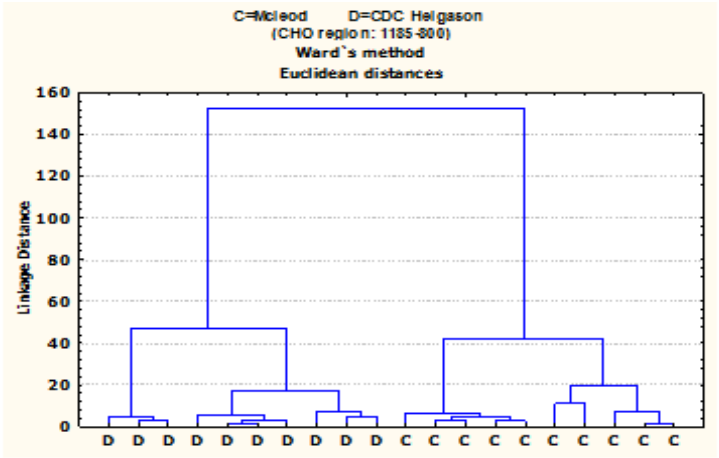

(3) Comparison of CDC Helgason (D) and McLeod (C)

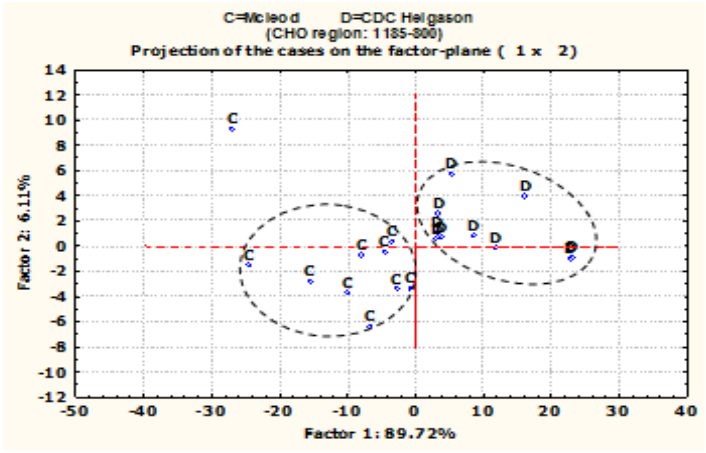

(3) Comparison of CDC Helgason (D) and McLeod (C): PC1 and PC2 explain 89.72 and 6.11% of the variances, respectively.

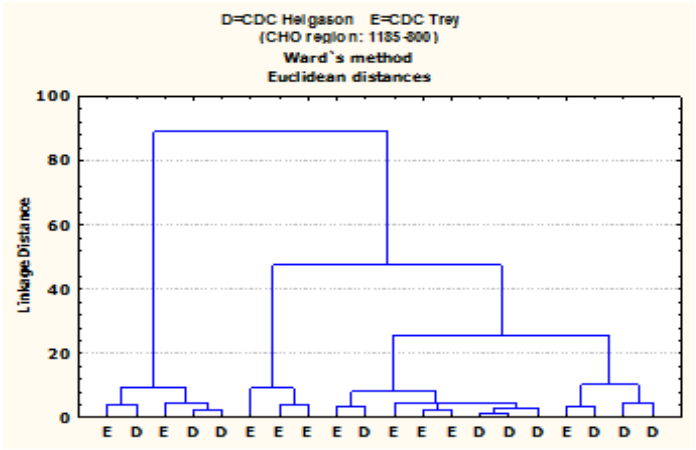

(4) Comparison of CDC Helgason (D) and CDC Trey (E)

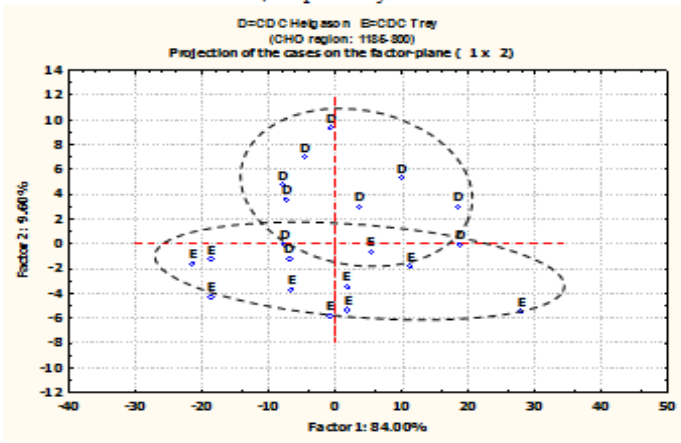

(4) Comparison of CDC Helgason (D) and CDC Trey (E): PC1 and PC2 explain 84.00 and 9.60% of the variances, respectively.

Figure 3.7 (continued) Multivariate spectral analyses of barley structures in the whole seed: comparison of CDC Helgason (D) with other five barley varieties (AC Metcalfe (A), CDC Dolly (B), McLeod (C), CDC Trey (E) and CDC Cowboy (F) I: cluster analysis (1) Select spectral region: carbohydrate region: ca. 1185 to 800 cm^{-1}; (2) Distance method: Euclidean; (3) Cluster method: Ward's algorithm; II: principal component analysis: Scatter plots of the 1st principal components (PC1) vs. the 2nd principal components (PC2).

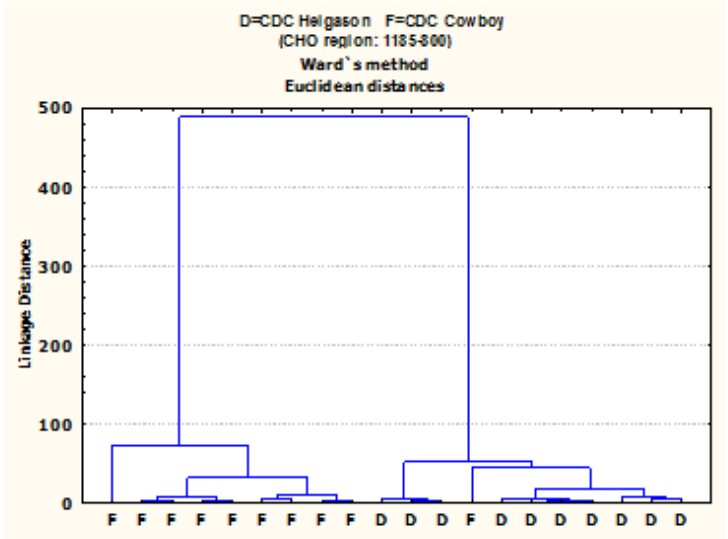

(5) Comparison of CDC Helgason (D) and CDC Cowboy (F)

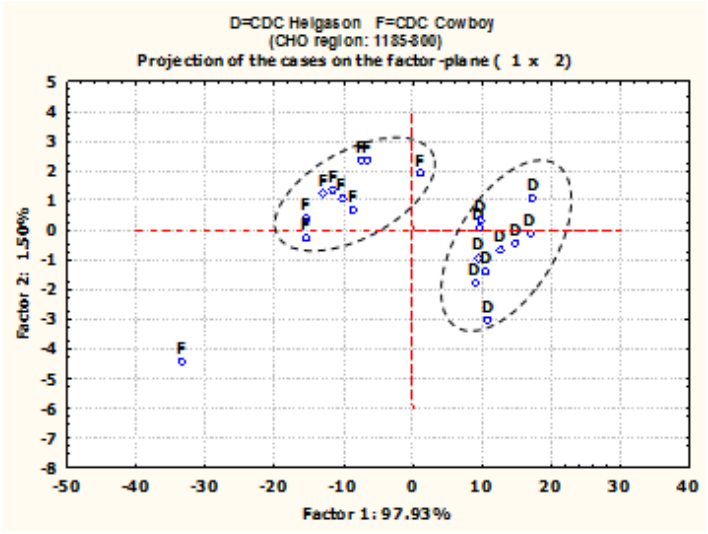

(5) Comparison of CDC Helgason (D) and CDC Cowboy (F): PC1 and PC2 explain 97.93 and 1.50% of the variances, respectively.

Figure 3.7 (continued) Multivariate spectral analyses of barley structures in the whole seed: comparison of CDC Helgason (D) with other five barley varieties (AC Metcalfe (A), CDC Dolly (B), McLeod (C), CDC Trey (E) and CDC Cowboy (F) I: cluster analysis (1) Select spectral region: carbohydrate region: ca. 1185 to 800 cm^{-1}; (2) Distance method: Euclidean; (3) Cluster method: Ward's algorithm; II: principal component analysis: Scatter plots of the 1st principal components (PC1) vs. the 2nd principal components (PC2).

Paired comparison of CDC Cowboy and four other varieties (AC Metcalfe, CDC Dolly, McLeod and CDC Trey) was computed. DRIFT spectral data of hull samples from six barley varieties and the SFTIRM data sets were also analyzed using these two multivariate methods. However, the results showed that it cannot be completely grouped in separate cluster (for AHCA) or ellipse (for PCA) because of overlapping of each paired comparison (data not shown). This may demonstrate that the microstructures of the hull and endosperm tissues from these barley varieties are quite similar to each other. Since this approach is so novel that few data have been reported, it should be pointed out that the structural information obtained from these two analysis methods is not the only determinant of cultivar variation. More study involving other structures of the barley kernel, such as pericarp or aleurone, may provide further insight into the varieties differences. Chemical mapping techniques may also provide further understanding on the similarities and dissimilarities.

3.4. Conclusions

Traditional chemical analysis methods are difficult to explore the structure or spatial conformation of feed samples. Failure to detect structural information and chemical distribution of complex biological organisms using traditional chemical analysis drives the development of novel research methodologies. DRIFT and SFTIRM techniques were used to investigate the structural and chemical features of barley varieties. The differences in chemical functional groups' characteristics, which are associated with feed nutrients, were determined in order to compare barley varieties. The results indicated that FTIR spectroscopy techniques could be applied to the detection of nutrients- related compounds that exist in barley grain. Therefore, the utilization of FTIR techniques for complex organic samples can be worthy to develop.

It is also conclusive that the differences in the chemical make-up features of whole seed and hull samples from the six barley varieties can be detected using DRIFT spectroscopy. The barley varieties can be differentiated with small sample volumes using this technique in comparison to traditional chemical analysis methodologies. The obtained results also indicated that the multivariate analysis methods (AHCA and PCA) can graphically

distinguish structural and chemical differences with spectroscopic information. With these two multivariate spectral analysis techniques applied to the whole seed samples, CDC Helgason was distinguished from AC Metcalfe, CDC Dolly, McLeod and CDC Cowboy in the fingerprint (1800-800 cm^{-1}) and CHO region (1185-800 cm^{-1}), from AC Metcalfe, McLeod and CDC Cowboy in the protein region (1715-1485 cm^{-1}). However, CDC Helgason could not be distinguished from CDC Trey in either protein/CHO region or fingerprint region even though they exhibited significantly different degradation rate and extent using *in situ* technique. In addition, the results indicated that these six barley varieties may have similar structures of hull, but significant differences in whole seed.

Ultra-spatial resolved synchrotron IR microspectroscopy was used to monitor the intrinsic distribution of chemical compounds associated with nutrition in barley endosperm tissue. The informative results reflected that SFTIR spectroscopic analysis with excellent ultra-spatial resolution allows the determination of spectral data with structural and chemical information of the specimens in microscopic regions. In addition, the synchrotron light source is preferred because of its superior brightness and S/N ratio.

The different grain properties of barley varieties may arise from their heterogeneous nature of barley endosperm tissue. The structural differences among the barley varieties may be one reason of various digestive behaviours and nutritive quality to ruminants. Information from this study involving probing the seed internal structure of barley may provide a further insight as to why barley varieties exhibit different biodegradation behaviours. To provide an informative characterization of samples on both the feed quality evaluation and breeding selection, this technique is worth developing practically from theories.

4. GENERAL DISCUSSION AND CONCLUSIONS

4.1. General discussion and conclusions

The results of this study show that there were significant differences in the mean and median particle size, and rumen degradation kinetics of each individual nutrient (DM, CP and starch) among the six barley varieties.

Based on the results obtained from *in situ* and mid-IR spectroscopy, it can be concluded that significant variation exists in structural and chemical composition among barley varieties. In addition, it is possible to select specific barley varieties for different purposes depending on these biochemical differences. Suitable barley grains for feed purpose are expected to have large particle size after simple processing and more starch and dietary protein can reach the small intestine to benefit the animal. Based on the *in situ* study, CDC Helgason exhibited the lowest degradation rate and extent of all nutrients (DM, CP and starch) among the six barley varieties, indicating that CDC Helgason may be the most ideal barley variety for feed purpose compared with the other five barley varieties. AC Metcalfe, a barley variety for malting purpose, has a faster degradation rate and greater degradation extent than feed type barely. An interesting result from this study is that CDC Trey, a barley variety for feed purpose, exhibits quite similar parameters in terms of particle size, degradation rate to the malting-purpose barley AC Metcalfe.

Inherent structural differences among the seeds of the six barley varieties in terms of hull, endosperm and whole seeds were detected by the DRIFT Spectroscopy and SFTIRM with univariate and multivariate spectral analyses. The results showed that the spectral profiling differed among the barley samples. The differences in particle size and structural and chemical make-up features may explain the various degradation characteristics exhibited in the rumen among the six barley varieties. Through application of these two multivariate techniques with the FTIR spectroscopy, it is possible to discriminate and classify the inherent molecular structural features among the different varieties. The AHCA and PCA enable us to deal with the informative data set. CDC

Helgason was distinguished from AC Metcalfe, CDC Dolly, McLeod and CDC Cowboy in fingerprint (1800-800 cm^{-1}) and CHO region(1185-800 cm^{-1}), from AC Metcalfe, McLeod and CDC Cowboy in protein region (1715-1485 cm^{-1}). However, CDC Helgason cannot be distinguished from CDC Trey in either protein/CHO region or fingerprint region using these two methods with spectroscopic information though they have significant different degradation features. This suggests further spectroscopic analysis, such as IR imaging, FSD and 2^{nd} derivative data treatment may be necessary. Mapping can also be utilized to identify the chemical compounds' distribution of region and track the difference. Besides the protein, CHO and fingerprint region, other spectral regions associated with nutrients (for example, CH component bands centered at 2925 cm^{-1} and CHO bands centered at 930 cm^{-1} and 860 cm^{-1}) can also be examined in the future.

Significant correlations were found between median particle size (not mean particle size) and the rate and extent of rumen degradation, but no strong correlations were found between spectral functional groups' intensity and their ratios and *in situ* data.

The studies demonstrated the potential of ultraspatially resolved synchrotron based technology (SFTIRM) to reveal the structural and chemical make-up within cellular and subcellular dimensions without destruction of the inherent structure of cereal seed tissue. With the SFTIRM techniques, the structural characteristics of the cereal seeds were illuminated among different cultivars at highly spatial resolution. The structural differences of barley seeds may be one reason for the various digestive behaviours and nutritive values for ruminants. Examination of other tissues such as aleurone layer and pericarp may provide further insight as to why barley verities exhibit different biodegradation behaviours, and provide a deeper and better indication of the chemical make-up and structural information.

The potential of mid-IR IR techniques in feed science has emerged from this study and other recent reports. More research is needed to achieve a deeper understanding of grains' complexity and improve these spectroscopic techniques to be more mature in feed science.

4.2. Industry application

Infrared spectroscopy can be used in industrial and related field for quantitative and qualitative analysis of organic or inorganic ingredients. The rising number of research publications involving FTIR techniques in feed science heralds a broader future for commercial application. Such a tool can enable plant breeders to optimize cultivar selection strategies by rapidly analyzing the grains without chemical degradation. The genetic relationship of plants can be characterized and identified according to the spectral information. Combined with the multivariate spectral analyses (for example, AHCA and PCA), the FTIR techniques make it possible to characterise varieties in a short time. It can also be used for grain evaluation. The main constituents of grains are water, carbohydrates, protein, fat, fibre, and minerals. Using FTIR techniques, the structural and chemical composition information associated with nutrients can be rapidly obtained from a small volume of samples and make it possible to predict the feed quality to diminish the risk of metabolic disorders.

It is worth doing more studies to establish a rapid, non-destructive analytical technique to meet analytical needs. It can be developed as an effective method for nutritionists, cereal breeders, food and feed chemists, grain processors and scientists. To serve the industrial analytical requirement, there is a need to select representative samples for model establishment. A large number of analyses are also needed to ensure the accuracy. However, with a mature prediction models, feed samples can be evaluated directly and rapidly with minimal pre-treatment to obtain detailed information on chemical compounds.

4.3. Future research

The application of FTIR techniques in combination with other chemical analysis can avoid structural information losses and evaluate the quality of barley grain more exactly and accurately. More study is needed to improve the effectiveness of analysis methods and provide further understanding of the relationship between structural and nutritional characteristics of feedstuffs. Suggestions for future research include expanded research to

determine the relationship between feed inherent structure and degradation behaviours by using many different feedstuffs with a large range in rumen degradability. Further analysis is needed to determine differences in protein and carbohydrate molecular conformation among feedstuffs. Additionally, grain hardness, small and large starch granule ratio and conformation in endosperm tissue are also of interest. Partial Least Squares (PLS) analysis associated with Mid-IR spectroscopy can also be employed to provide deeper understanding of the structural and chemical make-up information of the feedstuffs.

LIST OF REFERENCES

Association of Official Analytical Chemists. 1997. Official Methods of Analysis of the Association of Official Analytical Chemists, 16th ed. AOAC, Arlington, VA.

Bamba, T. 2002. In-situ chemical analyses of trans-polyisoprene by histochemical staining and Fourier transform infrared microspectroscopy in a rubber-producing plant, Eucommia ulmoides Oliver. Planta. 215 (6): 934.

Barth, A. 2007. Infrared spectroscopy of proteins. Biochim. Biophys. Acta. 1767 (9): 1073-1101.

Black, M. 2000. Seed technology and its biological basis. CRC Press, Boca Raton, Fla. 419 pp.

Bowman, J. G. P., Blake, T. K., Surber, L. M. M., Habernicht, D. K. and Bockelman, H. 2001. Feed-quality variation in the barley core collection of the USDA National Small Grains Collection. Crop Sci. 41 (3): 863-870.

Budevska, B. O. 2002. Vibrational spectroscopy imaging of agricultural products. Pages 3720-3732 *in* J. M. Chalmers, P. R. Griffiths, eds. Handbook of Vibrational Spectroscopy. J. Wiley, Hoboken, NJ.

Camm, G. A. 2008. Grain Hardness and Slow Dry Matter Disappearance Rate in Barley. M. Sc. thesis. University of Saskatchewan, Saskatoon, SK.

Canadian Council on Animal Care. 1993. Guide to the care and use of experimental animals. 2nd ed. Canadian Council on Animal Care, Ottawa. 298 pp.

Canadian Food Inspection Agency. 2007. List of varieties which are registered in Canada. [Online] Available: http://www.inspection.gc.ca/english/plaveg/variet/lovric.pdf [July, 2009].

Church, D. C. 1991. Livestock feeds and feeding. 3rd ed. Prentice Hall, Englewood Cliffs, NJ. 546 pp.

Davies, T. and Fearn, T. 2004. Back to basics: the principles of principal component analysis. Spectrosc. Eur. 16 (6): 20.

Diem, M., Romeo, M., Matthäs, C., Miljkovic, M., Miller, L. and Lasch, P. 2004. Comparison of Fourier transform infrared (FTIR) spectra of individual cells acquired using synchrotron and conventional sources. Infrared Phys. Technol. 45 (5-6): 331-338.

Doiron, K. 2009. Characterization of autoclaved flaxseed as feed for ruminants using conventional and Mid-IR spectroscopic based approaches. M. Sc. thesis. University of Saskatchewan, Saskatoon, SK.

Du, L. 2009. Hull, ferulic acid, para-coumaric acid content and particle size characteristics of various barley varieties in relation to nutrient availability in ruminants. M. Sc. thesis. University of Saskatchewan, Saskatoon, SK.

Du, L., Yu, P., Rossnagel, B. G., Christensen, D. A. and McKinnon, J. J. 2009. Physicochemical characteristics, hydroxycinnamic acids (ferulic acid, P-coumaric acid) and their ratio, and *in situ* biodegradability: comparison of genotypic differences among six barley varieties. J. Agric. Food Chem. 57 (11): 4777-4783.

Dumas, P., Jamin, N., Teillaud, J. L., Miller, L. M. and Beccard, B. 2004. Imaging capabilities of synchrotron infrared microspectroscopy. Faraday Discuss. 126: 289-302.

Dumas, P. and Miller, L. 2003. The use of synchrotron infrared microspectroscopy in biological and biomedical investigations. Vib. Spectrosc. 32 (1): 3-21.

Dumas, P., Sockalingum, G. D. and Sule-Suso, J. 2007. Adding synchrotron radiation to infrared microspectroscopy: what's new in biomedical applications? Trends Biotechnol. 25 (1): 40-44.

Dunteman, G. H. 1989. Principal components analysis. Sage Publications, Newbury Park, CA. 96 pp.

Figroid, W., Hale, W. H. and Theurer, B. 1972. An evaluation of the nylon bag technique for estimating rumen of grains. J. Anim. Sci. 35 (1): 113-120.

Foley, A. E., Hristov, A. N., Melgar, A., Ropp, J. K., Etter, R. P., Zaman, S., Hunt, C. W., Huber, K. and Price, W. J. 2006. Effect of barley and its amylopectin content on ruminal fermentation and nitrogen utilization in lactating dairy cows. J. Dairy Sci. 89 (11): 4321-4335.

Food and Agriculture Organization. 2007. Food balance sheet-excluding beer. [Online] Available: http://faostat.fao.org/default.aspx [July, 2009].

Gan, G., Ma, C. and Wu, J. 2007. Data Clustering: Theory, Algorithms, and Applications (ASA-SIAM Series on Statistics and Applied Probability). Society for Industrial and Applied Mathematics Philadelphia , PA. 466 pp.

Griffiths, P. R. and De Haseth, J. A. 1986. Fourier transform infrared spectrometry. Wiley, New York. 656 pp.

Hale, W. H. 1973. Influence of processing on the utilization of grains (starch) by ruminants. J. Anim. Sci. 37 (4): 1075.

Hart, K. J., Rossnagel, B. G. and Yu, P. 2008. Chemical characteristics and in situ ruminal parameters of barley for cattle: Comparison of the malting cultivar AC Metcalfe and five feed cultivars. Can. J. Anim. Sci. 88: 711-719.

Harvey, B. L. and Rossnagel, B. G. 1984. Harrington barley. Can. J. Plant Sci. 64(1): 193-194.

Herrera-Saldana, R. E., Huber, J. T. and Poore, M. H. 1990. Dry matter, crude protein, and starch degradability of five cereal grains. J. Dairy Sci. 73 (9): 2386-2393.

Himmelsbach, D. S., Khalili, S. and Akin, D. E. 1998. FT-IR microspectroscopic imaging of flax (Linum usitatissimum L.) stems. Cell. Mol. Biol. (Noisy-Le-Grand). 44 (1): 99-108.

Hindle, V. A., Vuuren van, A. M., Klop, A., Mathijssen-Kamman, A. A., van Gelder, A. H. and Cone, J. W. 2005. Site and extent of starch degradation in the dairy cow - a comparison between *in vivo*, *in situ* and *in vitro* measurements. J. Anim. Physiol. Anim. Nutr. 89 (3-6): 158-165.

Holopainen, U. R., Wilhelmson, A., Salmenkallio-Marttila, M., Peltonen-Sainio, P., Rajala, A., Reinikainen, P., Kotaviita, E., Simolin, H. and Home, S. 2005. Endosperm structure affects the malting quality of barley (*Hordeum vulgare* L.). J. Agric. Food Chem. 53 (18): 7279-7287.

Holtekjøen, A. K., Uhlen, A. K., Bråhen, E., Sahlstrø, S. and Knutsen, S. H. 2006. Contents of starch and non-starch polysaccharides in barley varieties of different origin. Food Chem. 94 (3): 348-358.

Homan, J. A., Radel, J. D., Wallace, D. D., Wetzel, D. L. and Levine, S. M. 2000. Chemical changes in the photoreceptor outer segments due to iron induced oxidative stress: analysis by Fourier transform infrared (FT-IR) microspectroscopy. Cell. Mol. Biol. (Noisy-Le-Grand). 46 (3): 663-672.

Jackson, M. and Mantsch, H. H. 1991. Protein secondary structure from FT-IR spectroscopy: Correlation with dihedral angles from three-dimensional Ramachandran plots. Can. J. Chem. 69 (11): 1639-1642.

Jackson, M. and Mantsch, H. H. 2000. Infrared spectroscopy ex vivo tissue analysis. Pages 131-156 *in* RA Myers, ed. Encyclopedia of Analytical Chemistry. John Wiley & Sons Ltd, Chichester, England.

Jain, A. K., Murty, M. N. and Flynn, P. J. 1999. Data clustering: a review. ACM computing surveys. 31 (3): 264 - 323.

Jolliffe, I. T. 2002. Principal component analysis. 2nd ed. Springer, New York, NY, 487pp.

Kaufman, L. and Rousseeuw, P. J. 1990. Finding groups in data: an introduction to cluster analysis. Wiley, New York. 342 pp.

Keunen, J. E., Plaizier, J. C., Kyriazakis, L., Duffield, T. F., Widowski, T. M., Lindinger, M. I. and McBride, B. W. 2002. Effects of a subacute ruminal acidosis model on the diet selection of dairy cows. J. Dairy Sci. 85 (12): 3304-3313.

Kellems, R. O. and Church, D. C. 2002. Livestock feeds and feeding. 5th ed. Prentice Hall, Upper Saddle River, NJ. 654 pp.

Khorasani, G. R., Helm, J. and Kennelly, J. J. 2000. *In situ* rumen degradation characteristics of sixty cultivars of barley grain. Can. J. Anim. Sci. 80 (4): 691-701.

Kulp, K. and Ponte, J. G. 2000. Handbook of cereal science and technology. 2nd , rev. and expand ed. Marcel Dekker, New York. 790 pp.

Langrell, D. E., Edney, M. J. and Izydorczyk, M. S. 2008. Quality of western Canadian malting barley. Canadian Grain Commission, Winnipeg.

Legge, W. G. 2003. AC Metcalfe barley. Can. J. Plant Sci. 83 (2): 381-384.

LeVine, S. M., Radel, J. D., Sweat, J. A. and Wetzel, D. L. 1999. Microchemical analysis of retina layers in pigmented and albino rats by Fourier transform infrared microspectroscopy. Biochim. Biophys. Acta. 1473 (2-3): 409-417.

LeVine, S. M. and Wetzel, D. L. 1994. *In situ* chemical analyses from frozen tissue sections by Fourier transform infrared microspectroscopy. Examination of white matter exposed to extravasated blood in the rat brain. Am. J. Pathol. 145 (5): 1041-1047.

LeVine, S. M. and Wetzel, D. L. 1998. Chemical analysis of multiple sclerosis lesions by FT-IR microspectroscopy. Free Radic. Biol. Med. 25 (1): 33-41.

Levine, S. M. and Wetzel, D. L. B. 1993. Analysis of brain tissue by FT-IR microspectroscopy. Appl. Spectrosc. Rev. 28 (4): 385-412.

Marinkovic, N. S. and Chance, M. R. 2005. Synchrotron infrared microspectroscopy. Page 671–708 *in* R. Meyers, ed. Encyclopedia of Molecular Cell Biology and Molecular Medicine. Wiley, New York.

Marinkovic, N. S., Huang, R., Bromberg, P., Sullivan, M., Sperber, E., Moshe, S., Miller, L. M., Jones, K., Chouparova, E. and Franzen, S. 2002. Center for Synchrotron Biosciences' U2B Beamline: an international resource for biological infrared spectroscopy. J. Synchrotron Rad. 9 (part 4): 189–197.

Messerschmidt, R. G. and Harthcock, M. A. 1988. Infrared microspectroscopy: theory and applications. H. Dekker, New York, NY. 282 pp.

Mikel, M. A. and Kolb, F. L. 2008. Genetic Diversity of Contemporary North American Barley. Crop Sci. 48 (4): 1399-1407.

Miller, L. M. 2002. Infrared microspectroscopy and imaging. National Synchrotron Light Source, Brookhaven National Laboratory, Internal publication. [Online] Available: http://www.nsls.bnl.gov/newsroom/publications/otherpubs/imaging/workshopmiller.pdf [July, 2009].

Miller, L. M., Carr, G. L., Jackson, M., Dumas, P. and Williams, G. P. 2000. The impact of infrared synchrotron radiation in biology: Past, present and future. Synchrotron Radiation News. 13 (5): 31-38.

Miller, L. M. and Dumas, P. 2006. Chemical imaging of biological tissue with synchrotron infrared light. Biochim. Biophys. Acta. 1758 (7): 846-857.

Miller, L. M., Wang, Q., Smith, R. J., Zhong, H., Elliott, D. and Warren, J. 2007. A new sample substrate for imaging and correlating organic and trace metal composition in biological cells and tissues. Anal. Bioanal. Chem. 387 (5): 1705-1715.

Mills, E. N. C., Parker, M. L., Wellner, N., Toole, G., Feeney, K. and Shewry, P. R. 2005. Chemical imaging: the distribution of ions and molecules in developing and mature wheat grain. J. Cereal Sci. 41 (2): 193-201.

National Research Council. 2001. Nutrient Requirements of Dairy Cattle. National Academy Press, Washington, D.C.

Nelson, D. L. and Cox, M. M. 2005. Lehninger principles of biochemistry. WH Freeman, New York, NY 1119 pp.

Nocek, J. E. 1988. *In situ* and other methods to estimate ruminal protein and energy digestibility: a review. J. Dairy Sci. 71 (8): 2051-2069.

Nocek, J. E. and Tamminga, S. 1991. Site of digestion of starch in the gastrointestinal tract of dairy cows and its effect on milk yield and composition. J. Dairy Sci. 74 (10): 3598-3629.

OMAF Feed Advisory Program. 2009. Cereal Crops - Barley, Oats, Wheat. [Online] Available: http://www.omafra.gov.on.ca/english/crops/field/cereal.html [July, 2009].

Ørskov, E. R. 1986. Starch digestion and utilization in ruminants. J. Anim. Sci. 63 (5): 1624-1633.

Ørskov, E. R. and McDonald, I. 1979. The estimation of protein degradability in the rumen from incubation measurements weighted according to rate of passage. J. Agric. Sci. 92 (part 2): 499-503.

Pietrzak, L. N. and Miller, S. S. 2005. Microchemical structure of soybean seeds revealed *in situ* by ultraspatially resolved synchrotron Fourier transformed infrared microspectroscopy. J. Agric. Food Chem. 53 (24): 9304-9311.

Plaizier, J. C., Krause, D. O., Gozho, G. N. and McBride, B. W. 2008. Subacute ruminal acidosis in dairy cows: The physiological causes, incidence and consequences. Vet. J. 176 (1): 21-31.

Raab, T. K. and Martin, M. C. 2001. Visualizing rhizosphere chemistry of legumes with mid-infrared synchrotron radiation. Planta. 213 (6): 881-887.

Romesburg, H. C. 1984. Cluster analysis for researchers. Lifetime Learning Publications, Belmont, CA. 334 pp.

Rossnagel, B. G. and Harvey, B. L. 1994. CDC Dolly Two-row Feed Barley. 38: 109. Barley Newsletter. American Malting Barley Association, Inc., Milwaukee, WI.

SAS. 2003. User's guide: Statistics. 9th ed. SAS Institute, Inc., Cary, NC.

Slafer, G. A. 2002. Barley science: recent advances from molecular biology to agronomy of yield and quality. Food Products Press, Binghamton, NY. 565 pp.

Sniffen, C. J., O'Connor, J. D., Van Soest, P. J., Fox, D. G. and Russell, J. B. 1992. A net carbohydrate and protein system for evaluating cattle diets: II. Carbohydrate and protein availability. J. Anim. Sci. 70 (11): 3562-3577.

Stuart, B. 2004. Infrared spectroscopy: fundamentals and applications. J. Wiley, Chichester, West Sussex, England; Hoboken, NJ.

Takeda, Y., Takeda, C., Mizukami, H. and Hanashiro, I. 1999. Structures of large, medium and small starch granules of barley grain. Carbohydr. Polym. 38 (2): 109-114.

Tamminga, S., Van Straalen, W. M., Subnel, A. P. J., Meijer, R. G. M., Steg, A., Wever, C. J. G. and Blok, M. C. 1994. The Dutch protein evaluation system: the DVE/OEB-system. Livest. Prod. Sci. 40 (2): 139-155.

Tamminga, S., Vuuren, A. M., Koelen, C. J., Ketelaar, R. S. and Togt, P. L. 1990. Ruminal behaviour of structural carbohydrates, non-structural carbohydrates and crude protein from concentrate ingredients in dairy cows. Neth. J. Agric. Sci. 38 (3): 513-526.

Tester, R. F., Karkalas, J. and Qi, X. 2004. Starch—composition, fine structure and architecture. J. Cereal Sci. 39 (2): 151-165.

Theurer, C. B. 1986. Grain processing effects on starch utilization by ruminants. J. Anim. Sci. 63 (5): 1649-1662.

Valentin, S. F., Williams, P. E. V., Forbes, J. M. and Sauvant, D. 1999. Comparison of the in vitro gas production technique and the nylon bag degradability technique to measure short-and long-term processes of degradation of maize silage in dairy cows. Anim. Feed Sci. Technol. 78 (1-2): 81-99.

von Bothmer, R. 2003. Diversity in barley: (*Hordeum vulgare*). 1st ed. Elsevier, Amsterdam; New York. 280 pp.

Waldo, D. R. 1973. Extent and partition of cereal grain starch digestion in ruminants. J. Anim. Sci. 37 (4): 1062-1074.

Welch, J. G. 1986. Physical parameters of fiber affecting passage from the rumen. J. Dairy Sci. 69 (10): 2750.

Wetzel, D. L. 1993. Molecular Mapping of Grain with a Dedicated Integrated Fourier Transform Infrared Microspectrometer. Dev. Food Sci. 32: 679-679.

Wetzel, D. L. 1998. Metabolically deuterated species determined in rat cerebella by FT-IR microspectroscopy as a novel probe of brain metabolism. Pages 294 AIP conference proceedings. American Institute of Physics, New York.

Wetzel, D. L. 2000. Infrared spectroscopy goes microscopic. Chem. Ind. (London). 9 (8): 308-313.

Wetzel, D. L., Eilert, A. J., Pietrzak, L. N., Miller, S. S. and Sweat, J. A. 1998a. Ultraspatially-resolved synchrotron infrared microspectroscopy of plant tissue *in situ*. Cell. Mol. Biol. (Noisy-Le-Grand). 44 (1): 145-168.

Wetzel, D. L. and LeVine, S. M. 1993. *In situ* FT-IR microspectroscopy and mapping of normal brain tissue. Spectroscopy. 8: 40-45.

Wetzel, D. L. and LeVine, S. M. 2000. Infrared microbeam analysis of intricate biological specimens. Inst. Phys. Conf. Ser. 165: 65-66.

Wetzel, D. L. and LeVine, S. M. 2001. Biological applications of infrared microspectroscopy. Pages 101-142 *in* Hans-Ulrich Gremlich and Bing Yan, ed. Infrared and Raman Spectroscopy of Biological Materials. Marcel Dekker Inc., NY.

Wetzel, D. L., Reffner, J. A., Carr, G. L. and Cho, L. 1998b. Synchrotron powered FT-IR microspectroscopy permits small spot ATR sampling of fiber finish and other materials. Pages 657-660 *in* J. A. d. Haseth, ed. Fourier Transform Spectroscopy. American Institute of Physics, Woodbury, NY.

Wetzel, D. L., Slatkin, D. N. and Levine, S. M. 1998c. FT-IR microspectroscopic detection of metabolically deuterated compounds in the rat cerebellum: a novel approach for the study of brain metabolism. Cell. Mol. Biol. (Noisy-Le-Grand). 44 (1): 15-27.

Yang, W. Z., Beauchemin, K. A., Farr, B. I. and Rode, L. M. 1997. Comparison of barley, hull-less barley, and corn in the concentrate of dairy cows. J. Dairy Sci. 80 (11): 2885-2895.

Yoshimoto, Y., Tashiro, J., Takenouchi, T. and Takeda, Y. 2000. Molecular structure and some physicochemical properties of high-amylose barley starches. Cereal Chem. 77 (3): 279-285.

You, S. G. and Izydorczyk, M. S. 2002. Molecular characteristics of barley starches with variable amylose content. Carbohydr. Polym. 49 (1): 33-42.

Yu, P. 2004. Application of advanced synchrotron radiation-based Fourier transform infrared (SR-FTIR) microspectroscopy to animal nutrition and feed science: a novel approach. Br. J. Nutr. 92 (6): 869-885.

Yu, P. 2005a. Application of cluster analysis (CLA) in feed chemical imaging to accurately reveal structural-chemical features of feeds and plants within cellular dimension. J. Agric. Food Chem. 53 (8): 2872-2880.

Yu, P. 2005b. Applications of hierarchical cluster analysis (CLA) and principal component analysis (PCA) in feed structure and feed molecular chemistry research, using synchrotron-based Fourier transform infrared (FTIR) microspectroscopy. J. Agric. Food Chem. 53 (18): 7115-7127.

Yu, P. 2005c. Multicomponent peak modeling of protein secondary structures: comparison of gaussian with lorentzian analytical methods for plant feed and seed molecular biology and chemistry research. Appl. Spectrosc. 59 (11): 1372-1380.

Yu, P. 2006a. An emerging method for rapid characterization of feed structures and feed component matrix at a cellular level and relation to feed quality and nutritive value. Arch. Anim. Nutr. 60 (3): 229-244.

Yu, P. 2006b. Synchrotron IR microspectroscopy for protein structure analysis: Potential and questions. Spectroscopy. 20 (5): 229-251.

Yu, P. 2007a. Molecular chemical structure of barley proteins revealed by ultra-spatially resolved synchrotron light sourced FTIR microspectroscopy: comparison of barley varieties. Biopolymers. 85 (4): 308-317.

Yu, P. 2007b. Protein secondary structures (α-helix and β-sheet) at a cellular level and protein fractions in relation to rumen degradation behaviours of protein: a new approach. Br. J. Nutr. 94 (05): 655-665.

Yu, P. 2007c. Ultra-spatial synchrotron radiation for imaging molecular chemical structure: Applications in plant and animal studies. Spectroscopy. 21 (4): 183-192.

Yu, P. 2008. Modeling protein structures in feed and seed tissues using novel synchrotron-based analytical technique. Anim. Feed Sci. Technol. 140 (1-2): 199-206.

Yu, P., Block, H., Niu, Z. and Doiron, K. 2007. Rapid characterization of molecular chemistry, nutrient make-up and microlocation of internal seed tissue. J Synchrotron Rad. 14 (part 4): 382-390.

Yu, P., Block, H. C. and Doiron, K. 2009a. Understanding the differences in molecular conformation of carbohydrate and protein in endosperm tissues of grains with

different biodegradation kinetics using advanced synchrotron technology. Spectroc. Acta Pt.A-Molec. Biomolec. Spectr. 71 (5): 1837-1844.

Yu, P., Christensen, C. R., Christensen, D. A. and McKinnon, J. J. 2005. Ultrastructural-chemical make-up of yellow-seeded (Brassica rapa) and brown-seeded (Brassica napus) canola within cellular dimensions, explored with synchrotron reflection FTIR microspectroscopy. Can. J. Plant Sci. 85 (3): 533-542.

Yu, P., Christensen, D. A., Christensen, C. R., Drew, M. D., Rossnagel, B. G. and McKinnon, J. J. 2004a. Use of synchrotron FTIR microspectroscopy to identify chemical differences in barley endosperm tissue in relation to rumen degradation characteristics. Can. J. Anim. Sci. 84 (3): 523-528.

Yu, P., Doiron, K. and Liu, D. 2008. Shining light on the differences in molecular structural chemical make-up and the cause of distinct degradation behavior between malting- and feed-type barley using synchrotron FTIR microspectroscopy: a novel approach. J. Agric. Food Chem. 56 (9): 3417-3426.

Yu, P., Jonker, A. and Gruber, M. 2009b. Molecular basis of protein structure in proanthocyanidin and anthocyanin-enhanced Lc-transgenic alfalfa in relation to nutritive value using synchrotron-radiation FTIR microspectroscopy: A novel approach. Spectroc. Acta Pt.A-Molec. Biomolec. Spectr. 73 (5): 846-853.

Yu, P., McKinnon, J. J., Christensen, C. R. and Christensen, D. A. 2004b. Imaging molecular chemistry of Pioneer corn. J. Agric. Food Chem. 52 (24): 7345-7352.

Yu, P., McKinnon, J. J., Christensen, C. R. and Christensen, D. A. 2004c. Using synchrotron-based FTIR microspectroscopy to reveal chemical features of feather protein secondary structure: comparison with other feed protein sources. J. Agric. Food Chem. 52 (24): 7353-7361.

Yu, P., McKinnon, J. J., Christensen, C. R. and Christensen, D. A. 2004d. Using Synchrotron Transmission FTIR Microspectroscopy as a Rapid, Direct, and Nondestructive Analytical Technique To Reveal Molecular Microstructural-Chemical Features within Tissue in Grain Barley. J. Agric. Food Chem. 52 (6): 1484-1494.

Yu, P., Meier, J. A., Christensen, D. A., Rossnagel, B. G. and McKinnon, J. J. 2003. Using the NRC-2001 model and the DVE/OEB system to evaluate nutritive values of Harrington(malting-type) and Valier(feed-type) barley for ruminants. Anim. Feed Sci. Technol. 107 (1-4): 45-60.

APPENDIX: SUPPLEMENTARY MATERIAL

A.1. Using Mid-IR spectroscopy with multivariate molecular spectral analyses to discriminate and classify molecular structure difference of barley seed: expanded comparison

Paired comparisons were conducted among the six barley varieties using AHCA and PCA analysis. Besides the results shown in Chapter 3 using DRIFT spectroscopic data collected from whole seed sample to compare CDC Helgason with other five varieties in fingerprint, protein and CHO region, the results also indicated that CDC Cowboy differed with McLeod and CDC Trey in fingerprint region (Figure A1); differed with CDC Trey in protein region(Figure A2); differed with CDC Dolly, McLeod and CDC Trey in CHO region (Figure A3). DRIFT spectral data of hull sample from the six barley varieties and the SFTIR spectral data of endosperm tissue were also analyzed using these two multivariate methods. However, all the varieties comparison could not be grouped in separated cluster (for AHCA) or ellipse (for PCA) due to overlapping.

I: Cluster Analysis (CLA): fingerprint region 1800-800 cm^{-1}

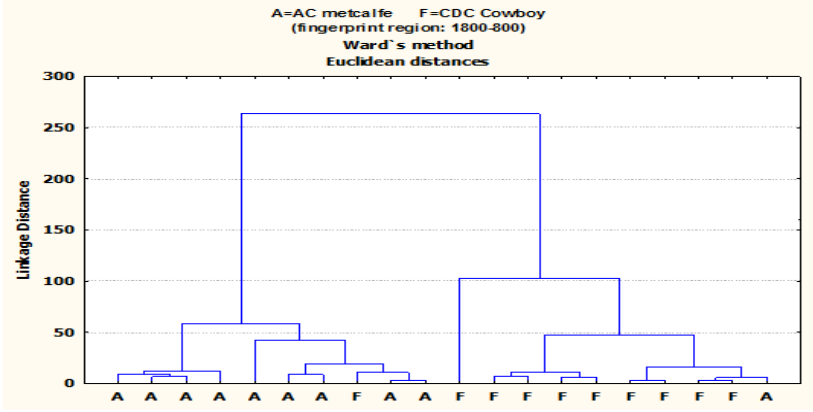

(1) Comparison of AC Metcalfe (A) and CDC Cowboy (F)

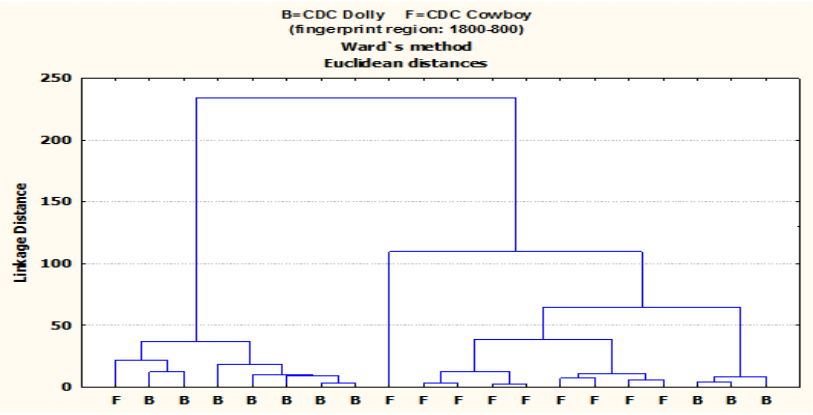

(2) Comparison of CDC Dolly (B) and CDC Cowboy (F)

II: Principal component analysis (PCA): fingerprint region 1800-800 cm^{-1}

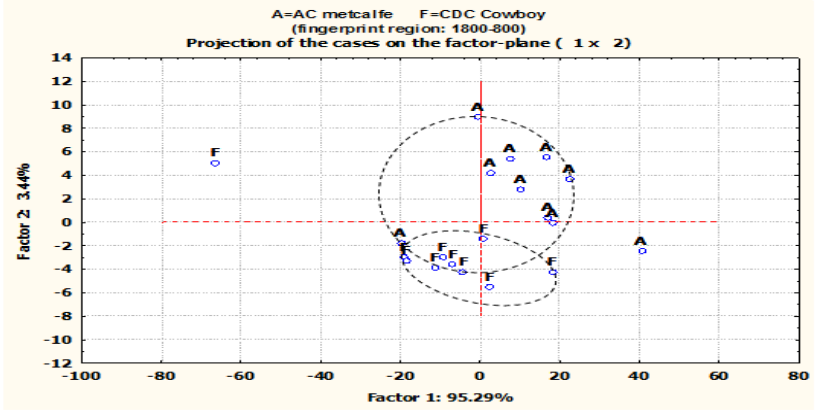

(1) Comparison of AC Metcalfe (A) and CDC Cowboy (F): PC1 and PC2 explain 95.29 and 3.44% of the variances, respectively.

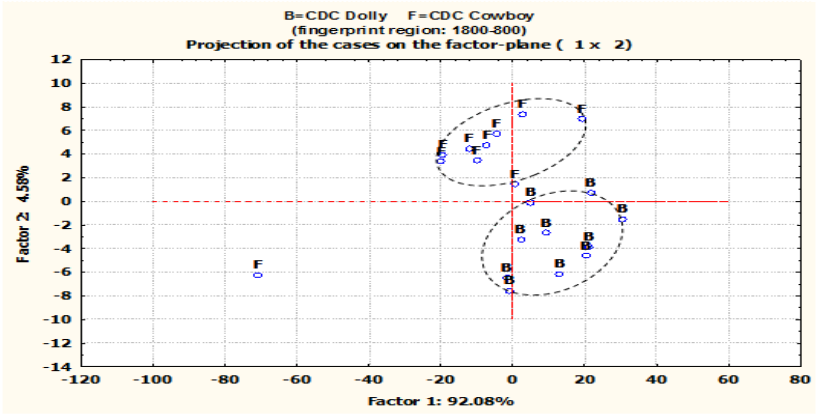

(2) Comparison of CDC Dolly (B) and CDC Cowboy (F): PC1 and PC2 explain 92.08 and 4.58% of the variances, respectively.

Figure A1. Multivariate spectral analyses of barley structures in the whole seed using DRIFT: comparison of CDC Cowboy (F) with other four barley varieties AC Metcalfe (A), CDC Dolly (B), McLeod (C) and CDC Trey (E) I: cluster analysis (1) Select spectral region: finger print region: ~1800 to 800 cm^{-1}; (2) Distance method: Euclidean; (3) Cluster method: Ward's algorithm; II: principal component analysis: Scatter plots of the 1st principal components (PC1) vs. the 2nd principal components (PC2).

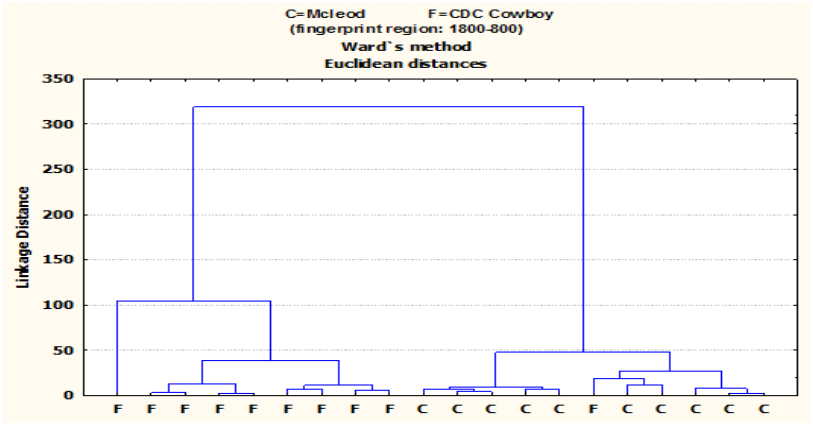

(3) Comparison of McLeod (C) and CDC Cowboy (F)

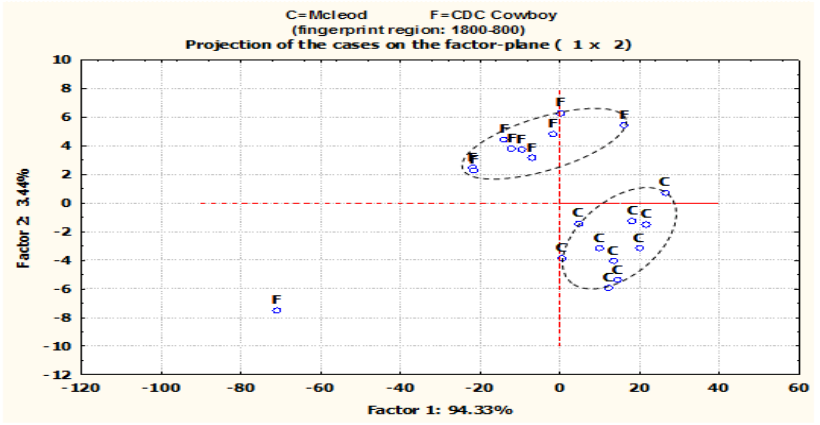

(3) Comparison of McLeod (C) and CDC Cowboy (F): PC1 and PC2 explain 94.33 and 3.44% of the variances, respectively.

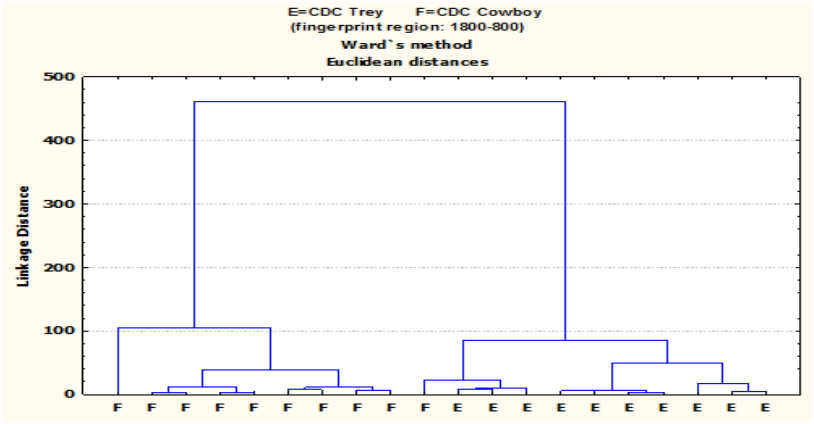

(4) Comparison of CDC Trey (E) and CDC Cowboy (F)

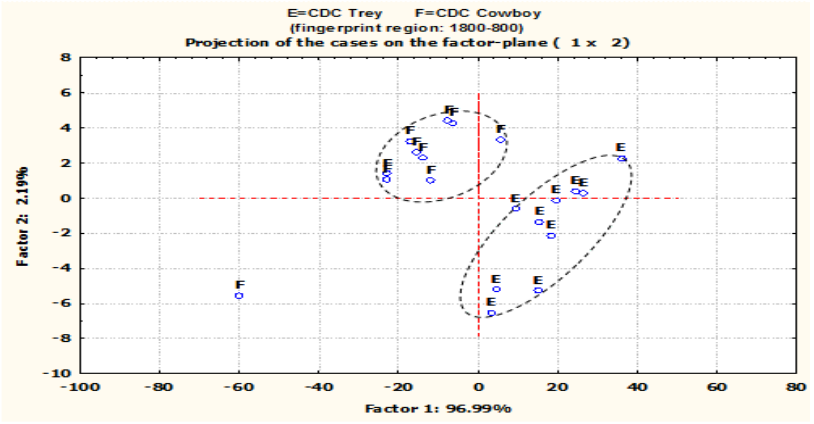

(4) Comparison of CDC Trey (E) and CDC Cowboy (F): PC1 and PC2 explain 96.99 and 2.19% of the variances, respectively.

Figure A1. (continued) Multivariate spectral analyses of barley structures in the whole seed using DRIFT: comparison of CDC Cowboy (F) with other four barley varieties AC Metcalfe (A), CDC Dolly (B), McLeod (C) and CDC Trey (E) I: cluster analysis (1) Select spectral region: finger print region: ~1800 to 800 cm^{-1}; (2) Distance method: Euclidean; (3) Cluster method: Ward's algorithm; II: principal component analysis: Scatter plots of the 1st principal components (PC1) vs. the 2nd principal components (PC2).

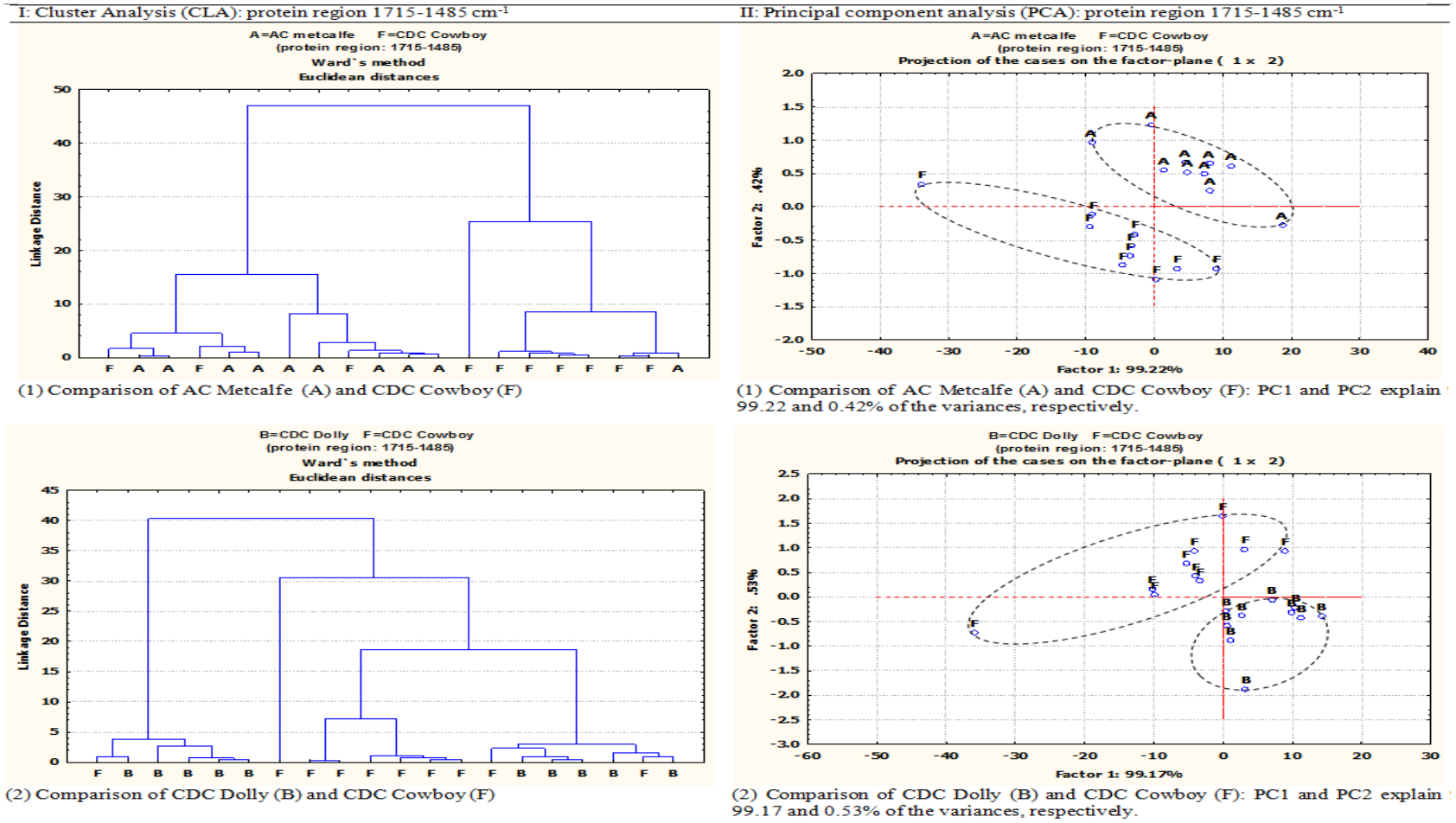

Figure A2. Multivariate spectral analyses of barley structures in the whole seed using DRIFT: comparison of CDC Cowboy (F) with other four barley varieties AC Metcalfe (A), CDC Dolly (B), McLeod (C) and CDC Trey (E) I: (1) Select spectral region: amide I and II region: ~1715 to 1485 cm-1; (2) Distance method: Euclidean; (3) Cluster method: Ward's algorithm; II: principal component analysis: Scatter plots of the 1st principal components (PC1) vs. the 2nd principal components (PC2).

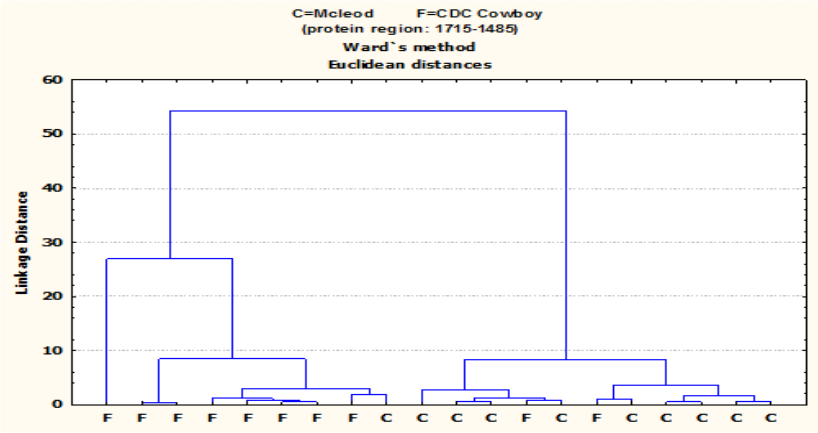

(3) Comparison of McLeod (C) and CDC Cowboy (F)

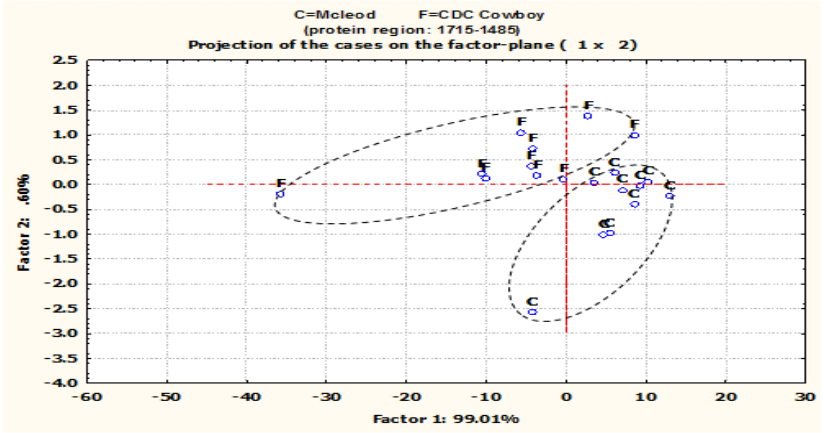

(3) Comparison of McLeod (C) and CDC Cowboy (F): PC1 and PC2 explain 99.01 and 0.60% of the variances, respectively.

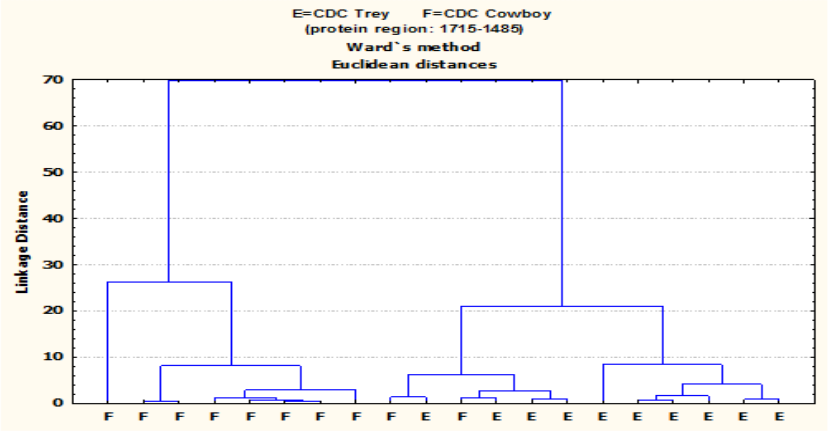

(4) Comparison of CDC Trey (E) and CDC Cowboy (F)

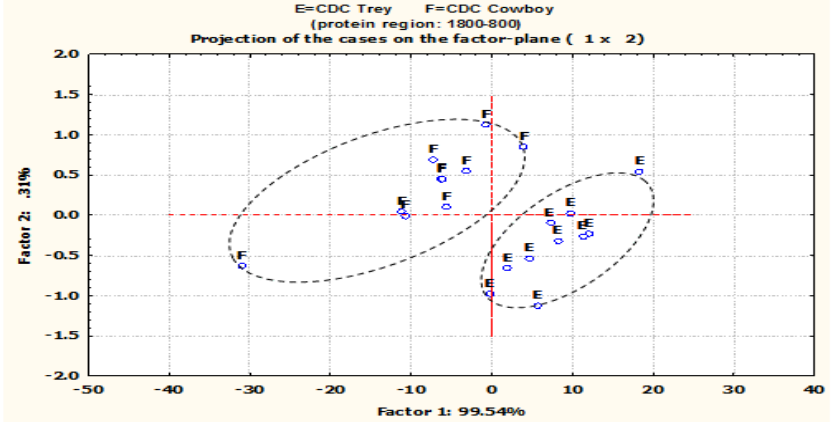

(4) Comparison of CDC Trey (E) and CDC Cowboy (F): PC1 and PC2 explain 99.54 and 0.31% of the variances, respectively.

Figure A2. (continued) Multivariate spectral analyses of barley structures in the whole seed using DRIFT: comparison of CDC Cowboy (F) with other four barley varieties AC Metcalfe (A), CDC Dolly (B), McLeod (C) and CDC Trey (E) I: (1) Select spectral region: amide I and II region: ~1715 to 1485 cm-1; (2) Distance method: Euclidean; (3) Cluster method: Ward's algorithm; II: principal component analysis: Scatter plots of the 1st principal components (PC1) vs. the 2nd principal components (PC2).

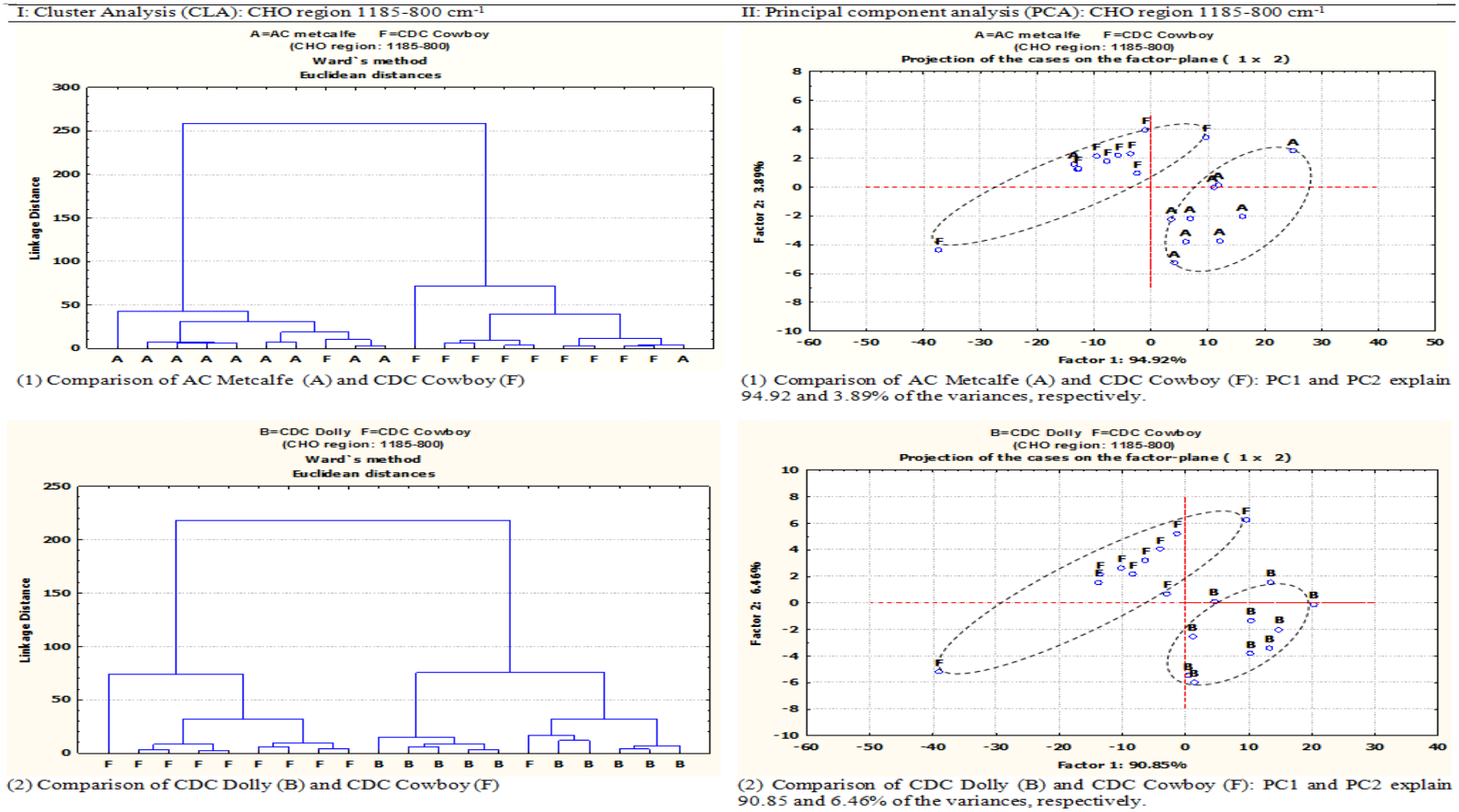

Figure A3. Multivariate spectral analyses of barley structures in the whole seed using DRIFT: comparison of CDC Cowboy (F) with other four barley varieties AC Metcalfe (A), CDC Dolly (B), McLeod (C) and CDC Trey (E) I: cluster analysis (1) Select spectral region: carbohydrate molecular region: 1185 to 800 cm^{-1}; (2) Distance method: Euclidean; (3) Cluster method: Ward's algorithm; II: principal component analysis: Scatter plots of the 1st principal components (PC1) vs. the 2nd principal components (PC2).

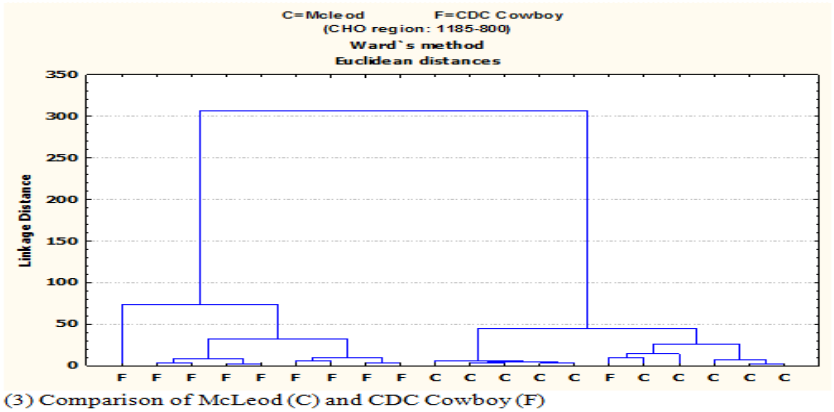

(3) Comparison of McLeod (C) and CDC Cowboy (F)

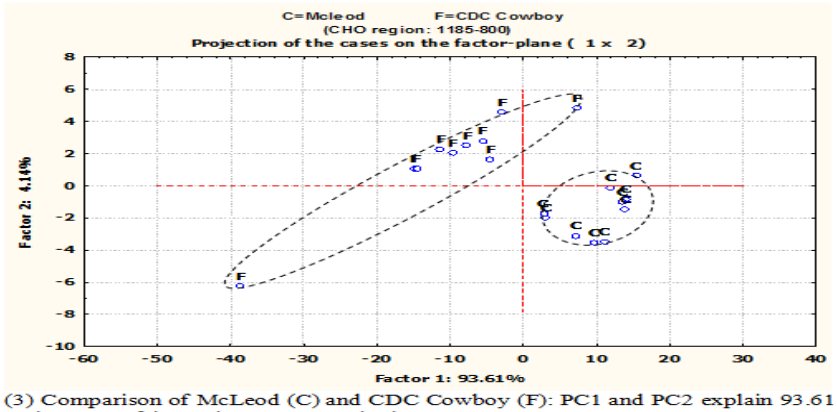

(3) Comparison of McLeod (C) and CDC Cowboy (F): PC1 and PC2 explain 93.61 and 4.14% of the variances, respectively.

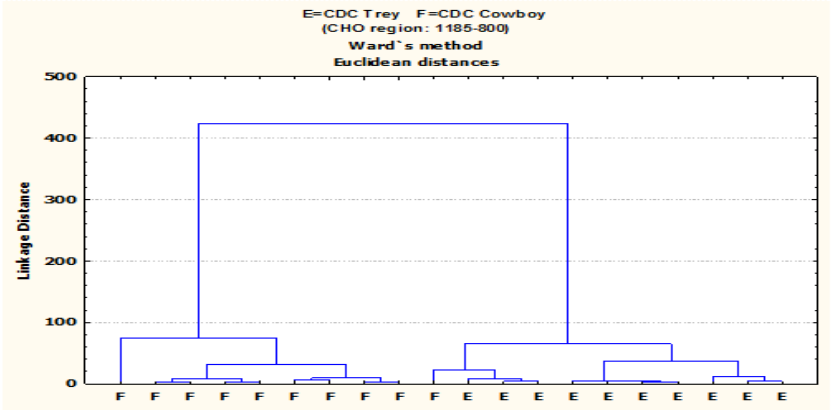

(4) Comparison of CDC Trey (E) and CDC Cowboy (F)

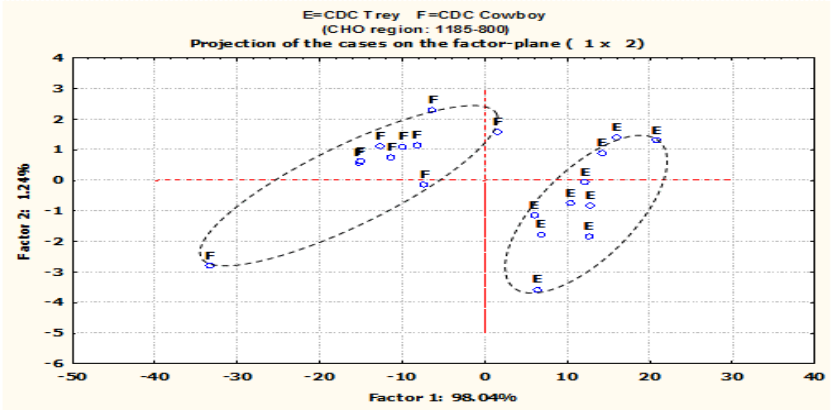

(4) Comparison of CDC Trey (E) and CDC Cowboy (F): PC1 and PC2 explain 98.04 and 1.24% of the variances, respectively.

Figure A3. (continued) Multivariate spectral analyses of barley structures in the whole seed using DRIFT: comparison of CDC Cowboy (F) with other four barley varieties AC Metcalfe (A), CDC Dolly (B), McLeod (C) and CDC Trey (E) I: cluster analysis (1) Select spectral region: carbohydrate molecular region: 1185 to 800 cm^{-1}; (2) Distance method: Euclidean; (3) Cluster method: Ward's algorithm; II: principal component analysis: Scatter plots of the 1st principal components (PC1) vs. the 2nd principal components (PC2).

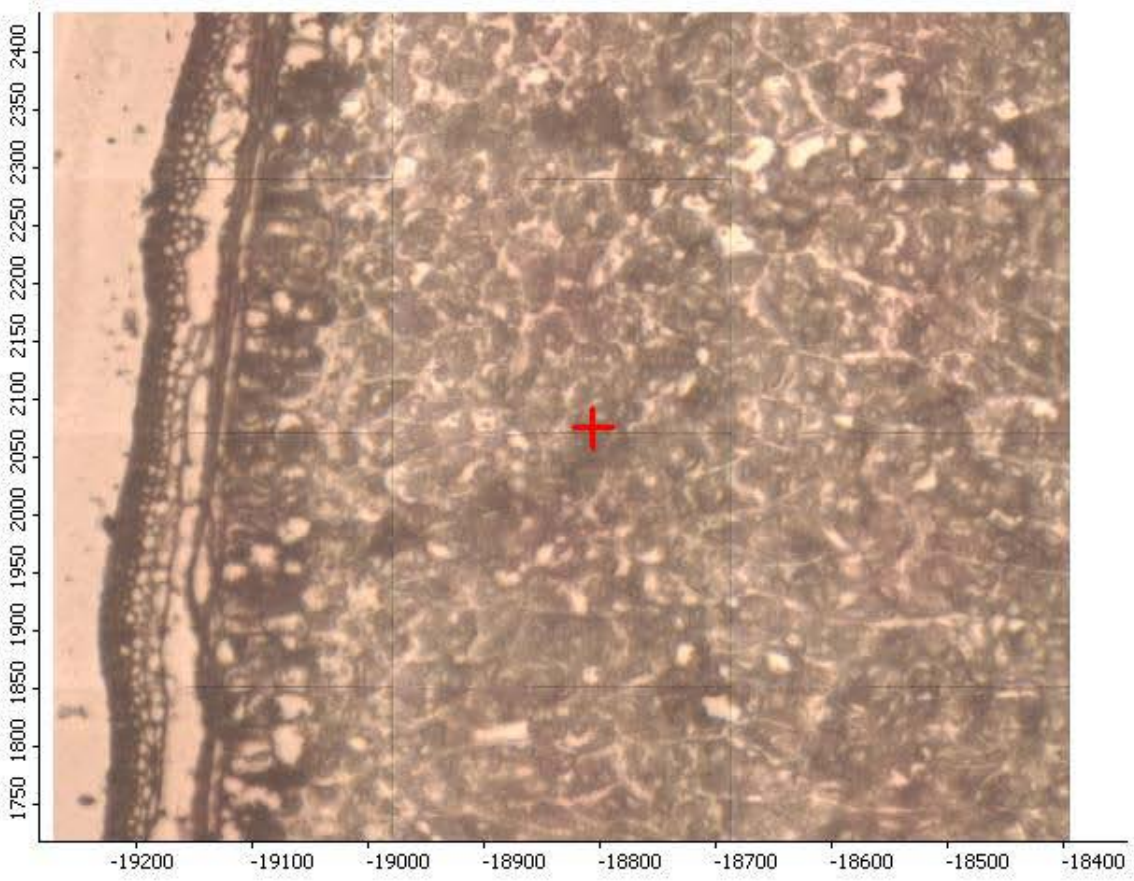

Figure A4. A photomicrograph of barley (cv. McLeod) section produced using ultra-spatial resolution synchrotron-based FTIR microspectroscopy at NSLS U2B station.

Table A.1 Trend of the comparison results of particle size, chemical file, *in situ* rumen degradation kinetics of dry matter (DM), crude protein (CP), starch (ST), and DRIFT and Synchrotron-based FTIR spectroscopic data among six barley varieties.

	AC Metcalfe	CDC Dolly	McLeod	CDC Helgason	CDC Trey	CDC Cowboy
			Particle size			
Mean (mm)	L[z]	H[z]		H		
Median (mm)	L	H		H		
			In situ rumen degradation kinetics of DM			
S				L	H	
D		L			H	
U		H			L	
Kd	H	L	L		H	
EDDM%	H			L	H	
			In situ rumen degradation kinetics of CP			
CP%	H				L	H
S	H				L	
D		L			H	
U		H	H		L	L
Kd	H		H	L	H	
EDCP%	H	L		L	H	
			In situ rumen degradation kinetics of ST			
ST%	H	H	L			
Kd	H	L		L	H	
EDST%	H	L		L	H	

	AC Metcalfe	CDC Dolly	McLeod	CDC Helgason	CDC Trey	CDC Cowboy
			DRIFT data			
Hull sample						
Lignin area	H	L		H		H
Cellulosic area	L	L		H		H
Total CHO area		L		H	L	
Whole seed sample						
Amide I area		L	L	L		H
Cellulosic area	H			L	L	H
Total CHO area				L		H
			SFTIR data			
Amide I area	L		H	L		
Amide II area	L		H	L		H
Total CHO area		H	L	H		
Cellulosic area	H	H	L	H		
CHO 1st area		H	L	H		
CHO2nd area		H	L	H		
CHO3th (starch)		H	L	H		

[z] H= numerically high value; L= numerically low value.